

Lehrstuhl für Molekulare Zellbiologie, Institut für Botanik I - Universität Karlsruhe

TOBACCO MUTANTS WITH REDUCED MICROTUBULE
DYNAMICS ARE MORE RESISTANT TO TOBACCO
MOSAIC VIRUS (TMV)

Zur Erlangung des akademischen Grades eines

DOKTORS DER NATURWISSENSCHAFTEN

(Dr. rer. nat.)

der Fakultät für Chemie und Biowissenschaften der

Universität Karlsruhe (TH)

vorgelegte

DISSERTATION

von

Ouko, Maurice Ochieng

aus

Kenia

Lehrstuhl für Molekulare Zellbiologie, Institut für Botanik I - Universität Karlsruhe

TOBACCO MUTANTS WITH REDUCED MICROTUBULE
DYNAMICS ARE MORE RESISTANT TO TOBACCO
MOSAIC VIRUS (TMV)

Thesis submitted

In

Partial fulfilment of the requirements

For Doctor of Philosophy (PhD.)

of the

Faculty of

University of Karlsruhe

Ouko, Maurice Ochieng

from

Kenya

Dekan: Prof. Dr. Stefan Bräse

Referent: Prof. Dr. Peter Nick

Koreferent: Herr Dr. Claus Buschmann (Priv Doz)

Tag der mündliche Prüfung: 06.02.08

Erklärung

Ich versichere, dass ich diese Arbeit selbstständig verfasst habe, keine anderen Quellen und Hilfsmittel als die angegebenen benutzt und die Stellen der Arbeit, die anderen Werken dem Wortlaut oder dem Sinn nach entnommen sind, kenntlich gemacht habe.

Die Arbeit hat in gleicher oder ähnlicher Form keiner anderen Prüfungsbehörde vorgelegen.

Karlsruhe, den 07-12- 2007

Maurice Ochieng Ouko

Dedication

I dedicate this work to my parents

Mrs Mary Ouko and the late Mr. P.F. Ouko

Who sacrificed selflessly for the sake of my education.

And for my son Romeo, future rocket scientist.

Table of Contents

Erklärung.....	i
Dedication	ii
Table of Contents.....	iii
List of Figures.....	vii
List of tables	viii
Abstract.....	ix
Abbreviations	xii
1 Literature Review	1
1.1 Viral Spread in Plants	1
1.1.1 Cell-To-Cell Movement.....	2
1.1.2 Long Distance Movement.....	4
1.2 Tobacco Mosaic Virus.....	5
1.2.1 Structure and Organisation of the TMV Genome.....	5
1.2.2 TMV Replication Cycle	6
1.2.3 TMV as a Model System for Studying Intracellular Trafficking in Plants. 7	
1.3 The Interaction of TMV with the Cytoskeleton	8
1.4 Microtubules	9
1.5 Movement Protein.....	12
1.6 Subcellular Distribution of MP during Infection	14
1.6.1 Plasmodesmata Association.....	15
1.6.2 Endomembrane Association.....	16
1.6.3 Microtubule Association.....	17
2 Statement of the Problem and Objectives of the Study.....	20

Table of contents

2.1	The Plant Lines.....	21
2.1.1	T-DNA Activation Tagging	21
2.1.2	Ethyl-N-Phenylcarbamate (EPC).....	22
2.1.3	EPC Resistance : The <i>ATER</i> Mutants	22
3	Justification and Significance of the Study.....	24
4	Materials and Methods.....	25
4.1	Plants.....	25
4.2	Chemicals	25
4.3	Equipment.....	26
4.3.1	Other Equipment.....	27
4.3.2	Protein marker	28
4.4	Antibodies	29
4.4.1	Primary Antibodies.....	29
4.4.2	Secondary Antibodies.....	29
4.5	Physiological studies.....	30
4.5.1	Immunodetection of Microtubules	32
4.5.2	Actin Staining.....	33
4.5.3	Soluble Protein Extraction	34
4.5.4	Fractionation by EPC Sepharose Affinity Chromatography	34
4.5.5	TCA Precipitation.....	35
4.5.6	Preparation of Samples for SDS-PAGE.....	35
4.5.7	Total Protein Extracts	36
4.5.8	SDS-PAGE (Sodium Dodecyl Sulphate -Poly Acrylamide Gel Electrophoresis)	37
4.6	Western Blotting (semi-dry) and Protein Detection.....	38

Table of contents

4.6.1	Protein Transfer and Detection.....	38
4.6.2	Signal Development with Alkaline Phosphate.....	40
4.6.3	TMV-RNA Plant Inoculation.....	40
4.6.4	The Plasmids.....	40
4.6.5	Heat Shock Transformation.....	41
4.6.6	Plasmid Amplification.....	41
4.6.7	Quantification of Nucleic Acids.....	42
4.6.8	Plasmid Purification.....	42
4.6.9	In-vitro Transcription.....	43
4.6.10	Verification of the Transcription.....	44
4.6.11	Preparation of Plants for Inoculation.....	44
4.6.12	Transcript Inoculation.....	44
4.6.13	Agroinfiltration.....	44
5	Results.....	46
5.1	Microtubule Dynamics and EPC Sensitivity.....	47
5.2	Tyrosinylated and De-Tyrosinylated Tubulin Differ in EPC Affinity....	48
5.3	Determining the Levels of Tyrosinylated and Detyrosinylated Tubulin	51
5.4	Microtubule Orientation in the <i>ATER</i> mutants.....	53
5.5	Actin Orientation in the <i>ATER</i> mutants.....	56
5.6	Spread of TMV in Mutants with Reduced Microtubule Dynamics.....	58
5.7	Intracellular Localisation of TMV.....	61
5.7.1	Are Microtubules Involved in the Spread of TMV?.....	61
5.7.2	TMV:MP Association during TMV Spread in Tobacco.....	63
5.8	TMV:MP Intracellular Association in the Absence of Viral Infection...	65
5.9	<i>ATER</i> mutants are Less Susceptible to TMV Infection.....	67

Table of contents

5.10	Summary of the Results.....	69
6	Discussion.....	71
6.1	Resistance to EPC is Dependant on Microtubule Dynamics.....	71
6.2	Tubulin Separation using EPC Affinity Chromatography.....	74
6.3	Microtubule Stability and Detyrosinylation	75
6.4	Microtubule Stability Depends on their Orientation	76
6.5	Microtubules Influences the Orientation of Actin Filaments	77
6.6	MP Phosphorylation is a Viral Strategy.....	80
6.7	Reduced Microtubule Dynamics Lower TMV Cell-To-Cell Movement Efficiency	82
6.8	Intracellular Association of MP:GFP during Viral Infection.....	83
6.9	Association of MP with the Cytoskeleton in the Absence of Infection.	86
6.10	<i>ATER</i> Mutants are More Resistant to TMV.....	87
7	Conclusions and Future Outlook.....	90
	Acknowledgements	93
8	References.....	94
9	Appendix.....	109

List of Figures

Figure 1: Tobacco seedlings grown in petridishes.	31
Figure 2: Schematic representation of correct layering of blots, for transfer of proteins from gel to membrane during Western blot.	39
Figure 3: Growth response of tobacco plants to EPC	47
Figure 4: EPC sepharose protein profiling in tobacco.	49
Figure 5: Separation of tyrosinylated and detyrosinylated α tubulin in tobacco.	50
Figure 6: Detection of α tubulin in total protein extracts from leaves.	51
Figure 7: Tyrosinylation levels in mutant and wild type tobacco plants	52
Figure 8: Cortical microtubules in epidermal cells of <i>N. tabacum</i>	54
Figure 9: Schematic rep. of an epidermal cell showing cytoskeletal filaments.	54
Figure 10: Cortical microtubule orientation in tobacco.	55
Figure 11: Actin filament orientation in epidermal cells of <i>N. tabacum</i>	56
Figure 12: Orientation of actin filament in epidermal cells of <i>N. tabacum</i>	57
Figure 13 Successful inoculation of SR1 (A), ATER 2 (B) and ATER 5 (C)	58
Figure 14: Schematic representation of TMVMP: GFP spread following successful inoculation.	59
Figure 15: Infection band in tobacco plants showing direction of spread.	59
Figure 16: TMVMP:GFP movement in tobacco.	60
Figure 17: Intracellular localization of TMVMP:GFP in epidermal cells of tobacco.	61
Figure 18: Differences in MP localization between <i>N. tabacum</i> and <i>N. benthamiana</i>	62
Figure 19: MP labelling at the leading edge of infection in <i>N. benthamiana</i> plants.	63
Figure 20: Pd labelling at the leading edge in <i>N. tabacum</i>	64
Figure 21: Association of MP with ER inclusion bodies at the ME of infection.	64
Figure 22: Association of MP with microtubules at the leading edge of infection in <i>N.</i> <i>tabacum</i>	65
Figure 23: Intracellular localization of MP in <i>N. tabacum</i> in the absence of viral infection.	66
Figure 24: Visualization of filaments in leaf epidermis of <i>N. tabacum</i> plants.	67
Figure 25: Tobacco plants infected with TMV at 6 weeks post inoculation.	68
Figure 26: Symptom expression in <i>N. tabacum</i> at 6 weeks post inoculation.	68
Figure 27: working model depicting TMV movement via microtubule treadmilling.	89
Figure 28: Effect of high tubulin levels on viral spread in <i>N. tabacum</i>	109

List of tables

Table 1: List of chemicals used during the study	26
Table 2: List of equipment used in the study.....	27
Table 3: Specific materials used in the study.....	28
Table 4: Marker 2, Prestained Protein Marker, Broad Range (6-175 kDa).....	29
Table 5: List of items required for surface sterilization of tobacco seedlings.....	30
Table 6: List of materials used for growing tobacco seedlings.....	31
Table 7: List of solutions used for indirect immunolocalization of microtubules in leaf tissue.....	32
Table 8: Solutions required for actin staining in leaf tissue.....	33
Table 9: Solutions required for extraction of soluble proteins from plant tissue.....	34
Table 10: Solutions required for TCA precipitation.....	35
Table 11: Solutions required for protein isolation from a total plant extract.....	36
Table 12: Solutions used for preparation of SDS PAGE gels.....	37
Table 13: Composition of resolving and stacking gel.....	37
Table 14: Solutions required for semi dry blotting and protein detection.....	38
Table 15: Solutions required for transfer of proteins from gel to membrane, and for protein detection	38
Table 16: Solutions required for signal development with alkaline phosphatase.....	40
Table 17: Solutions used for plasmid DNA purification.....	42
Table 18: Solutions required for <i>in vitro</i> transcription of template DNA.....	43

Zusammenfassung

Wenn ein Virus in eine Pflanze eindringt ist es zunächst auf nur eine oder wenige Zellen beschränkt. Damit eine erfolgreiche Infektion stattfinden kann, muss das Virus vom Wirt repliziert werden und sich auf benachbarten Zellen ausbreiten können.

Der Transfer des viralen Genoms von Zelle zu Zelle beinhaltet eine Interaktion zwischen cytoplasmatischen Wirtskomponenten und den vom Virus codierten Bewegungsproteinen (*movement protein*, MP). Insbesondere die Komponenten des Zellskeletts wie die Aktinmikrofilamente und Mikrotubuli, sowie das Endoplasmatische Reticulum (ER) wurden bereits als signifikante Mitspieler in der interzellulären Bewegung des Tabakmosaikvirus (TMV) erwähnt.

Obwohl die Mitwirkung der Mikrotubuli im lokalen Transport des TMV unbestritten erscheint, liegt die genaue Rolle im Transport der viralen Komplexe noch im Dunkeln. Das so genannte *Treadmilling* und ein Führungsschienenmodell wurden als mögliche Mechanismen vorgeschlagen.

Der Schwerpunkt dieser Arbeit war es, ein Modell für die Mitwirkung von Mikrotubuli im Transport des TMV von Zelle zu Zelle zu entwerfen.

Als Untersuchungsobjekt wurden Tabakpflanzen (*Nicotiana tabacum*) verwendet. Diese waren charakterisiert durch ihre Resistenz zu Ethyl-N-Phenylcarbamate (EPC). Diese *ATER*-Mutanten (*Activation Tagged EPC Resistant*) wurden mit TMV-Derivaten infiziert, in welchen das MP mit GFP (*Green fluorescent protein*) fusioniert vorliegt. Das fluoreszierende MP wurde als Indikator für das Vorhandensein des viralen Komplexes verwendet.

Die *ATER 2*-Mutante mit verminderter Mikrotubulidynamik zeigt eine ebenso verminderte Effizienz in der Verbreitung der viralen Komplexe, sowie weniger Symptome eines viralen Infekts. Diese Beobachtungen lassen auf ein Bewegungsmodell schließen, in welchem der virale Komplex per *Treadmilling* bewegt wird. Somit hat sich die in der vorliegenden Arbeit untersuchte reduzierte Mikrotubulidynamik direkt auf die Resistenz der Pflanze gegen das TMV ausgewirkt.

Abstract

Systemic viruses offer a useful model system to unravel the mechanisms by which selected macromolecules are transported to and through plasmodesmata. When a virus is introduced into a plant, it is usually deposited in a few cells or even a single cell. For successful infection to occur the virus has to replicate in these cells and spread from there into the neighbouring cells, and eventually to the rest of the plant, this results in visible disease.

The transfer of the viral genome from cell to cell involves an interaction between specific cytoplasmic host components and the encoded viral movement protein (MP) (Heinlein *et al.*, 1998a Oparka *et al.*, 1999; Boyko *et al.*, 2000a; 2000b). More specifically, the cytoplasmic components; microtubules (Heinlein *et al.*, 1995; Boyko *et al.*, 2007), actin microfilaments (Mclean *et al.*, 1995), and endoplasmic reticulum (Kawakami *et al.*, 2004; Liu *et al.*, 2005) have been implied as significant players in the cell-to-cell movement of tobacco mosaic virus (TMV).

Even though microtubules have been conclusively shown to be involved in local transport of TMV (Boyko *et al.*, 2002, Boyko *et al.*, 2007), it remains unclear as to what mode the microtubules use to convey the viral complex. Treadmilling (Más and Beachy 1999) and guiding tracks (Carrington *et al.*, 1996) have been proposed as possible mechanisms by which microtubules transport the MP/vRNA complex.

The focus of this study was to elucidate the involvement of microtubules in cell-to-cell transport of TMV.

Activation tagged EPC resistant (*ATER*), *Nicotiana tabacum* tobacco plants with reduced microtubule dynamics were inoculated with transcripts of TMV derivatives in which the MP was fused to a green fluorescent protein (GFP). The detected fluorescence of the MP was used as an indicator for the presence of the viral complex. Its distribution as well as its association with subcellular components was followed over a time.

Abstract

In the mutant *ATER 2*, where microtubule turnover is reduced, the efficiency of viral spread is reduced as well. These observations suggested that the viral complex moves via treadmilling. A model based on these results suggests that MP/vRNA binds onto one end of the microtubules and via polymerisation and depolymerisation arrives at the other end.

In consequence of the reduced efficiency of viral trafficking infected plants of *ATER 2* exhibit lowered symptom expression, thereby suggesting a link between microtubules and TMV infection.

Based on these observations, this study concludes that the reduced microtubule dynamics in *ATER 2* confer resistance to the plant in the face of TMV infection.

Abbreviations

(v/v)	volume per volume (percentage volume)
(w/v)	weight per volume (percentage weight)
μM	micrometer
<i>A. thaliana</i>	<i>Arabidopsis thaliana</i>
APS	Ammonium peroxydisulfate
ATT	Anti tyrosinated tubulin
BSA	bovine serum albumin
BY-2	tobacco cell line bright yellow-2
CaMV	cauliflower mosaic virus
CBB	Coomassie brilliant blue
cDNA	complementary DNA
CLSM	confocal laser scanning microscope
CP	capsid protein
cv	cultivar
DNA	Deoxyribonucleic acid
DNase	Desoxyribonuclease
dpi	days post infection
dsDNA	double stranded DNA
DTT	Dithiothreitol
E.col	<i>Escherichia coli</i>
EB1	Microtubule End Binding protein 1
EDTA	Ethylenediamine tetraacetic acid
EGTA	Ethylene glycol tetraacetic acid
ER	Endoplasmic reticulum

Abbreviations

F-actin	Filamentous actin
FITC	Fluorescein 5(6)-isothiocyanate
GFP	Green fluorescent protein
GTP	Guanosine 5'-triphosphate
kb	kilobase pairs
MAP	Microtubule associated protein
MFP	Microfilament Buffer
min	minutes
MP	Movement protein
mRNA	messenger RNA
MSB	Microtubule Stabilizing Buffer
MT	Microtubules
MW	molecular weight
<i>N. tabacum</i>	<i>Nicotiana tabacum</i>
<i>N. benthamiana</i>	<i>Nicotiana benthamiana</i>
OD	optical density
ORF	Open reading frame
PAGE	Polyacrylamide gel electrophoresis
PBS	Phosphate buffered saline
Pd	Plasmodesmata
PIPES	1,4-Piperazinediethanesulfonic acid
PVDF	Polyvinylidene Difluoride
RFP	Red fluorescent protein
RNA	Ribonucleic acids
RNase	Ribonuclease

Abbreviations

RNP	ribonucleoprotein
SDS	Sodium dodecyl sulphate
SDS-PAGE	Sodium dodecyl sulfate-polyacrylamide gel electrophoresis
SEL	size exclusion limit
siRNA	small interfering RNA
ssDNA	single-stranded DNA
TMV	Tobacco Mosaic Virus
Tris	Tris-(Hydroxymethyl)-Aminomethane
VRC	viral replication complexes
vRNA	viral Ribonucleic acids
vRNP	viral Ribonucleic protein
WT	wild type

1 Literature Review

1.1 Viral Spread in Plants

When a virus is introduced into a plant, usually by mechanical means or by an insect mediated vector, it is usually deposited in a few cells or in a single cell. For successful systemic infection of a susceptible host leading to visible symptom expression, the virus has to move from where it is deposited, to adjacent cells and eventually the rest of the plant.

Unlike animal cells, plant cells possess a cell wall in addition to a cell membrane. In contrast to animal cells, cells in plants are connected to each other symplastically via plasmodesmata. In mesophyll cells only small molecules, metabolites and dextrans of a molecular mass upto 1 kDa (stokes radius 0.75 nm) can pass through the plasmodesmata freely.

Viral spread in plants has long been considered to occur in two distinct modes; slow movement from cell to cell occurring via the plasmodesmata and also referred to as local transport, and a rapid distribution known as system or long distance transport that occurs via the plants vascular system (Samuel, 1934).

It has long been established that animal and bacterial viruses exploit and modify pre-existing pathways for macromolecular movement within cells, between cells and between organs (Thivierge *et al.*, 2005). This knowledge has helped to advance the theory that plant viruses make use of a similar strategy for trafficking, the relatively large viral genome to overcome the barrier imposed by the plant cell wall and hence spread from cell to cell through the plasmodesmata.

Early studies on viral movement involved the extraction of a suspect plant tissue and inoculation of the extract onto a susceptible indicator host to determine if the virus was present (i.e. had moved) into the sampled tissue (susceptible

host). With this kind of technology it was not possible to track neither viral movement nor the viral-host components that were significant for movement.

The current use of fluorescent proteins to label viruses enables us to track the movement of the virus in near real time. This ability to locate viruses in plant cells, coupled with the ability to alter the expression of viruses and host encoded genes has helped to outline the significance that cytoskeletal components play in viral movement (Heinlein *et al.*, 1995, Mclean *et al.*, 1995, Citovsky *et al.*, 1999, Boyko *et al.*, 2000).

For successful movement of a plant virus through the plasmodesmata, interaction of the virus with the host is important. These host dependent factors either support viral movement or defeat the host's defence that might limit or hinder viral movement.

Studies conducted by Wolf *et al.*, (1989) demonstrated that, the SEL of plasmodesmata in host plants was modified by the MP of TMV to allow the passage of the macromolecules 10 fold as that in the absence of the MP. This process where the MP increases the SEL is referred to as "gating".

1.1.1 Cell-To-Cell Movement

Cell to cell movement is an active process and it has been shown previously that "gating" alone is not sufficient to allow cell to cell movement of plant viruses.

The process of cell to cell movement occurs in three steps:

- i) The viral replication complexes (VRCs) with the newly synthesized viral genomes are transferred from the sites of replication to the intracellular transport system.
- ii) The VRCs are targeted and transported to the plasmodesmata.
- iii) The VRC is directed through the plasmodesmata and to the adjacent cell.

It has been shown that, early in TMV infection, there is an accumulation of endoplasmic reticulum (ER) associated complexes that contain TMVMP,

genomic RNA and viral replicase. These complexes represent viral replication complexes (VRCs) where virus production occurs (Asurmendi *et al.*, 2004). The VRCs associates with the ER either through the 126 kDa replicase protein or the MP; an association of the VRCs with microfilaments is suggested to occur at this point.

The VRCs are then transported to the plasmodesmata and associate with a certain region of the cell wall through its interaction with microfilaments. It has been suggested that the VRCs move along microtubules to cell wall adhesion sites and that these sites are somehow linked to plasmodesmata via actin, myosins or ER (Beachy and Heinlein 2000; Más and Beachy 2000). Pectinmethylesterase (PME), a 38 kDa protein (P38), is suggested to represent a cell wall receptor for TMVMP that helps to target the VRC to the plasmodesmata. Deletion of the PME-binding region resulted in activation of TMV cell-to-cell movement (Citovsky *et al.*, 1999; Chen *et al.*, 2000).

Once the virus arrived at the plasmodesmata, other viral and host factors become necessary for transport of the VRCs to adjacent cells (Heinlein *et al.*, 1995; Mclean *et al.*, 1995; Boyko *et al.*, 2000). Mutations in host or viral genes required for any step in this process prevents the expression of systemic symptoms and/or cell to cell movement (Boyko *et al.*, 2000; Heinlein *et al.*, 2000).

However, the nature of the viral entity that moves through the plasmodesmata during cell to cell movement is not known. It is postulated that it occurs in the form of a viral ribonucleoprotein (vRNP) complex comprising the MP and vRNA as it has been shown that the MP interacts with single stranded nucleic acids (Citovsky *et al.*, 1990).

Interaction of the viral movement protein with the plasmodesmata most likely interferes with normal intercellular communication of the host plant; it is therefore likely that a mechanism exists to regulate the activity of TMVMP (Lucas *et al.*, 1995). It has been postulated that the phosphorylation of TMVMP performs this function minimizing interference of TMVMP with plasmodesmatal permeability during viral infection.

TMVMP is phosphorylated by a cell wall associated protein kinase at its carboxyl terminal serine and threonine residues (Citovsky *et al.*, 1993). Phosphorylation was shown to downregulate the biological activity of TMVMP, by hindering its ability to increase the SEL of plasmodesmata (Sokolova *et al.*, 1997; Waigmann *et al.*, 2000; Matsushita *et al.*, 2002b).

TMVMP mutations that blocked cell-to-cell viral movement in *Nicotiana tabacum* allowed movement in *Nicotiana benthamiana*. This was very uncharacteristic since both species of tobacco phosphorylated the MP normally (Waigmann *et al.*, 2000). This implies that the mechanisms of MP transport through the plasmodesmata must be different in *N. tabacum* and *N. benthamiana*. This may explain why *N. benthamiana* is the more susceptible of the two species to viral diseases.

It has been suggested that the replication proteins play a role in cell-to-cell movement by interaction with the viral MP and performing transport functions not associated with their genome replication function or by affecting a cellular processes (Hirashima and Watanabe, 2001; Hirashima and Watanabe, 2003). The 126-kDa replicase protein has been shown to influence the quantity and timing of the synthesis of MP thus indirectly affecting cell to cell movement functions (Watanabe *et al.*, 1987; Nelson *et al.*, 2004; Nelson *et al.*, 2005).

1.1.2 Long Distance Movement

Long distance or phloem-dependent movement requires that viruses are able to enter and exit bundle-sheath cells and sieve elements. Systemic viral spread involves host-viral interactions that are different from those in cell-to-cell movement. Most viruses that show cell-to-cell movement in a similar manner as TMV require a capsid protein (CP) for long distance transport (Dawson *et al.*, 1988; Siong *et al.*, 1993). It has however been demonstrated that groundnut rosette umbravirus (GRV) does not code for a CP and that the protein encoded by ORF3 of GRV can functionally replace the CP of tobacco mosaic virus (TMV) for long distance movement. The capsid function of the CP in long distance

transport is only necessary after the virus has crossed the plasmodesmata at the boundary between bundle sheath and phloem cell.

Our knowledge on viral trafficking into and out of the vascular system is limited. Minor veins are generally sheathed by bundle-sheath cells and contain various cell types including vascular parenchyma cells, companion cells and enucleate sieve elements (reviewed in Nelson and van Bel, 1998). The transport of the viral complex throughout the vascular system implies movement from mesophyll cells to bundle-sheath cells, from bundle-sheath cells to vascular parenchyma and companion cells, and entry into sieve elements. It has been suggested that the plasmodesmata linking these types of cells differ from those interconnecting mesophyll cells (Kempers *et al.*, 1993; Nelson and van Bel, 1998). Analysis of virus-host systems in which systemic virus movement was impaired has provided evidence of the need for specific viral factors, different from those required for cell-to-cell movement (Goodrick *et al.*, 1991; Ding *et al.*, 1995; Carrington *et al.*, 1996, Nelson and van Bel, 1998).

1.2 Tobacco Mosaic Virus

1.2.1 Structure and Organisation of the TMV Genome

TMV belongs to the *tobamovirus* group of viruses. TMV virions are not enveloped, are usually straight and have a regular length of 300 nm and a width of 18 nm. The TMV genome comprises a single stranded positive sense RNA (ssRNA) molecule that is 63595 nucleotides (nts) in length and contains four open reading frames (ORFs). This ssRNA is encapsidated by 2160 helically arranged coat protein (CP) subunits.

The 5' terminus of the TMV genomic RNA is capped with 7-methyl guanosine and forms a histidine accepting transfer RNA (tRNA)-like structure within the 3'-untranslated region. The 5' proximal ORFs that encode the overlapping 126 and 183-kDa replication proteins initiate at nt 69 and terminate with amber and ochre stop codons at nt 3417 – 3419 and nt 4917 – 4919 respectively. These two proteins are translated directly from genomic RNA and constitute the

replicase function of TMV (Ishikiwa *et al.*, 1991; Lewandrowski and Knapp, 2001). Viral constructs containing only the 126-kDa replicase gene were unable to cause infection whereas infection occurred, when only the 183-kDa was present, although to a lesser extent as compared to the wild type TMV containing both replicase proteins (Ishikawa *et al.*, 1986). The 30-kDa movement protein (MP), nt 4903 – 5709, and the 17.5-kDa capsid protein (CP), nt 5712 – 6191, are translated from individual 3' – co-terminal subgenomic mRNAs (sgRNAs) that are produced during virus replication.

TMV and the red clover necrotic mosaic virus (RCNMV) represent the simplest versions of RNA viruses that infect mesophyll cells, encode a single MP and do not need coat proteins for cell-to-cell movement. The CP is, however, necessary for systemic infection.

1.2.2 TMV Replication Cycle

TMV is not transmitted by insects, nematodes or similar vectors. It infects plants via direct contact with the wounded areas on plant surfaces. Once TMV enters the host cell, the virus particles disassemble in an organized manner to expose the TMV RNA. This uncoating process is thought to require ribosomes in the 5' to 3' removal of CP subunits during translation in the process, and is therefore termed co-translational disassembly (Wilson, 1984). Translation of the replicase-associated proteins (126- and 183-kDa) begins within a few minutes after infection. When viral RNA is mechanically inoculated or used in cell-to cell movement assays, the first step is direct synthesis of the replication proteins.

As in many positive strand RNAs, the synthesis of progeny negative strand TMV is thought to be coupled to viral disassembly, translation of the replication proteins and RNA synthesis (Buck, 1999; Lewandowski and Dawson, 1998).

Once the complementary negative strand is synthesized, a presumed double-strand intermediate is used as a template for synthesis of positive strands. Subsequently, progeny negative strands are synthesized using the positive strand as a template. In protoplasts of the tobacco cell line bright yellow (BY-2), the synthesis of negative strands ceases early in infection (6 – 8 hours post

inoculation), whereas positive strands continue to be synthesized up to 2 - 4 hours longer (Ishikawa *et al.*, 1991b; Lewandowski and Dawson, 1998). This continued synthesis of positive strands results in an asymmetric excess of positive strands.

During early to mid infection, MP is expressed transiently and accumulates to relatively low levels (Lehto *et al.*, 1978). In contrast, CP accumulates to high amounts later during replication (Siegel *et al.*, 1978; Ooshika *et al.*, 1984) and when synthesis of negative strand RNA has ceased, encapsidates the genomic positive strand RNA to form virions, thus completing the cycle (Aoki and Takebe, 1975; Palakaitus *et al.*, 1983).

1.2.3 TMV as a Model System for Studying Intracellular Trafficking in Plants.

Tobacco mosaic virus (TMV) was the first virus to be isolated and identified when M.W. Beijerinck showed that the filterable agent of TMV was neither a bacteria nor any other corpuscular body, but that it was a *contagium vivum fluidum* (Beijerinck, 1898). The mosaic symptoms associated with tobacco mosaic virus (TMV) were however already described in Russia and in the USA a decade earlier by Mayer (1886) and Iwanowski (1892). The birth of virology is as such generally accredited to TMV as its identification helped define what a virus is. TMV is used as a model system in plant virology

It is now recognized that invading pathogens have evolved in such a way that they can make use of the metabolic pathways of the host and adapt these pathways to their own advantage (Kimura *et al.*, 1996; Moulard *et al.*, 2001, Rietdorf *et al.*, 2001; Martin *et al.*, 2002). Animal viruses such as influenza, herpes simplex and adenovirus rely on the cytoskeleton for the transport of their viral genomes to the nucleus (Ben-Ze'ev *et al.*, 1983; Topp *et al.*, 1994; Avalos *et al.*, 1997; Li *et al.*, 1998). The ability of viruses to cross cellulosic cell walls and propagate infection throughout plants is of particular interest for plant biology and virology. Studies of virus - plant interactions in addition to improving our understanding of viral life cycles and mechanisms of viral infection, can be

used in studying cellular processes such as gene expression, intercellular communication and molecular transport.

The importance of TMV in molecular biology has been enhanced by the consideration that virus replication might be analogous to synthesis of cellular components (Bawden and Pirie, 1936). In molecular biology, TMV is one of the most studied pathogens and is now considered as a model system for studying cellular processes in plants.

TMV is a single stranded positive sense RNA virus, cell-to-cell spread of the virus occurs via the plasmodesmata which are intercellular communication channels between plant cells (Tomenius *et al.*, 1987; Atkins *et al.*, 1991). The movement of the virus is considered to occur in the form of a viral nucleoprotein complex (vRNP) (Dorokhov *et al.*, 1983; Citovsky *et al.*, 1990). This movement is mediated by a virus encoded, 30-kDa movement protein (MP), also referred to as P30. The MP has been shown to dilate the size exclusion limit of the plasmodesmata (Wolf *et al.*, 1989) thus easing the passage of the viral complex through the plasmodesmata. The discoveries by Heinlein *et al.*, (1995) and Mclean *et al.*, (1995) showing that the MP of TMV localizes specifically with microtubules and actin, have helped focus interest on the role of the cytoskeleton in directing transcytoplasmic movement and regulating plasmodesmata. The MP of tobacco as such represents an indirect marker for the presence of vRNA during TMV infection (Más and Beachy, 1999). And is now used to understand the mechanisms by which macromolecular transport is directed and integrated within and between plant cells.

1.3 The Interaction of TMV with the Cytoskeleton

Synthesis of TMVMP, replication of TMV and probably formation of the MP-TMV complex all occur within the host cell. This implies that P30 moves through the cytoplasm to the plasmodesmata, although the underlying mechanism is not well understood. It has been suggested that the cytoskeleton acts as a trafficking system for the intracellular transport of proteins, organelles, vesicles and even mRNA (Williamson, 1986; Vale, 1987; Dingwall, 1992; Hesketh,

1994). It is therefore possible that the movement of the TMVMP-RNA complex through the cytoplasm is mediated by cytoskeletal components.

Many animal viruses spread through the host cell by interacting with the cytoskeletal components of the cell. Specifically, the microtubule network appears to play a significant role in viral protein distribution in animal cells (Pasick *et al.*, 1994).

Analogous to the animal cytoskeleton, the plant cytoskeleton is composed of filamentous networks of actin and tubulin (microtubules). Experimental data and evolutionary conservation of the cytoskeletal proteins suggest that both the general mechanisms and the functions of the cytoskeleton are conserved between animals and plants (reviewed in Lloyd, 1982; Staiger and Lloyd, 1991; Shibaoka and Nagai; 1994). It is therefore probable that both plants and animals may use cytoskeletal filaments and motor proteins to move macromolecular complexes such as ribonucleic proteins. Evolutionary studies suggest that viruses exploit host cellular genes and pathways, adapting them for the viral life cycle (Haselhof *et al.*, 1984; Citovsky, 1993; Koonin and Dolja, 1993). Based on this, Mclean *et al.*, (1995) hypothesize that the viral P30-RNA complexes may mimic ribonucleic protein particles and use the cytoskeleton as a pathway through the cytoplasm to the plasmodesmata.

1.4 Microtubules

The great interest evoked by microtubules is due to the fact that they are regarded as morphogenetic tools in eukaryotic cells. Plant microtubules are highly dynamic cytoskeletal components that are involved in maintaining cell shape and polarity, specifying the site and determining the plane of cell division. In addition, they are involved in cellular movement (Shibaoka, 1994), control the mechanical properties of the expanding cell wall (Staehelin, 1991), participate in the response of plants to biotic and abiotic stresses, and are essential for an effective defence against fungal pathogens (Kobayashi *et al.*, 1999). The major structural unit of microtubules is the protein tubulin. Tubulin is a dimer that is composed of alternating α - and β - polypeptide subunits of almost equal

molecular weight (55 kDa). Polymerisation of the α - and β -tubulin subunits results in a long protofilament. In plants, 13 of these protofilaments bundle to form a hollow cylinder.

The polarity in microtubules results from polymerisation of α - and β -dimers end to end. The end of the protofilament with β -dimers exposed is referred to as the plus (+) end whereas the end with the α -dimers exposed is known as the minus (-) end. Elongation of microtubules is dependant on a relatively faster growth rate at the plus end as compared to the minus end. When growth at the plus end drops, this will result in shrinkage of the microtubule. Polymerisation and depolymerisation occur at both microtubule ends, the rate of polymerisation is faster at the plus end ensuring dynamic stability and in consequence growth. However when hydrolysis catches up to the tip of the microtubule, it begins a rapid depolymerisation and shrinkage. This switch from growth to shrinking is called a catastrophe.

The activity and function of microtubules seems to be related to the ratio between the polymerized und the depolymerised form of tubulin (Jordan and Wilson, 1998). In addition, cortical microtubules undergo both global and regional rearrangements (Boevink *et al.*, 1998; Marc *et al.*, 1998).

The construction of infectious TMV derivatives that express MP as a MP:: GFP fusion proteins (Heinlein *et al.*, 1995; Epel *et al.*, 1996) has paved the way for the identification and characterisation of cytoplasmic components of the host cell that are involved in targeting and trafficking of the viral genome to plasmodesmata and adjacent cells (Padget *et al.*, 1996; Heinlein *et al.*, 1998). Microtubules have emerged as key players (Aaziz *et al.*, Boyko *et al.*, 2000a; Heinlein, 2002), which is in line with their documented role in trafficking mRNAs, vesicles, viruses and proteins in yeast and animal cells (Bassell and Singer, 1997; Jansen, 1999; Schnorrer *et al.*, 2000, Sodeik, 2000; Ploubidou and Way, 2001).

Despite its central role in virus infection, little is known on the mechanisms of intracellular movement of virus components within the infected cells. Based on findings of colocalization of the MP with microtubules (Heinlein *et al.*, 1995) and

actin microfilaments (McClean *et al.*, 1995), it has been suggested that these two components of the cytoskeleton interact with the MP and thereby mediate cell-to-cell movement of the complexes that contain vRNA and MP (Zambryski, 1995; Carrington *et al.*, 1996). Más and Beachy (1999) showed that TMV RNA colocalizes with microtubules thus lending further credence to the aforementioned hypothesis. These studies also showed dramatic changes in the distribution of vRNA when pharmacological agents were used to disrupt the cytoskeleton.

Boyko and co-workers have recently identified a conserved tobamovirus MP sequence exhibiting similarity to a tubulin motif and postulated that this conserved region mediates the association of MP with microtubules during the cell-to-cell movement process. Viruses that display point mutations in the putative tubulin binding domain of the MP showed reduced cell-to-cell spread and did not label microtubules, suggesting that the spread of vRNA is linked closely to the ability of MP to interact with microtubules (Boyko *et al.*, 2001).

These observations suggested that MP may mimic tubulin interfaces for direct interactions with the microtubule lattice (Boyko *et al.*, 2000a). They also found that MP-associated microtubule complexes to be highly stable against microtubule disrupting conditions (Boyko *et al.*, 2000a).

The findings of Boyko *et al.*, (2002) confirm the significance of MP interacting microtubules in the spread of viral infection, however their particular role in this complex was not elucidated. It has been suggested that microtubules support the spread of infection by serving as a track for the translocation of vRNA from replication sites to plasmodesmata (Heinlein *et al.*, 1995; Zambryski, 1995; Carrington *et al.*, 1996; Aaziz *et al.*, 2001). It was also proposed that microtubules might transport and anchor ER associated replication sites (Más and Beachy, 1999); mediate the storage, turnover or degradation of MP, or alternatively that binding of MP to microtubule results in RNA silencing (Ding, 2000).

In recent years the use of different drugs to suppress microtubules dynamics has made it possible to examine how microtubules regulate a wide spectrum of cellular activities.

1.5 Movement Protein

To establish systemic infection in a susceptible host, a plant virus must move from the inoculation site to the remaining parts of the plant. In most plant viruses (with one notable and biologically relevant exception in the Gemini viruses) this migration is facilitated by a virus encoded protein known as movement protein (MP). The MP actively mediates viral movement through plasmodesmata (Gibbs, 1976; reviewed in Doem *et al.*, 1992, Citovsky and Zambryski, 1993, Carrington *et al.*, 1996; Mclean *et al.*, 1997).

The viral movement protein that mediates the spread of TMV is a 30-kDa protein (also referred to as TMVMP or P30) and is one of the most thoroughly studied MPs. P30 is proposed to form a complex with the genomic TMV RNA, to target this protein-nucleic acid complex to plasmodesmata and to transport it through the plasmodesmata.

To date, four biological activities have been postulated for P30:

- a) Binding to TMV-RNA, forming an extended P30-RNA complex that can penetrate the plasmodesmatal channel (Citovsky *et al.*, 1990; 1992a).
- b) Interacting with cytoskeletal elements to facilitate transport of the P30-TMV RNA complex from the cell cytoplasm to the plasmodesmata (Heinlein *et al.*, 1995, Mclean *et al.*, 1995).
- c) Increasing the size exclusion limit of plasmodesmata thereby allowing the passage of larger macromoles (Wolf *et al.*, 1989).
- d) Interacting with a cell wall associated receptor, this then phosphorylates the bound MP and inactivates its ability to dilate the plasmodesmata (Chen *et al.*, 2000).

The estimated diameter of plasmodesmata in wild type tobacco mesophyll cells is 2.5 nm (Ding *et al.*, 1992) and allows the passage of dextrans 0.75-1.0-kDa. When the lower surface leaf of transgenic tobacco plants expressing the TMV MP gene were micro injected with Fluorescein isothiocyanate (FITC)-labelled dextrans (F-dextrans). It resulted in an increase in the size exclusion limit (SEL) of plasmodesmata to allow the passage of dextrans upto 10-kDa corresponding to a Stokes radius of 2.4 nm to 3.1 nm (Wolf *et al.*, 1989). Experiments conducted whereby TMVMP was co microinjected with F-dextrans, demonstrated that, this increase in SEL was transmitted to a distance 20-25 cells away from the transfection site. This initially led to the suggestion that the MP induces a signalling pathway that causes this modification in SEL for cells that far away. However, detection of MP in cells distant from the point of transfection indicates that MP itself moves through the plasmodesmata (Waigmann *et al.*, 1994). It has since been shown that the SEL differs dependent on the plant species and cell type. In trichomes it is about 7-kDa (Waigmann and Zambyski, 1995) and between 10 and 40-kDa in companion cells of *Vicia faba* (Kampen and Van Bel, 1997), whereas in similar tissues of *Arabidopsis thaliana* it can be upto 67-kDa.

The active expression of the MP eliminates the barrier presented by the cell wall to viral movement, which suggests that MPs alter cell architecture and overcome this barrier. Using a plant virus with a null mutation in MP it has been shown that movement of the viral genome from the initially deposited cell to adjacent cells did not occur (Atabekov and Dorokhov, 1984; Hull, 1991)

The modification of the plasmodesmatal permeability has long been regarded as the fundamental property of MPs and indispensable for cell-cell viral movement. It is, however, not clear, how the plasmodesmal aperture is regulated in the plant. Callose is known to hinder viral spread; Fridburg *et al.*, (2003), have suggested that gating occurs via acceleration of callose degradation. The interaction of MP with PME regulates the activity of PME and thereby loosens the cell wall around the plasmodesmata to open more easily; it

is therefore possible that MP recruits additional PME to the plasmodesmata in order to assist in gating.

1.6 Subcellular Distribution of MP during Infection

The intercellular and intracellular distribution/localization of TMVMP in plant cells and protoplasts can directly be monitored by using a MP gene fused to the gene encoding the green fluorescent protein (GFP) of *Aequorea victoria* (Heinlein *et al.*, 1995; Epel *et al.*, 1996; Padget *et al.*, 1996).

By following the distribution of the MP: GFP, following infection with TMVMP: GFP the subcellular structures involved in vRNA trafficking at equivalent stages of TMV infection can be inferred.

In both *N. benthamiana* and *N. tabacum*, a modified virus where the endogenous CP gene was replaced by a MP: GFP fusion (TMVMP:GFP) caused infection. The infection spots were observed to appear in the form of expanding fluorescent rings.

Microscopy of the infected epidermal cells revealed subcellular localisation patterns of MP:GFP which differed depending on their position in the fluorescent ring (Heinlein *et al.*, 1995; Oparka *et al.*, 1997; Padget *et al.*, 1996; Heinlein *et al.*, 1998):

In *N. benthamiana*, at 3 days post inoculation (dpi), it has been observed that at the initiation of infection (leading edge of the ring) the MP:GFP strongly co-localized with plasmodesmata; this finding indicates the involvement of plasmodesmata in the mediation of cell-to-cell vRNA transport. It also supports a role of MP in increasing the size exclusion limit of plasmodesmata (Wolf *et al.*, 1989; Waigmann *et al.*, 1994). As infection spreads (central region of the ring), the MP associates with ER bodies, these appear in the form of irregularly shaped cytoplasmic punctae, which over time decrease in number but increase in size over time (Heinlein *et al.*, 1995). Analyses of these ER bodies reveals that they are sites for virus synthesis and replication hence the term viral replication centres (VRCs) has been used synonymously to inclusion bodies. As

infection progresses and the ER aggregates disappear, the MP associates with a filamentous, cytoskeletal, structure (trailing edge of the ring). Initially, these structures were thought to be actin filaments, but immunofluorescence data have shown this filamentous network to consist of microtubules (Mclean *et al.*, 1995; Boyko *et al.*, 2000b; Gillespie *et al.*, 2002). It has, in addition, been suggested that MP associates to a limited extent with actin (Mclean *et al.*, 1995). Late during infection the MP-microtubule association ceases and plasmodesmata labelling is resumed.

When tobacco BY-2 protoplasts were infected with TMVMP:GFP, a similar pattern of MP localization was observed to that in *N. benthamiana* epidermal cells with the exception of plasmodesmata targeting.

1.6.1 Plasmodesmata Association

In the initially infected cell, the TMV-encoded MP is produced by the transcription of RNA derived from the invading virus. The MP then associates with viral RNA molecules and mediates cell-to-cell trafficking. This nucleoprotein complex is directed toward the plasmodesmata via interactions with the cytoskeleton of the host cell. It has been suggested that the targeting of TMV MP/vRNA complexes to plasmodesmata involves binding to cell wall pectin methylesterase (PME) (Rhee *et al.*, 2000; Citovsky *et al.*, 1992).

Gating of plasmodesmata is an active process that is mediated by TMVMP, and is a precondition for cell-to-cell movement.

Using viral derivatives of TMV expressing functional and dysfunctional MP: GFP mutations, Heinlein *et al.*, (2000), showed that the association of the MP and its accumulation in plasmodesmata at the leading edge of infection is necessary for vRNA transport. In mutants with N-terminal deletions of 3 to 28 amino acids, respectively, there was no association of MP to plasmodesmata. This indicates that the N-terminus is important for the targeting or anchorage of MP to plasmodesmata. Plants infected with these TMV derivatives exhibited association of MP with inclusion bodies as well as with microtubules, but did not show cell-to-cell movement, thus confirming that the association of MP with the

plasmodesmata is essential for vRNA trafficking, and that the association of MP with inclusion bodies and/or microtubules alone is not sufficient for vRNA trafficking. The authors concluded that microtubules are not involved in targeting MP to plasmodesmata. This confers with results of Boyko *et al.*, (2000) in which temperature sensitive MP:GFP variants were used to show that disruption of the microtubules affected targeting of MP with microtubules but did not interfere with association of MP with the plasmodesmata.

Large deletions at the C-terminus (66 amino acids) resulted in TMVMP:GFP derivatives that associated with plasmodesmata at the trailing edge but not at the leading edge. This suggests that targeting of MP to plasmodesmata is differentially regulated at the leading edge as compared to the trailing edge of infection. In MP-variants where the MP associated to plasmodesmata only during the late stages of infection, cell-to-cell movement did not occur. The authors suggest that two forms of MP exist: an active form at the leading edge that supports cell-to-cell movement, and an inactive form at the late stage that does not support movement. This hypothesis is supported by data presented by Oparka *et al.*, (1997), where the authors showed that plasmodesmatal gating only occurred within the fluorescent band. At the centre of infection the plasmodesmal SEL is maintained, implying that MP at the late stage of infection is down-regulated or inactivated to limit interference with normal intercellular communication.

1.6.2 Endomembrane Association

The cortical endoplasmic reticulum in plants fulfils specialized functions in cell growth and development (Allen and Brown, 1998; Hepler *et al.*, 1990; Staehlin, 1991). Of particular relevance to the role of the endoplasmic reticulum in intercellular virus movement is the apparent direct association between the cortical endoplasmic reticulum and both cortical actin and the desmotubule that forms the centre structure of the plasmodesmata (Hepler, 1982; Ding *et al.*, 1992b; 1996).

It has long been assumed that the endomembrane including the endoplasmic reticulum plays an important role in RNA virus replication in both animals and plants (Richards and Ehrenfeld, 1990; Buck, 1996; Lai, 1997).

Studies of TMV using MP fused GFP revealed that MP associates with ER forming cortical bodies (aggregates), that change in size, number and shape throughout virus infection (Epel *et al.*, 1996; Padget *et al.*, 1996; Oparka *et al.*, 1997; Heinlein *et al.*, 1998). These aggregates contain the 126-kDa and 183-kDa proteins (components of viral replicase) and were suggested to be sites of protein synthesis and viral replication (Mathos, 1981; Saito *et al.*, 1987).

When plants are initially infected with TMV this results in severe disruption of the ER, during this initial period, ER inclusion bodies are formed (Reichel and Beachy 1998). The ER associated sites grow in size over time forming cortical bodies that contain MP as well as replicase proteins. During later stages of infection, the large aggregates dissipate and the ER network returns to the pre-infection state of a well organised cortical reticulum (Reichel and Beachy 1998). These changes in the ER structure parallel MP accumulation and degradation in the infected cell (Heinlein *et al.*, 1998; Gillespie *et al.*, 2002), thus providing evidence for MP:ER association throughout the cell.

It is tempting to suggest that the association of the replication complexes (MP:vRNA) with the ER is a pre-requisite for cell-to-cell spread. However Boyko *et al.*, (2000c), showed that the formation of ER inclusion bodies is not a pre-requisite for cell-to-cell spread of TMV. Using a TMVMP:GFP viral construct in which 55 amino acids were deleted from the C-terminus, it was observed that cell-to-cell spread of TMV proceeded in the absence of aggregated inclusion bodies.

1.6.3 Microtubule Association

In TMV infected *N. benthamiana* plants as well as in protoplasts derived from the tobacco BY-2 suspension culture, the association of MP with microtubules occurs in the mid and late stages of infection when the size and number of ER

cortical bodies decreases and eventually disappears (Heinlein *et al.*, 1998; Heinlein *et al.*, 2000).

Boyko *et al.*, (2000) showed that microtubules play a significant role in determining the rate of vRNA spread. In TMV infected *N. benthamiana* plants incubated at 32°C, microtubule-MP association appeared earlier than when similarly treated plants were incubated at 22°C. Even though the level of MP expression did not increase in the plants where MP microtubule association was observed earlier, the efficiency of intercellular transport of RNA was enhanced, thereby revealing a correlation between early MP-microtubule association and the efficiency of vRNA trafficking.

The involvement of microtubules in intracellular transport of vRNA has further been strengthened by the identification of a conserved TMV-MP sequence exhibiting significant similarity to a tubulin motif known to mediate lateral contacts between microtubule protofilaments (Boyko *et al.*, 2000). It has been suggested that the MP of TMV mimics tubulin to ensure the association of microtubules to the MP.

Studies using virus derivatives expressing MP in fusion with GFP showed that mutations in the putative tubulin binding domain of the MP disrupted the binding of MP to microtubules as well as vRNA transport. This provides evidence for the significance of microtubule association in the migration of vRNA.

The fact that MP is not associated with microtubules at the leading edge of infection in *N. benthamiana* has stimulated a debate on the significance of this association with regard to TMV spread.

Gillespie *et al.*, (2002), describe in their report a viral MP with improved transport functions which they developed via DNA shuffling. TMV vectors expressing this shuffled MP (shuff3MP) moved from cell to cell faster than the same vectors expressing a wild type MP (wtMP). The fact that the shuff3MP did not associate strongly with microtubules at the leading edge of infection led the authors to conclude that microtubules are not involved in vRNA transport of TMV.

Further data suggesting that microtubules are not required for vRNA transport were shown by Gillespie *et al.*, (2002) and Kawakami *et al.*, (2004). Using the microtubule eliminating drug colchicine, the microtubule network was disrupted in *N. benthamiana* plants expressing Arabidopsis α -tubulin (TUA6) fused to GFP (TUA6-GFP). In these plants, the cell-to-cell spread of TMV was shown to proceed even in the absence of an intact microtubule network.

However, the studies of Gillespie and Kawakami challenging the role of microtubules in vRNA movement of TMV have been questioned. Recent studies (Seemanpillai *et al.*, 2006) present evidence showing that colchicine does not completely destroy the microtubule network. This and the fact that the spread of infection requires the movement of only very few virus genomes (Li and Roossinick, 2004; Sacristan *et al.*, 2003), weaken the conclusions of Gillespie and Kawakami on the dispensable nature of microtubules for vRNA trafficking. In addition, compelling evidence exists co-relating efficiency of viral movement to the association of MP to microtubules (Boyko *et al.*, 2000; 2002). Using temperature sensitive mutants Boyko *et al.*, (2007) have irrefutably shown that microtubules are indispensable for TMV spread.

2 Statement of the Problem and Objectives of the Study

The capacity of viruses to successfully replicate in the cell and spread locally and systematically in the host is determined by specific virus-host interactions. However, despite the significance of the intracellular and intercellular movement of virus components within infected cells, little is known on the mechanisms involved in the transport of viral RNA–protein complexes through the cytoplasm, anchorage and replication in cellular membranes, and targeting to plasmodesmata to initiate spread to adjacent plant cells.

Defining these mechanisms will give newer insights about specific virus-host interactions that ultimately determine the success of viral infection.

The following options of how microtubules are involved in the cell-to-cell movement of TMV have been suggested:

1. The MP:RNA complex binds to stable microtubules, which are then moved via microtubule motors (kinesin and dynein). The MP is either transported as cargo of such motors, or it docks to a microtubule and is indirectly moved along with other microtubules.
2. The MP:RNA complex binds to dynamic microtubules and is then transported by “treadmilling” (Shaw *et al.*, 2003). In this case a given microtubule “walks” through the cytoplasm through continuous polymerisation at the plus end (+) and depolymerisation at the minus end (-). Cargo that docks at the “+” end would in time be released at the “-“end
3. The MP binds onto microtubules. However the movement of the MP is not via microtubule motors or treadmilling but through the transport of microtubules along actin filaments which are usually found along microtubules.

It is the objective of this study to determine, which of the three possibilities is realized in plants infected with TMV.

2.1 The Plant Lines

The streptomycin resistant, diploid tobacco line SR1 (*Nicotiana tabacum* cv Petit Havana, Maliga *et al.*, 1973) was used for T-DNA activation tagging. In addition, *Nicotiana benthamiana* was used in further experiments.

2.1.1 T-DNA Activation Tagging

Insertional mutagenesis has the advantage that the inserted element acts as a tag for gene identification. When a T-DNA sequence is inserted into a transcriptional unit, it results in a recessive mutation due to gene disruption or inactivation. In contrast, dominant mutations with a particular phenotype are usually rare. When a particular trait dominates, this is generally regarded as a gain-of-function phenotype caused by either a mutation in the coding region that lead to constitutive activity of the resulting protein or by mutations that stimulate the expression of the respective gene (Chang *et al.*, 1993; Walden *et al.*, 1995).

In T-DNA activation tagging, multiple transcription enhancer elements originating from the cauliflower mosaic virus (CaMV)-35S promoter are fused to the complete CaMV-35S promoter linked to the left border of the transformation plasmid. The insert harbours a Hygromycin resistance on the right border as a selection marker for transformed plant cells and an Ampicillin resistance along with an *E. coli* origin of replication between the Hygromycin resistance and the multiple enhancers (Feldman, 1991).

Once this insert is integrated, dominant *cis*-activation of the genes located near the T-DNA integration site occurs: As a result of the influence of multiple enhancers, flanking genes are overexpressed which produces dominant traits, such that selection is possibly directly in the primary transformants. Based on this principle, Dr Abdul Ahad (Umea-University, Sweden), developed transgenic protoplasts which were then screened and selected based on their microtubule dynamics.

2.1.2 Ethyl-N-Phenylcarbamate (EPC)

The mode of action of many commercial herbicides relies on disruption of the cytoskeleton network. Disassembly of the microtubule network by the herbicides in turn leads to disruption of growth processes. Carbamate based herbicides such as Ethyl-N-phenylcarbamate (EPC) or its derivatives bind directly to tubulin and prevent incorporation onto the growing end of the microtubule (Vaughn, 2000). Using such herbicides it is possible to analyze physiological functions of microtubules, and to demonstrate clearly that microtubules play a significant role in growth processes in plants. EPC has proved to be an important drug in microtubule studies, Wiesler *et al.*, (2002) showed that sensitivity of growth to EPC (phenyl urethane, EPC) is elevated after addition of auxin even though the affinity of α -tubulin for this antimicrotubular herbicide is reduced by auxin, indicating that under these conditions it is the turnover of the microtubules and not the affinity of the inhibitor that limits the tolerance of the microtubules against EPC.

2.1.3 EPC Resistance : The *ATER* Mutants

The list of compounds, which bind to tubulin or microtubules, is large and consists of chemically unique compounds that bind to the tubulin dimers and thus indirectly destabilize microtubules (*Vinca* alkaloid- and colchicine-binding site drugs) and those that bind to the microtubule polymer and stabilize microtubules, such as the taxanes (Taxol and Taxotere)

EPC hinders microtubule assembly by binding to tubulin heterodimers and thereby preventing their addition to the growing end of the microtubule (Mizuno and Suzaki, 1991; Escuin *et al.*, 2005). As a result of depolymerisation at the minus end with none or reduced corresponding polymerisation at the plus end of the microtubule, microtubules are eliminated. Using a rice mutant resistant to EPC, Nick *et al.*, (1994) showed that resistance to assembly blockers is either due to reduced affinity of tubulin to the inhibitor or to reduced dynamics of assembly and disassembly, meaning that, microtubules with a high turnover are more sensitive to such inhibitors whereas microtubules with reduced turnover

can tolerate a reduced rate of assembly because disassembly is also slow as such microtubules persist longer in the presence of assembly blockers. Based on the ideas proposed in Nick *et al.*, (1994), Ahad Abdul designed a screen using activation tagging combined with EPC as a selection marker for generation of tobacco mutants with reduced microtubule turnover. EPC binds to the carboxyterminus of the α -tubulin; the terminal tyrosine is known to be significant for affinity to EPC (Wiesler *et al.*, 2002).

Callus from these activation tagged EPC resistant (*ATER*) mutants, was able to tolerate EPC concentrations of up to 500 μ M. 7 genetically stable mutant lines (*ATER 1* to *ATER 7*) exhibiting the *ATER* trait were raised. In addition to tolerance to cold, the microtubules of these mutants showed corresponding tolerance to EPC. Tolerance to EPC could either be due to lowered affinity of tubulin to this blocker of microtubule assembly, increased levels of tubulin that compensate for loss of dimers bound to EPC, or lowered sensitivity of the microtubules to EPC. Recent studies on *ATER 2* have revealed that the activation tag was inserted shortly before the start codon of a novel cytochrome-P450. This cytochrome-P450 has been identified earlier in rice (Chaban *et al.*, 2003) during a search for auxin-regulated genes that were differentially regulated in the EPC-resistant mutant *Yin-Yang* (Wang and Nick, 1998).

3 Justification and Significance of the Study

Invading pathogens have generally evolved to usurpate the metabolic pathways of their hosts and adapt these pathways for their own use. Studies of plant-virus interactions offer valuable insights for further understanding the mechanisms of viral diseases as well as shedding light on cellular processes such as gene expression, hormonal response, intercellular communication and molecular transport.

Historically, TMV research has been a pacemaker for the development of cell and molecular biology. To spread inside the host TMV probably exploits the innate mechanisms for RNA transport, which is very important for plant development and gene regulation. A survey of the literature shows that the role of microtubules for the spread of TMV is still under debate. In this study, tobacco plants with reduced microtubule dynamics were used to show that this property confers comparative advantage following TMV infection.

This study gives new insights about specific virus-host interactions and paves the way for methods of how microtubule dynamics may be exploited to fight plant viral infections (worldwide, the estimated damage from plant viruses is several billion Euros). Secondly, findings from this study would have a positive impact in biotechnology when applied in gene silencing. In “virus induced gene silencing” (VIGS) the spreading of the viral vector is the key factor. Once the movement mechanism is known, it might become possible to optimise such vectors to spread faster and to increase VIGS efficiency profoundly. A third possibility to use these results would be in the production of commercially valuable bio-molecules such as vaccines in plants with the help of viral vectors, similarly optimising viral spread would be the key to profit.

4 Materials and Methods

Materials

4.1 Plants

Wild type

For this study, streptomycin resistant (SR-1) tobacco plants raised from the callus of haploid *Nicotiana tabacum* cv Petit Havana (1973) were used. These plants do not differ genotypically or physiologically from *N. tabacum* cv. Petit Havana apart from the fact that they are resistant to streptomycin. They are therefore referred to as wild type or control plants.

Mutants

The mutant lines used in the study were generated by Dr. Abdul Ahad from protoplasts of SR-1 tobacco plants that had been mutated via activation tagging (Ahad *et al.*, 2003) and were selected for tolerance to the antimicrotubular herbicide ethyl-N-phenyl carbamate (EPC).

4.2 Chemicals

The chemicals used were all molecular biology grade unless otherwise specified. **Table 1**, lists some of the chemical used that were specific for this study. Standard chemicals for day to day laboratory work were bought from BioRad, Fluka Merck, Serva or Sigma. Bidistilled water was used to dissolve the chemicals. Where necessary solutions were autoclaved before use.

Formatie

Gelöscht

Table 1: List of chemicals used during the study

ITEM	MANUFACTURER
Phenol	Carl Roth GmbH,
3-Aminobenzoic acid	Fluka
3-Nitro-L-Tyrosine	Sigma-Aldrich
Acrylamide-Bisacryamide solution 37,5:1	Carl Roth GmbH
BCIP 5-Bromo-4-chloro-3-indolylphosphat-p-tuloidin	Carl Roth GmbH
Bromphenol blue	Carl Roth GmbH
Carbodiimide	Carl Roth GmbH
Chloroform	Merk
CNBr-activated Sepharose 4B	Amersham Biosciences
Coomassie Brilliant Blue R-250	Carl Roth GmbH
Cyanamide solution	Fluka
Ethylchlorocarbonate	Carl Roth GmbH
Ethylendiamine	Carl Roth GmbH
GTP Guanosin-5'-triphosphate	Fluka
Hoechst 33258 (BisBenzimide H 33258)	Sigma-Aldrich
Macerocyme Cellulase Onozuka R-10	Serva
Milk powder (non fat)	Heiler GmbH
NBT Nitroblue Tetrazolium	Carl Roth GmbH
Pectolyase	Sigma-Aldrich
PFA Paraformaldehyde	Sigma-Aldrich
PMSF Phenylmethylsulfonylfluoride	Sigma-Aldrich
Bovine Serum Albumin (BSA)	Sigma-Aldrich
Macerozyme r-10	Duchefa
Cellulase „Onozuka“ R-10	Duchefa
Primary antibodies (DM1A and ATT)	Sigma

4.3 Equipment

Equipment used in the study, that played a significant role, is listed in [Table 2](#).
Standard laboratory equipment is not listed.

Formatie
Gelöscht

Table 2: List of equipment used in the study

EQUIPMENT	MANUFACTURER
Agarose gel-chamber (Model 40-0911)	PeQlab, Erlangen Germany)
SDS-PAGE gel chamber	Atto
Semi dry blot chamber	BIO-RAD
Thermocycler (cyclone 25)	PeQlab
Table centrifuge (Rotor PP 1/96 #3324)	Heraeus
Ultracentrifuge (TL-100, Rotor TLA 100.2)	Beckmann
Speed Vacuum (Eppendorf concentrator 5301)	Eppendorf Germany
Photometer (Eppendorf BioPhotometer)	Eppendorf Germany
Silmat S5	Ivoclar vivadent, New York, USA
NanoDrop® ND-1000 spectrophotometer	Eppendorf Germany
Eppendorf thermomixer comfort	Eppendorf Germany

4.3.1 Other Equipment

Microscopes/Cameras

At Karlsruhe University, the samples were examined under an AxioImager Z.1 microscope (Zeiss, Jena, Germany) equipped with an ApoTome microscope slider for optical sectioning and a cooled digital CCD camera (AxioCamMRm). For observation of GFP fluorescence the filter sets 46 HE (excitation at 470 nm, beamsplitter at 495 nm and emission at 525 nm), using either a 63x or 40x plan apochromat oil-immersion objective. Images were processed using AxioVison 4.5 software.

In Strasbourg at the Institut de Biologie Moléculaire des Plantes (IBPM), Epifluorescence microscopy of infection sites, leaf epidermis, immunostained cytoskeletal complexes, and motor protein assays was performed with Nikon Eclipse E800 and Nikon Eclipse 80i microscopes equipped with CFI Plan Apochromat objectives (Nikon Corp. Tokyo Japan) and filter sets for visualization of GFP/Alexa fluor 488/fluoresceinisoithiocyanate and rhodamine/Alexa fluor 568 fluorescence, respectively. Images were acquired either with a Nikon Eclipse DXM1200 digital camera (mounted on the Nikon Eclipse E800)

and Nikon ACT-1 software or with a Hamamatsu ORCA-100 progressive scan interline charge-coupled device camera (mounted on the Nikon Eclipse 80i) and Openlab software (Improvision).

Fluorescence infection sites were viewed with the 4x lens, while for high magnification of leaf discs, the 63x lens was used.

Images for publication were processed using Image J 1.38 (<http://rsb.info.nih.gov/ij/>).

Other materials specific to the study are listed in [Table 3](#).

Formatie

Gelöscht

Table 3: Specific materials used in the study

ITEM	MANUFACTURER
PVDF-Membrane	Pall Gelman Laboratory
Gel-Blotting Paper	Schleicher & Schuell
Perfusion chambers 32 x 19 x 1 mm	Schleicher & Schuell
Separating Glas Column with a sintered filter	Thoma Glas

4.3.2 Protein marker

A pre-stained protein marker was used to help determine the size of the separated proteins following SDS PAGE and Western-blot analysis. Transfer of the marker during western blot was used as an indicator of successful blotting.

Table 4: Marker 2, Prestained Protein Marker, Broad Range (6.5-175 kDa).

Size[kDa]	Protein	Origin
175	MBP- β -Galactosidase	<i>Escherichia coli</i>
83	MBP-Paramyosin	<i>Escherichia coli</i>
62	Glutamat Dehydrogenase	Cow liver
47.5	Aldolase	Rabbit muscle
32.5	Triosephosphat Isomerase	<i>Escherichia coli</i>
25	β -Lactoglobulin A	Cow milk
16.5	Lysozym	Egg white
6.5	Aprotinin	lungs (Cow)

4.4 Antibodies

4.4.1 Primary Antibodies

ATT (Anti -Tyrosine Tubulin)

This is a monoclonal anti-tyrosine tubulin (mouse IgG3) antibody. It is specific for tyrosinated α -tubulin and recognizes the last 12 amino acids of the C-terminus of α -tubulin. It can be used for immunocytochemical localization as well as in immunoblotting studies (Kreis, 1987).

Monoclonal Anti α -Tubulin (DM1A)

To detect detyrosinylated α -tubulin, a monoclonal anti α -tubulin (mouse IgG) derived from mouse was used. It can be used for immunoblotting procedures as well as for microtubule detection by immunofluorescence (Breitling and Little, 1986).

4.4.2 Secondary Antibodies

Secondary anti-mouse IgG antibody conjugated to Alkaline Phosphatase

For Western blot analysis, a polyclonal antibody against mouse (raised in goats) was used. This antibody is coupled to Alkaline Phosphatase and converts the substrates NBT and BCIP into a violet precipitate, which allows the detection of the primary antibody.

Secondary anti-mouse IgG antibody conjugated to FITC

A polyclonal antibody against mouse immunoglobulin (anti-mouse IgG) coupled to a Fluorescein-isothiocyanat (FITC) as fluorescent label was used to detect microtubules by indirect immunofluorescence; FITC is excited by light of 488 nm (blue) and emits a green fluorescence (530 nm).

Methods

4.5 Physiological studies

Tobacco seedlings were grown and used to study their growth response to various stimuli. To avoid contamination and hence interference during growth, the seeds were first surface sterilized. A list of the items required for surface sterilization is listed in [Table 5](#).

Formatie
Gelöscht

Table 5: List of items required for surface sterilization of tobacco seedlings.

Component	Composition
Ethanol	70%
Ca(ClO) ₂	1.4%
Triton	0.1%
Sterile distilled water	

A sterile 1ml Eppendorf® tube was filled up to 250 µl with air dried tobacco seeds. To minimize contamination, the following steps were performed under a hooded sterile bench.

1 ml of Ethanol was added to the seeds and then vortexed for 90 seconds, the ethanol was then removed and 1ml of Calciumhypochloride containing triton was added to the seeds and vortexed for 2 minutes. This was done twice. The seeds were then were then washed 5 times with sterilized distilled water and air dried and stored at 4°C.

Materials and methods

Table 6: List of materials used for growing tobacco seedlings.

Component	Concentration	Manufacturer
MS medium	4.409 g/l	Duchefa
Phytigel	1.2 % (w/v)	Sigma
Gibberelic acid (GA3)	10 μ M	Fluka
EPC	0 to 500 μ M	

Several aliquots of MS medium (Murashige and Skoog, 1976) complemented with Phytigel and varying concentrations (0 - 500 μ M of ethyl-N-phenyl carbamate (Wako Pure Chemical Industries, Osaka, Japan) were prepared and autoclaved. These were then left to cool to 50 °C before adding gibberellic acid to each sample to a final concentration of 10 μ M. The plates were poured under sterile conditions in laminar-flow bench (25 ml of medium into 80-mm diameter petri dishes) and left under the hood to solidify.

Using sterile pipette tips, sterile seeds were then sown equidistantly from each other and aligned to the diameter of the petri dish.

The petri dishes were then sealed using Parafilm®, tilted such that the surface of the agar was vertical (Figure 1) and incubated at 25 °C in the dark for up to 25 days. The length of hypocotyls and roots was measured at 12, 14 and 21 days after sowing.

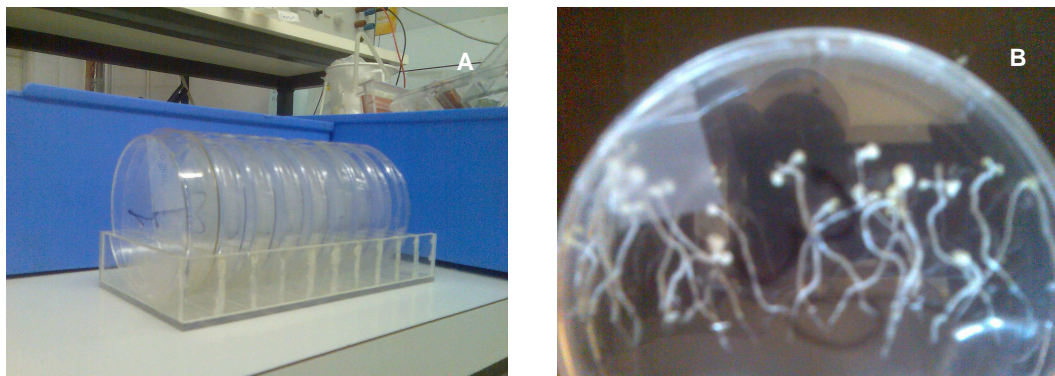


Figure 1: Tobacco seedlings grown in petridishes. Petridishes were placed vertically against each (A) other to ensure that seedlings grew upright (B).

Formatie
Absatz-Sta
Deutsch (I
Gelöscht

4.5.1 Immunodetection of Microtubules

The network of cortical microtubules was visualised through indirect immunofluorescence. The materials used for this procedure are listed in [Table 7](#).

Table 7: List of solutions used for indirect immunolocalization of microtubules in leaf tissue.

Component	Composition	Concentration
MSB pH 6,9 (Microtubule Stabilizing Buffer)	PIPES	50 mM
	EGTA	2 mM
	MgSO ₄	2 mM
	Triton X100	0,1 % (v/v)
	Glycerol	0,25 % v/v
Fixing solution	Paraformaldehyde (PFA)	3,7 % (w/v) in MSB
PBS pH 7,2 (Phosphate Buffered Saline)	NaCl	8 g/l
	KCl	0,2 g/l
	KH ₂ PO ₄	0,158 g/l
	Na ₂ HPO ₄ x 2 H ₂ O	2,31 g/l
Blocker	BSA (Bovine-Serum-Albumin)	0,5 % w/v in PBS
Antibodies	Primary antibody (ATT)	1:100 in PBS
	Secondary antibody (FITC antimouse IgG)	1:25 in PBS

Immunodetection of microtubules was carried out as described in Nick *et al.*, (1990) with modifications. Leaf petioles were harvested freshly from tobacco plants, these were then cut into 2-cm sections, placed in a 15 mm falcon tube and fixed for 60 minutes in fixing solution at room temperature.

The petiole sections were then washed in MSB 3 times for 10 minutes, and then, the epidermis was carefully peeled using a razor blade and fine tweezers; the epidermal strips were collected in buffer on a slide and covered with a perfusion chamber.

Unspecific reactions were blocked using 5% BSA in PBS for 20 minutes.

The epidermal strips were then incubated for 60 minutes at 37°C with the primary antibody ATT diluted to a concentration of 1:100 in PBS. This was followed by another wash step using PBS, 3 times for 10 minutes.

Secondary antibody diluted to 1:25 with PBS was then used to incubate the strips for another 60 minutes at 37°C, the sections were then washed 5 times

for 5 minutes, mounted immediately in PBS and observed using fluorescence microscopy.

4.5.2 Actin Staining

Table 8: Solutions required for actin staining in leaf tissue.

Component	Composition	Concentration
Microfilament Buffer (MFB) pH 7.3	K-phosphate buffer	100 mM
	Triton X100	0,25 % v/v
	KCl	100 mM
FITC Phalloidin stock	6,6 µM in ethanol	5% v/v in MFB
Paraformaldehyde (PFA) stock	37% in MFB (frozen)	1.8 % in MFB

Actin filaments were visualized following a procedure described by Waller and Nick (1997) with modifications. Solutions required for this procedure are listed in

Table 8. Freshly harvested petioles from the leaves of growing tobacco plants were cut into 2 cm² sections.

The sections were then placed in a 15 mm falcon tube and fixed with 1.8 % (w/v) PFA in MFB and rotated for 15 minutes at room temperature.

Following this, the epidermis was peeled from the leaf petioles using fine tweezers; the strips were then collected in a drop of buffer on slides and covered with a perfusion chamber.

The strips were washed 3 times for 5 minutes using MFB. The MFB was then removed and the strips incubated with freshly prepared FITC-labelled Phalloidin (5 % of the stock solution in MFB) for 1 hour in the dark at room temperature.

The sections were again washed 3 times with MFB at 5 minute intervals, mounted on slides containing PBS and observed immediately using fluorescence microscopy.

Formatie
Gelöscht

4.5.3 Soluble Protein Extraction

Table 9: Solutions required for extraction of soluble proteins from plant tissue.

Component	Composition	Concentration
Extraction buffer	MES	25 mM
	EGTA	5 mM
	MgCl ₂	5 mM
	Glycerol	1 M
Additives	PMSF (in extraction buffer)	100 mM
	DTT (in propanol)	100 mM

The following procedure for obtaining soluble microtubule extract was adapted from the procedure outlined in Nick *et al.* (1995). Solutions that were used in this procedure are listed in [Table 9](#). 6 cm² freshly harvested leaf tissue were placed in 2- ml Eppendorf® tubes containing 8-10 glass beads (Roth GmbH, Germany) of 1.7 to 2.0 mm diameter, and shock-frozen in liquid nitrogen. These were then homogenized in a Silamat S5 Dental Homogenizer (Ivoclat vivadent, New York, USA) until a fine powder was obtained; care was taken during this process to ensure that the samples remained frozen to avoid loss of the released proteins.

The powder was then left to thaw before adding 1 volume of extraction buffer with 1/100 of the additives PMSF and DTT.

This was then centrifuged at 16,500 g for 1 minute, at room temperature. The supernatant was removed and placed in ultra centrifuge tubes and the sediment discarded. The supernatant was then centrifuged at 300,000 g for 10 minutes at 4°C.

4.5.4 Fractionation by EPC Sepharose Affinity Chromatography

Aminoethyl Sepharose was prepared as described in Cuatrecasas (1970) and then coupled to Carboxy-EPC as described in Mizuno *et al.*, (1985).

The following steps were carried out at 4°C in a cold room. The Aminoethyl Sepharose coupled to carboxy EPC (EPC-sepharose) was loaded onto a separating column equipped with a sintered glass filter and then washed 3

times using 50 ml extraction buffer for each wash (Using a vacuum pump the extraction buffer was drained through the column) to remove any salts present.

To the supernatant collected previously, 1 volume of sepharose was added and the mixture incubated in batch under constant rotation for 1 h at 4°C to allow for binding of tubulin to EPC.

The sepharose-extract mixture was then loaded onto a column and eluted using increasing concentrations of KCl dissolved in extraction buffer (0, 0.05, 0.1, 0.15, 0.2, 0.25, 0.3, 0.4, 0.5, 1.0, 3.0 mM) by help of a mild vacuum and collected in falcon tubes.

4.5.5 TCA Precipitation

The solutions listed in [Table 10](#) were required for TCA precipitation of the protein fractions.

Formatie
Gelöscht

Table 10: Solutions required for TCA precipitation.

Component	Concentration
Solution A	1,5% (w/v) sodium desoxycholate
	1% (w/v) sodium azide
Solution B	72 % Trichlor acetic acid
Acetone	80% acetone, stored at -20 °C

1% of solution A was added to the collected fractions, these were then vortexed and incubated for 15 minutes at room temperature, followed by addition of 10% solution B, vortexing and centrifugation using a Sorvall SM24 for 30 minutes at 13,000 rpm at room temperature.

The supernatant was discarded and 1 ml of cold (-20°C) acetone added to the precipitate, followed by vortexing and centrifugation under room temperature for 30 minutes at 16,500 g. The sediment containing the proteins was then left to air dry overnight.

4.5.6 Preparation of Samples for SDS-PAGE

SDS sample buffer (20 µl per gel) prepared according to Freudenreich and Nick (1998) was added to the sediment from the TCA-preparation. A few drops of 1N

NaOH were added to samples that were not blue after addition of sample buffer (as a result of TCA residue to prevent hydrolyzation during the heating step.

The samples were then vortexed and heated for 10 minutes at 95°C, this was followed by centrifugation for 2 minutes at 16, 500 g.

4.5.7 Total Protein Extracts

Total protein extracts from tobacco leaves were generated as described in Nick *et al.*, (1995) with modifications. The solutions used are listed in [Table 11](#).

Formatie
Gelöscht

Table 11: Solutions required for protein isolation from a total plant extract.

Components	Composition	Concentration
Sample buffer	1 M Tris/HCl 6.8	5 %
	Glycerin	10%
	SDS	2 %
	Bromphenolblue	0.1 % (w/v)
	1 M DTT	10 % (v/v) added just before use

1 g of freshly harvested leaf tissue was placed in 2-ml Eppendorf® tubes containing 6-8 glass beads and shock-frozen in liquid nitrogen. Using a silomat S5 dental homogenizer (Ivoclar vivadent, New York, USA) the leaf samples were ground to a fine powder, care was taken to avoid thawing.

The sample buffer (100 µl) was directly added to the samples, vortexed and centrifuged for 5 min at 16,500 g; the supernatant was transferred to a new tube and boiled at 95°C for 10 minutes (this made loading in the SDS-PAGE easier and there was no reduction in protein amounts extracted compared to if boiling was done before transferring supernatant to a new tube). The samples were centrifuged again for 1 minute at 16,500 g, placed on ice for 5 minutes and loaded onto the freshly prepared polyacrylamide gel. This was run at 20 mA per mini gel for 90 minutes.

4.5.8 SDS-PAGE (Sodium Dodecyl Sulphate -Poly Acrylamide Gel Electrophoresis)

Table 12: Solutions used for preparation of SDS PAGE gels.

Component	Composition	Concentration
Acrylamide	Acrylamide	29.2 %
	Bisacrylamide	0.8 %
S – Buffer pH 8.8	Tris/HCl	1.5 M
C – Buffer pH 6.8	Tris/HCl	0.5 M
SDS		10% (w/v)
TEMED		
APS (Ammoniumperoxydisulphate)		10%

Using the components listed in [Table 12](#), a 10% polyacrylamide gel was prepared as described in [Table 13](#). It was composed of a 1 cm stacking gel layer and a resolving gel of approximately 6 cm.

Table 13: Composition of resolving and stacking gel.

	RESOLVING GEL				STACKING GEL
	7,5 %	10 %	12,5 %	15 %	
Acrylamide [ml]	5	6,7	8,3	10	1,7
S-Buffer [ml]	5	5	5	5	-
C-Buffer [ml]	-	-	-	-	2,5
H ₂ O [ml]	9,7	8	6,4	4,7	3,3
10 % SDS [µl]	200	200	200	200	100
10 % APS [µl]	80	80	80	80	80
TEMED [µl]	10	10	10	10	10

20 µl each of the prepared samples were then loaded onto the chambers in polyacrylamide gel and run at 20 mA per minigel for 90 minutes in an electrophoresis tank with a buffer containing 186 mM Glycin, 3.5 mM SDS and 0.025 mM Tris. The protein marker was used as recommended by the manufacturer.

4.6 Western Blotting (semi-dry) and Protein Detection.

Table 14: Solutions required for semi dry blotting and protein detection.

Component	Composition	Concentration
Coomassie Brilliant Blue	Coomassie R-250	2.5 g w/v
	Methanol	50%
	Acetic acid	0.9 %
Destainer	Ethanol	30%
	Acetic acid	10%
Drying buffer	Methanol	25%
	Isopropanol	10%
	Glycerol	2%

For Coomassie staining, from a freshly obtained SDS PAGE gel the separation gel was separated from the stacking gel and then placed in a plastic box containing Coomassie Brilliant Blue (CBB) and gently shaken for 1 hour. The CBB was replaced by destainer and the gel incubated over night at 4°C to get rid of the excess colouring. The stained gels were then placed together with cellophane sheets in a drying buffer bath for another 24 hours then placed between two of the cellophane sheets and sealed (care was taken to avoid air bubbles). This set-up was then left for 48 hours to dry.

4.6.1 Protein Transfer and Detection

Table 15: Solutions required for transfer of proteins from gel to membrane, and for protein detection

Component	Composition	Concentration
Transfer buffer	Glycin	14.4 g/l
	Tris/HCl	12.07 g/l
	MeOH	200 ml/l
TBS buffer pH 7.4 %	Tris/HCl	20 mM
	NaCl	150 mM
	Triton X100	1%
Milk buffer		2.5% (w/v) in TBS
Primary antibody	DM1A or ATT	1:300 in TBS
Secondary antibody	IgG-anti-mouse (Alkaline Phosphate conjugated)	1:2500 in milk buffer

Western blotting was performed based on the procedure described in Horwitz *et al.*, (1966) with some modifications.

Gel blotting paper as well as polyvinylidene fluoride (PVDF) membrane was cut out to the exact size of the resolving gel. The blotting paper was soaked in transfer buffer for 1 minute and the PVDF membrane activated by dipping in methanol for 30 seconds.

Starting from the anode end, the membrane was prepared for blotting as follows: 2 layers of blotting paper, PVDF membrane, the freshly run resolving gel and finally 2 layers of blotting paper (**Figure 2**). Care was taken to avoid air bubbles between the layers by rolling a 50-ml falcon tube on top of the layers. The cathode lid of the apparatus was then fixed and the transfer of the proteins from the gel onto the membrane proceeded at 100 mA for 60 minutes per mini gel.

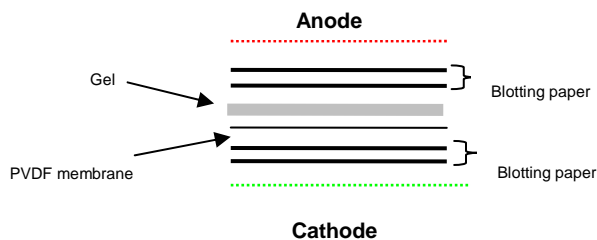


Figure 2: Schematic representation of correct layering of blots, for transfer of proteins from gel to membrane during Western blot.

The membrane was then incubated with milk buffer for 60 minutes to block unspecific binding sites; this was followed by rinsing twice using TBS for 1 minute. The blot was incubated overnight at 4°C with either DM1A or ATT as primary antibody, both dissolved 1:300 in TBS. On the following day, the membranes were washed 3 times for 15 minutes using TBS, and then incubated with the secondary antibody for 60 minutes. Following this, the membranes were washed once with milk buffer and twice for 5 minutes with TBS and were now ready for developing.

4.6.2 Signal Development with Alkaline Phosphate

Table 16: Solutions required for signal development with alkaline phosphatase.

Component	composition	concentration
Staining buffer pH 9.7	Tris/HCl	100 mM
	NaCl	100 mM
Magnesium stock	MgCl ₂ .6H ₂ O	500 mM
Nitrobluetetrazolium (NBT) solution	NBT	75 mg/ml in 75% Dimethylformamide
5-Bromo-4-Chloro-3-Indoxylphosphate-p-Tuloidin (BCIP)	BCIP	50 mg/ml in 100% Dimethylformamide

After the secondary antibody had been washed away, the membranes were incubated for 15 minutes in staining buffer containing 1/10 magnesium stock solution.

5 ml of freshly prepared developer (66 µl NBT and 33 µl BCIP in 5 ml staining buffer with 1/10 magnesium stock solution) were used to incubate the membrane in the dark for 15 minutes or until bands appeared, the reaction was then stopped by rinsing in water. The membranes were then left to dry and photographed or scanned.

4.6.3 TMV-RNA Plant Inoculation

Template Preparation

4.6.4 The Plasmids

Infectious viral RNA of TMVMPC55:GFP was produced by in-vitro transcription of the plasmid pTf5nx2 c55 using a MEGAscript® T7 kit (Ambion (Europe) Ltd, UK). This construct carries a deletion on its 55 C-terminal amino acids and exhibits enhanced microtubule association. It was obtained from Prof. Manfred Heinlein (Institut Biologie Moléculaire des Plantes, CNRS, Strasbourg, France) and was constructed as described in Heinlein *et al.*, (2000).

A wild-type TMV construct, TMV-pTLW (Meshi *et al.*, 2003) which carries the full length TMV cDNA was obtained from the Plant Physiology Department, National Institute of Agrobiological Sciences, Kannondai, Japan). In-vitro

transcription of this plasmid construct yields infectious RNA that is capable of long distance transport in susceptible tobacco plants and hence causes expression of visible symptoms.

For in-vitro transcription, 15 µg of each plasmid was digested using Acc651 (New England Biolabs). This restriction enzyme removes 3'-single strand overhang that would result in extraneous transcripts in addition to the expected transcript (Schenborn and Mierendorf, 1985). To confirm if the plasmid DNA was completely linearised, the digested plasmid was eletrophoresed on a 0.8% agarose gel. Following this the DNA concentration was determined.

4.6.5 Heat Schock Transformation

For transformation, 50 µl of XL-1 blue chemicompetent cells, (stored at -80°C) were used. The tube with the cells was placed on ice before adding 100 ng of the plasmid DNA. The sample was inverted several times, and then incubated on ice for 30 minutes. The tube was then placed in a thermoblock (42°C) for 90 seconds to administer a heat shock, and then incubated on ice for further 10 minutes.

To the sample 1 ml of Lysogeny broth (LB) medium was added and incubated at 37°C under constant shaking (1400 rpm) on an Eppendorf® Thermomixer comfort for 1 h. After 60 minutes, most of the supernatant was decanted (only 200 µl was left), and the sediment resuspended in the residual liquid. This suspension was then plated on LB agar plates containing 50 µg/ml of ampicillin as a selective agent, and incubated overnight.

The LB Medium contained 10 g/l Trypton, 5 g/l yeast extract, 5 g/l NaCl (7 g/l of agar, for LB agar plates) and was adjusted to a pH of 7.0.

4.6.6 Plasmid Amplification

Single colonies were picked from the LB-Ampicillin plates using a sterile pipette tip; these were cultured overnight at 37°C and constant shaking (200 rpm) in liquid LB-Ampicillin medium and amplified using the JETSTAR 2.0 plasmid midiprep kit (Genomed, Bad Oeynhausen, Germany).

4.6.7 Quantification of Nucleic Acids

The concentrations of nucleic acids in solutions were determined by measuring their absorbance at 260 nm using the NanoDrop® ND-1000 spectrophotometer (Eppendorf Netheler-Hinz GmbH, Hamburg Germany). The instrument was first standardized using either Tris-EDTA buffer solution or distilled water (dependent on the solution in which the nucleic acid was eluted in). Following this, 2 µl of the sample was directly pipetted onto a fibre optical measurement surface. The purity of the samples as well as nucleic acid concentration was determined by the ND-1000 associated software. No dilution of the sample was necessary as the instrument automatically detects high concentrations and uses the 0.2 mm path length to calculate absorbance.

4.6.8 Plasmid Purification

Phenol/Chloroform Extraction and Phenol Precipitation.

The linearised plasmids (using Acc651) were first purified before use for in-vitro transcription. Solutions used are listed in [Table 17](#).

Table 17: Solutions used for plasmid DNA purification.

Component	Composition
Chloroform	Mixed 24:1 with IAA (IsoAmyl Alcohol)
Ethanol	70 %
Ethanol	99 %
Phenol	
Sodium acetate	3 M pH 5.2

To the linearised DNA sample in a microfuge tube, an equal volume of a 1:1 mixture of phenol/chloroform was added, vortexed immediately and directly spun down for 30 seconds. The top aqueous layer was carefully removed and transferred to a fresh tube, complemented by an equal volume of chloroform and centrifuged as before. The top aqueous layer was again transferred to a fresh tube.

Formatie
Gelöscht

Ethanol Precipitation

1/10 volume of sodium acetate was added to the sample in the microfuge tube, this was then inverted once before adding 2 volumes of 99% Ethanol. The mixture was then incubated for 30 minutes at -80°C (alternatively overnight at 20°C). The sample was then centrifuged at 10,000 g for 10 minutes at 4°C, the supernatant was discarded and 3 volumes of 70% ethanol were added and the samples centrifuged as before. The supernatants were again discarded and the precipitates air dried. The air dried precipitates were resuspended in RNase free water (alternatively Tris-EDTA buffer, pH 8.0) stored at -20°C for later use or used immediately for in-vitro transcription

4.6.9 *In-vitro* Transcription

For in-vitro transcription of the linearised purified plasmids, a T7 MEGAscript® transcription kit was used. The reagents were all thawed on ice and the transcription assembled on the bench to avoid precipitation of the spermidine in the reaction buffer. Immediately before use the reaction buffer was vigorously vortexed to ensure that the spermidine was fully resuspended. The transcription was assembled as shown below to a total volume of 20 µl for each transcript. All the equipment used was RNase free.

Table 18: Solutions required for *in vitro* transcription of template DNA.

Component	Composition	Amount used
Reaction buffer	X10	2 µl
NTP mix	25mM CTP,UTP,ATP and 5 mM GTP	8 µl
GTP cap analog (m7G(5')ppp(5')G)	40 mM	1µl
DNA template	TMVMP:GFP	0,7-2.0 g (maximum volume 7 µl)
T 7 polymerase		2 µl
RNase free water		7 µl minus the template volume

The reaction was assembled on the bench as shown in [Table 18](#); addition of each component was followed by quick centrifugation. When all components had been added, the reaction was incubated at 37 °C for 2 hours.

Formatie
Gelöscht

4.6.10 Verification of the Transcription

A 0.8 % agarose gel was prepared in an RNase free tank. 1 µl each of the transcript and the template were separated by electrophoresis at 100 V for 20 minutes.

4.6.11 Preparation of Plants for Inoculation

The expanding 4 to 6 week old plants at the 6 leaf stage were used; these were approximately 3-5 cm long. The plants were grown and maintained in a greenhouse with a 16/8 h (day /night) photoperiod at 18-25 °C. The leaf petiole was marked using a permanent marker (for later identification of the inoculated leaves). The leaves were cleaned using distilled water. Two thirds of the upper leaf surface was then dusted using silicon carbide powder (grain size 400; Sigma-Aldrich).

4.6.12 Transcript Inoculation

Mechanical inoculation of the plants was conducted as follows. The solution with the transcript was spread the dusted leaf, and gently spread over the leaf surface. The inoculated leaves were then washed with distilled water (rubbing the leaves opens vacuoles which release acids that cause necrosis, washing removes these acids).

The plants were then placed in the green house at 22°C/20°C (day/night) and a 16 h L/8 h D photoperiod and 70% humidity. At 3, 5, 7 and 10 days post inoculation, the lower side of the leaf was examined for determination of successful infection. Infection spots were excised, vacuum-infiltrated with MS medium and examined under the microscope.

4.6.13 Agroinfiltration

Agrobacterium tumefaciens strain LBA 4404 (Life Technologies, Grand Island, NY) harbouring the appropriate plasmids; MP: GFP, MP: RFP, microtubule associated protein 4 (MAP4) and microtubule end binding protein 1 (AtEB1) were cultured as described in Wroblewski *et al.*, (2005), adjusted to an optical

Materials and methods

density at 600 nm of 1.0 and used to infiltrate small leaves of 4-week old tobacco plants. A cut was made on the upper leaf surface, and the culture infiltrated into the leaf with the help of a syringe. The infiltrated area was marked with a permanent marker pen. The plants were then placed under green house conditions of 22/20°C and a 16 h L/8 h D photoperiod for 48 hours before microscopy was carried out.

5 Results

This section presents the results from experiments conducted to assess the relationship between microtubule dynamics and the spread of Tobacco mosaic virus in 7 mutant tobacco lines showing differences in microtubule dynamics and a wild type tobacco plant that did not.

First, the extent of microtubule dynamics was estimated from the dose-response relations of growth on the microtubule disrupting drug EPC.

Further experiments were designed to probe for differences in the relative levels of tyrosinylated and detyrosinylated forms of α -tubulin. It has been shown that detyrosinylated α -tubulin is the abundant form in situations where microtubules are less dynamic (more stable); experiments were therefore conducted to determine the relative levels of these tubulin modifications in mutant and wild type tobacco plants.

The cytoskeletal components, actin and microtubules are known to interact; we therefore visualized actin in addition to microtubules to test for possible effects of microtubule dynamics on actin organization.

To establish whether microtubule dynamics play a role in TMV infection and spread, a viral construct in which the MP was fused to GFP, but still retained infectivity was used to mechanically inoculate plants. Movement of the virus as well as the interaction of MP with cytoskeletal components was assessed by following the movement of the fluorescent MP.

In addition, the mode of viral spread was compared to the virological model system *N. benthamiana*.

Experiments using TMV constructs capable of long distance transport were used to assess differences in susceptibility to TMV between the mutant and wild type plants.

5.1 Microtubule Dynamics and EPC Sensitivity

The *ATER* mutants were selected for Ethyl-N-Phenylcarbamate (EPC) tolerance, which in this case was an attribute of reduced microtubule treadmilling (Ahad *et al.*, 2003). To confirm this and to test, whether there are differences between functionally different microtubule populations, i.e. cortical microtubules in the hypocotyls which are involved in cell expansion versus mitotic arrays in the roots which are involved in cell division, we measured both hypocotyl growth (exclusively based on cell expansion, i.e. cortical microtubules) and root growth (based on both cell division and cell expansion).

Seedlings of the wild type and the 7 tobacco mutants were grown in MS medium containing different concentrations of EPC ranging from 0 μM to 60 μM . The dose response for hypocotyl lengths, as well as plants root growth at 14 days after sowing is shown in [Figure 3](#).

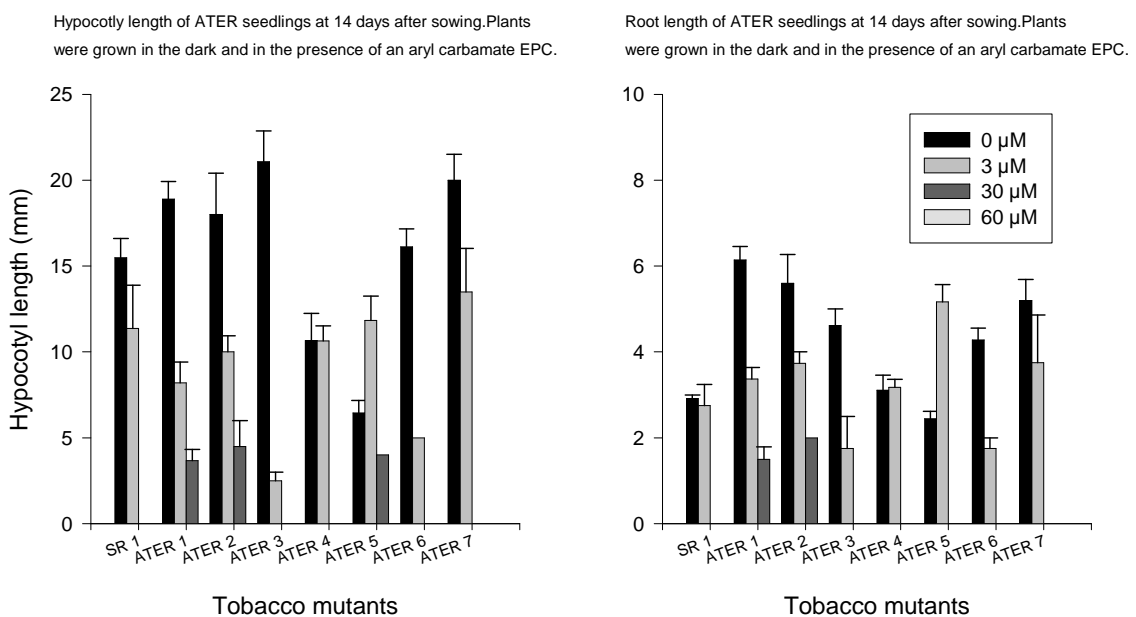


Figure 3: Growth response of tobacco plants to EPC. Mutants show a higher tolerance to EPC concentrations as indicated by growth in both hypocotyls and roots. (20 seedlings per plant were used).

Differences in the growth response of the plants in both hypocotyls and roots are dependent on the EPC concentration and the plant type ([Figure 3](#)). Hypocotyl length was reduced with increasing concentrations of EPC in all the plants. However, it was observed that at a concentration of 30 μM only the

mutants *ATER 1*, *ATER 2* and *ATER 5* were able to grow, indicating a superior tolerance of these plants to EPC as compared to the wild type (SR 1). The study concentrated on *ATER 2* and *ATER 5* even though *ATER 1* appeared promising, as studies by Ahad *et al.*, (2003) implied that *ATER 2* and 5 showed highest tolerance to EPC. Microtubules in *ATER 1* were not cross-tolerant to cold stress. The reduced sensitivity of these mutants could either be due to a reduced treadmilling of microtubules or, alternatively, to a reduced affinity of tubulin for EPC. Therefore, the affinity of tubulin for EPC was directly measured by EPC-affinity chromatography.

5.2 Tyrosinylated and De-Tyrosinylated Tubulin Differ in EPC Affinity

The high tolerance to EPC exhibited by the mutant plants might be caused by reduced affinity of the detyrosinylated α -tubulin that prevails in conditions where microtubule dynamics are reduced. EPC and other microtubule “disrupting” drugs act by interfering with microtubule assembly, i.e. by blocking the addition of tubulin dimers at the growing end of a microtubule. Therefore, alternatively, the tolerance of the *ATER* mutants could be caused by reduced rates of polymerisation and depolymerisation such that the mutants are less sensitive to the block of microtubule assembly that is triggered by EPC. In such plants the levels of detyrosinylated tubulin are expected to be higher than those of tyrosinylated tubulin.

To discriminate between the two possibilities, the affinity was measured by EPC affinity chromatography (Freudenreich and Nick, 1998). Carboxylated EPC was coupled to aminoethyl-sepharose and incubated with soluble protein extract derived from mutant and wild type tobacco (*N.tabacum*) plants. Fractions of the bound proteins were then eluted with increasing ionic strength of KCl. Using SDS PAGE and Coomassie Brilliant Blue (CBB) the fractionalized proteins were stained and visualized [Figure 4](#).

Results

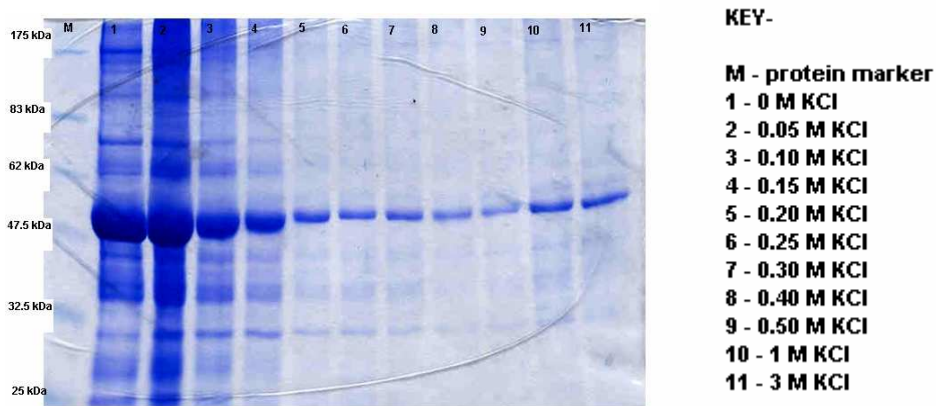


Figure 4: EPC sepharose protein profiling in tobacco. The key shows concentrations of KCl used to elute the protein fractions. A strong tubulin band is observed at approximately 50 kDa.

Figure 4 shows that separation of the protein fractions was successful, unbound proteins are found in the flow-through (lane 1) as well as in lanes 2 -11 where increasing salt concentrations were used to elute the protein. With increasing salt concentrations, there is a reduction in the amounts of proteins eluted as indicated by the weakening signal intensity. Weakly bound protein fractions are eluted first, with low salt concentrations, while the tightly bound proteins require higher salt concentrations for their elution.

Using western blot analysis with the antibodies DM1A and ATT, the eluted protein profiles were probed. With these antibodies, it is possible to distinguish between two populations of α -tubulin with differing affinity to EPC (**Figure 5**).

Results

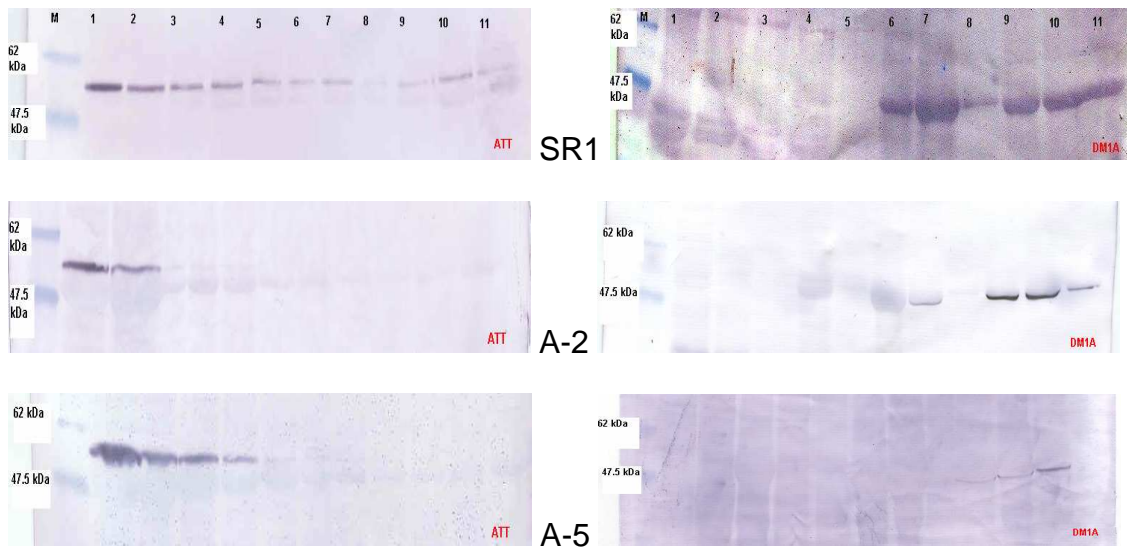


Figure 5: Separation of tyrosinylated and detyrosinylated α tubulin in tobacco. The affinity of tyrosinylated α tubulin to EPC in the wild type is higher than in the mutants, whereas the mutants show a higher affinity of detyrosinylated α tubulin to EPC than the wild type. (Key for lanes M to 11 see Fig 4).

Two distinct protein fractions are obtained. Tyrosinylated α -tubulin, which is recognized by ATT is weakly bound to EPC (and easily eluted by low KCl concentrations) compared to the detyrosinylated α -tubulin (recognized by DM1A) in both mutants and in the wild type. In *ATER 2*, the tyrosinylated α -tubulin is most weakly bound to EPC, no significant amount of tyrosinylated α -tubulin is eluted at concentrations higher than 0.05 M KCl, while that in *SR1* is most strongly bound and requires up to 0.2 M KCl for its elution. The detyrosinylated α -tubulin is more strongly bound and is eluted at high KCl concentrations. In contrast, *ATER 2* has higher amounts of detyrosinylated tubulin compared to *ATER 5* and *SR1* (Figure 5). These results confirm that tyrosinylated and detyrosinylated forms of α -tubulin in tobacco leaves can be distinguished based on their affinity to EPC and that tobacco plants with differing microtubule dynamics also differ in their levels of tyrosinylated and detyrosinylated α -tubulin. They also show that the affinity of detyrosinylated α -tubulin is more pronounced in the mutants as compared to the wild type. In contrast, the affinity of tyrosinylated α -tubulin is reduced (more pronounced in *ATER 2*, less in *ATER 5*). In order to relate these findings to the reduced sensitivity of growth to EPC, it is necessary to compare the relative levels of tyrosinylated versus detyrosinylated α -tubulin in wild type and mutants.

Formatie
Gelöscht

5.3 Determining the Levels of Tyrosinylated and Detyrosinylated Tubulin

We have confirmed that with the use of the antibodies ATT and DM1A it is possible to distinguish between two modifications of α -tubulin and that in the *ATER* mutants and wild type tobacco plants, the tyrosinylated and detyrosinylated α -tubulin differ in their affinity to EPC. In the next step it was tested, whether there was a relationship between microtubule dynamics and the levels of tyrosinylated and detyrosinylated α -tubulin forms

SDS PAGE and Western blot analysis using total protein extracts obtained from tobacco leaves was conducted for each plant type (**Figure 6**), and the relative amounts of tyrosinylated and detyrosinylated α -tubulin in the mutants to that in the wild-type were quantified.

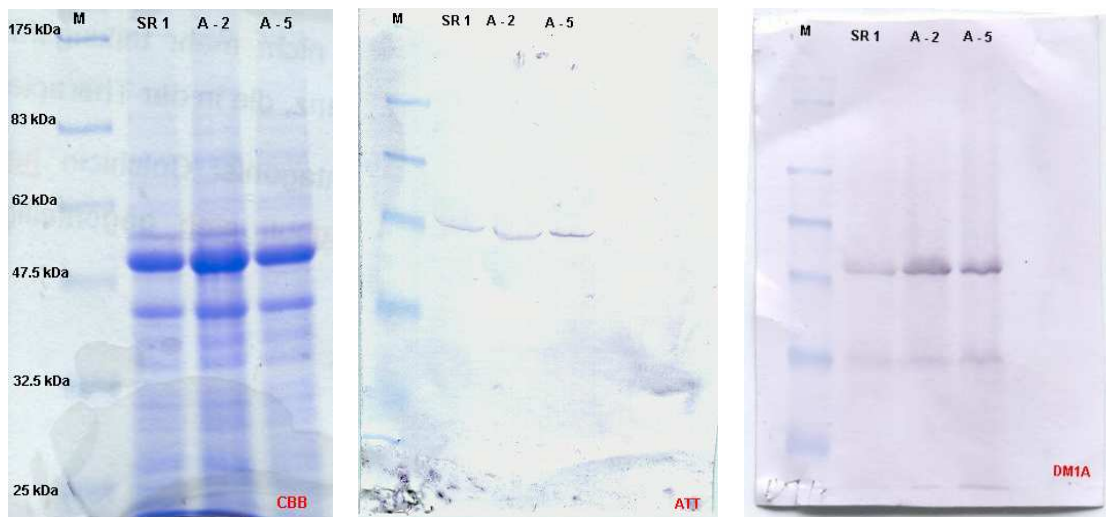


Figure 6: Detection of α tubulin in total protein extracts from leaves. Coomassie Brilliant Blue (CBB) showing equal loading of each lane. Western blot probed using the antibodies ATT and DM1A for detection of tyrosinylated α tubulin and de tyrosinylated α tubulin respectively.

The CBB gel was used as a control to ensure that the total protein loaded in each lane was equal, and hence to provide the basis for comparison of the ATT and DM1A blots.

The signal intensities for both DM1A and ATT probed blots differ among the plants; it is clear that the differences observed in the lanes on the blots is not

due to different amounts/concentrations of the loaded samples as evidenced by the CBB gel.

The signal intensities of the 50-kDa bands observed (tyrosinylated and detyrosinylated tubulin) in the mutants were analysed and related as a percentage to that of the wild type (**Figure 7**).

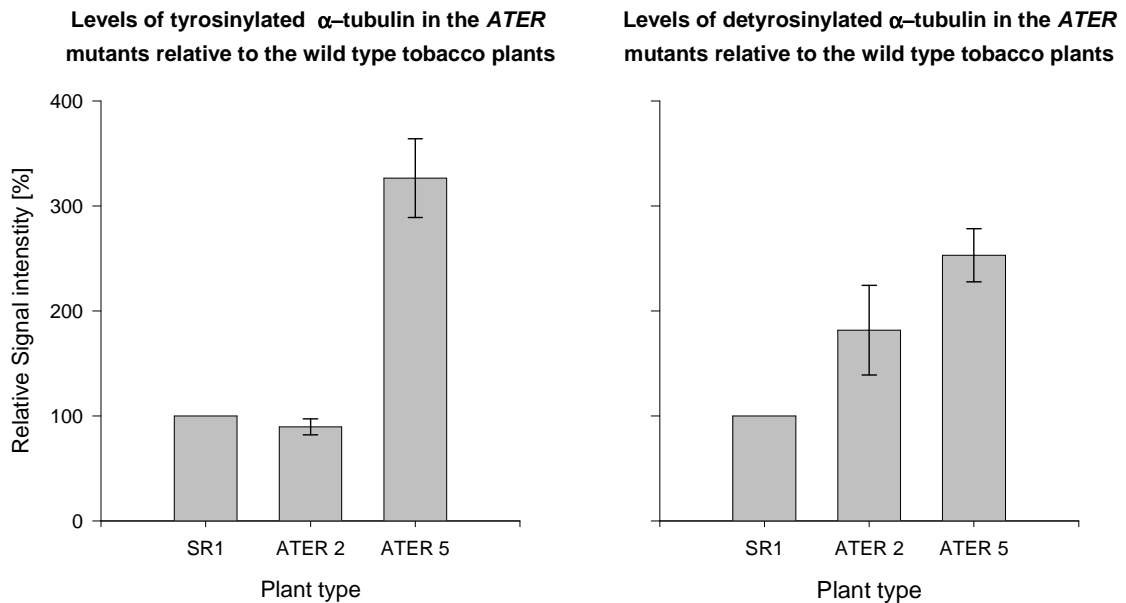


Figure 7: Tyrosinylation levels in mutant and wild type tobacco plants. Detyrosinylation levels are related to microtubule dynamics. (n =16 for ATT and n = 10 for DM1A).

An increase in the level of detyrosinylated tubulin (determined using the antibody DM1A) in the following order SR1, ATER 2, ATER 5 was noticed. Tyrosinylated tubulin (determined using the antibody ATT) was not increased as compared to the wild type in ATER 2, but strongly elevated in the mutant ATER 5 relative to both the wild type and ATER 2.

In the mutant ATER 2, the amount of detyrosinylated α -tubulin was higher, whereas the abundance of tyrosinylated α -tubulin was not altered as compared to the wild type. Therefore, in ATER 2, α -tubulin is clearly shifted from the tyrosinylated into the detyrosinylated form. Therefore, the contribution of the higher EPC-affinity of detyrosinylated α -tubulin (**Figure 5**) is expected to be dominant in comparison to the reduced EPC-affinity of tyrosinylated α -tubulin. Thus, the reduced EPC-sensitivity of growth in ATER 2 cannot be attributed to a generally reduced affinity of α -tubulin for this inhibitor.

The situation in *ATER 5* is more complex. Here, both forms of tubulin are strongly elevated as compared to the wild type. The relative increases (around a factor of 2.5) are comparable though, which means that the ratio between tyrosinylated and detyrosinylated α -tubulin is not altered as compared to the wild type. The affinity of tyrosinylated tubulin is comparable to that of the wild type (Fig. 3), that of the detyrosinylated tubulin is, however, increased even stronger than in case of *ATER 2*. Therefore, the impact of the reduced EPC-affinity of tyrosinylated tubulin on the EPC-sensitivity of growth is expected to be minor as compared to the effect of detyrosinylated tubulin. This means, again, that the reduced EPC-sensitivity of growth in *ATER 5* cannot be explained in terms of a globally reduced affinity of α -tubulin for EPC. However, in contrast to *ATER 2*, it might be the consequence of a generally increased abundance of α -tubulin (by a factor of 2.5).

Since the situation in *ATER 2* was clearer, we focussed in the following on this mutant, although *ATER 5* was tested in parallel.

5.4 Microtubule Orientation in the *ATER* mutants

The stability of cortical microtubules in maize coleoptiles has been shown to depend on their orientation (Nick *et al.*, 2002). To test whether this applied to the *ATER* mutants, immunolabelling experiments were conducted to visualize the microtubule network. **Figure 8** shows exemplarily the cortical microtubule network in epidermal cells of leaf petioles in the tobacco plants examined.

Formatie
Gelöscht

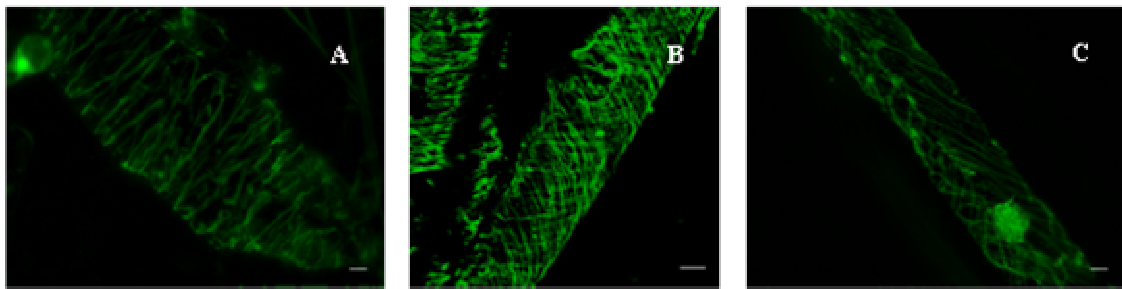


Figure 8: Cortical microtubules in epidermal cells of *N. tabacum*. Indirect Immunolocalization of microtubules was done using the anti α -tubulin antibody ATT. Oblique microtubules are visible in SR 1 (A), *ATER* 2 (B) and *ATER* 5 (C); these show no uniformity in their alignment (angle of orientation). Scale bars = 10 μ m.

To assess, whether there were significant differences in microtubule orientation between wild type and *ATER* mutants, the frequency of occurrence of microtubules showing a specific orientation was analyzed.

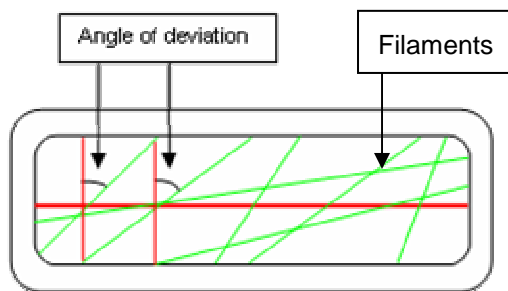


Figure 9: Schematic representation of an epidermal cell showing cytoskeletal filaments (green lines). The alignment of the filaments (microtubules in this case) was determined by calculating the angle of deviation (arrows) of the filaments from the long axis of the cell.

A schematic interpretation of how microtubule orientation was measured is shown in [Figure 9](#).

Formatie

Gelöscht

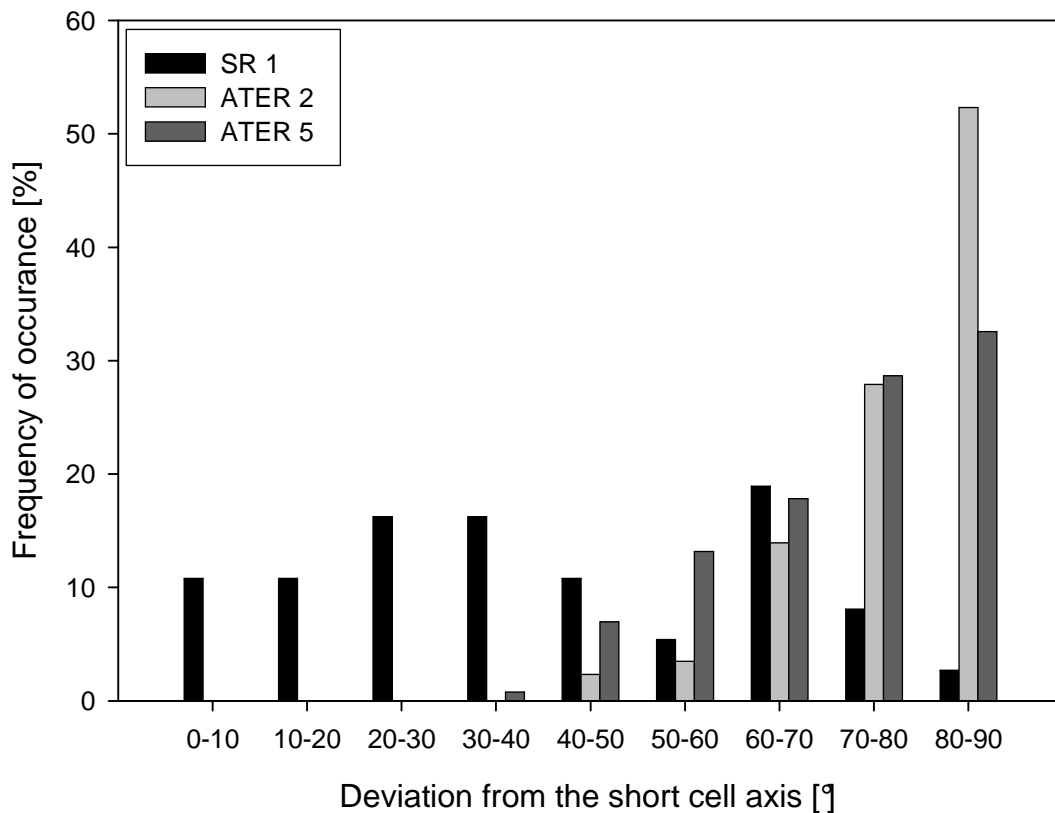
Cortical microtubule orientation in epidermal cells of tobacco (*N. tabacum*)

Figure 10: Cortical microtubule orientation in tobacco. In the mutants, the frequency by which longitudinal trending microtubules occur is higher than in the wild type. ATER 2 had a higher number of cells with longitudinal microtubules ($n = 56, 85,$ and 73 for SR1, ATER 2 and ATER 5 respectively).

Both mutants and the wild type have longitudinal and transverse microtubules. However the mutants have a greater number of microtubules that deviate from the short cell axis as compared to the wild type, which means that there are more longitudinal microtubule arrays in the mutants, which was most pronounced in ATER 2, while SR1 had the highest number of transverse inclined microtubules (Figure 10).

The results show that there is a correlation between microtubule orientation and reduced microtubule dynamics (enhanced microtubule stability).

Formatie
Gelöscht

5.5 Actin Orientation in the *ATER* mutants

In both, plants and animals, actin filaments are known to interact with microtubules (Heil-Chapdelaine *et al.*, 1999; Goode *et al.*, 2000; Bisgroove *et al.*, 2004). The extent of this interaction is, however, not known. It was of interest therefore to check whether the reduced microtubule dynamics (stable microtubules) exhibited by the *ATER* mutants are accompanied by alterations of the actin filament network. Actin labelling experiments using FITC Phalloidin were designed to reveal the structure and orientation of actin filaments in epidermal cells of *N. tabacum* (Figure 11).

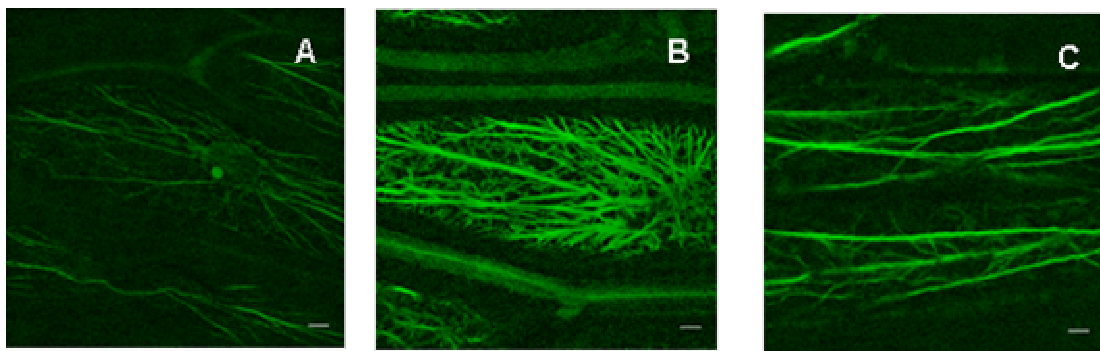


Figure 11: Actin filament orientation in epidermal cells of *N. tabacum*. Actin Filaments were stained using FITC phalloidin. Differing populations of transverse and longitudinally oriented filaments are present in SR1 (A), ATER 2 (B) and ATER 5 (C). Scale bars = 10 μ m.

Similar to microtubules, mixed populations of longitudinally and transverse inclined filaments were observed. The orientation of filaments was observed to differ between the plants. To elucidate the significance of these differences, frequency distributions over the orientation of actin filaments were constructed (Figure 12).

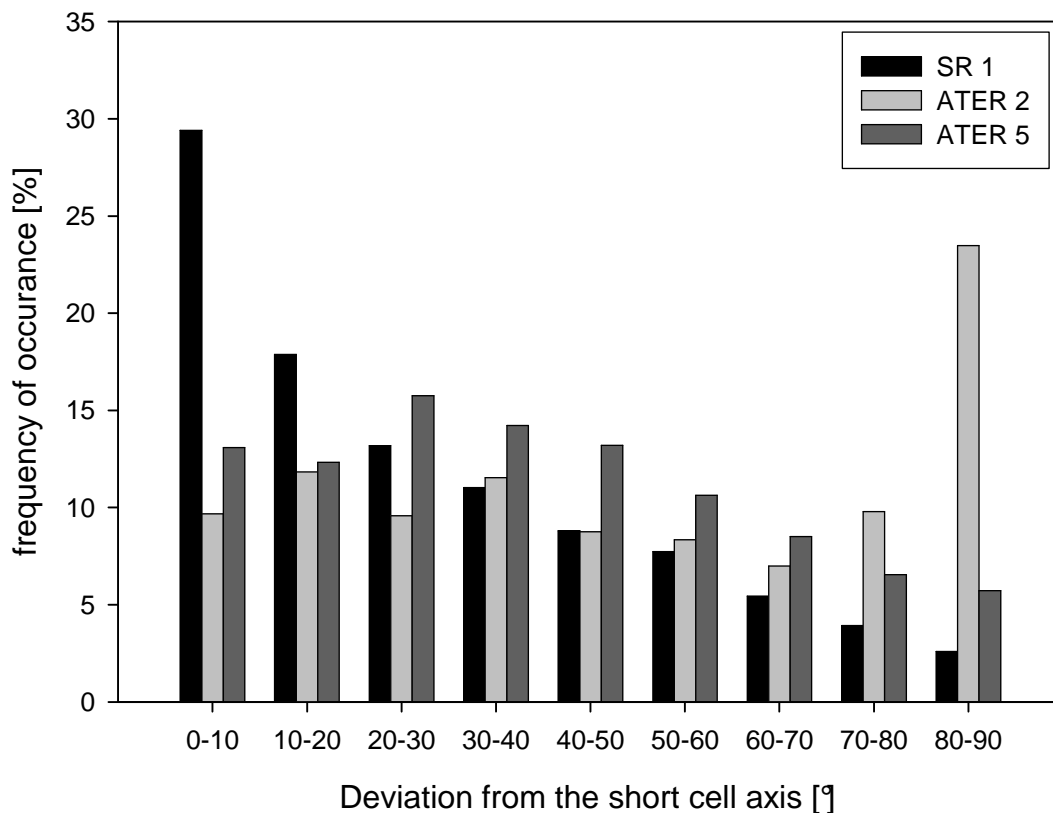
Actin filament orientation in epidermal cells of tobacco (*N. tabacum*)

Figure 12: Orientation of actin filament in epidermal cells of *N. tabacum*. Differences in orientation are related to plant type. *ATER 2* has the highest number of longitudinally oriented actin filaments whereas *SR1* has the lowest. (n =1577 cells for mutants and 868 for the wild type).

In *SR1*, cells with actin filaments that were transverse occurred with the highest frequency, with increasing angle of deviation the frequencies decreased. Both mutants had a higher incidence of cells with longitudinally inclined filaments compared to the wild type. The highest incidence of longitudinally inclined cells was observed in *ATER 2*. The *ATER 2* plants also had the least number of cells in which the actin filaments were transversely oriented. In *ATER 5*, the incidence of orientation of the actin filaments in the cells was intermediate to that of *ATER 2* and the wild type.

Based on the frequency distribution over orientation, these results suggest that in tobacco plants, the angle of orientation of actin filaments can be correlated to microtubule stability and in consequence to microtubule dynamics.

5.6 Spread of TMV in Mutants with Reduced Microtubule Dynamics

Successful infection of TMV in a systemic host such as *N. tabacum* requires inoculation followed by movement of the viral RNA from cell to cell. It has been suggested that microtubules play a significant role in this process. A series of experiments were therefore conducted to measure the extent to which the spread of TMV is influenced by the altered microtubules in the *ATER*-mutants. Using a TMV viral construct in which the MP is coupled to GFP but still retains infectivity, 4 week old tobacco plants were mechanically inoculated with the virus. Successful inoculation and infection in tobacco was evidenced by fluorescent “halo”-shaped rings [Figure 13](#).

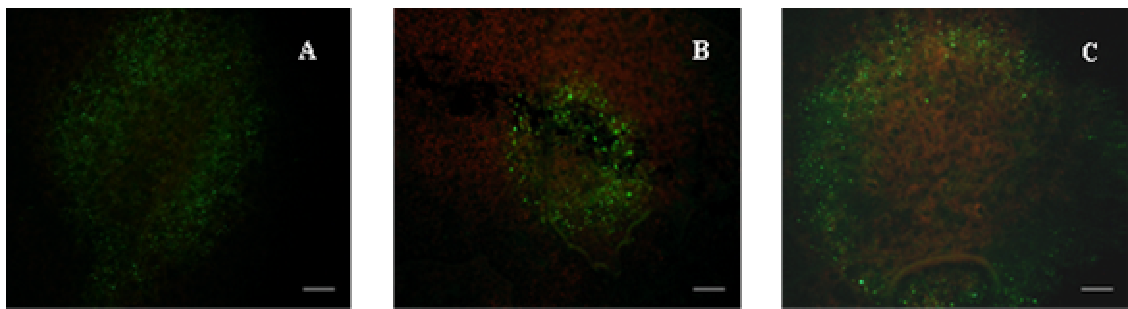


Figure 13 Successful inoculation of SR1 (A), ATER 2 (B) and ATER 5 (C) using an in vitro transcript of TMVMP:GFP. The MP spreads at the leading edge and is degraded at the trailing edge resulting in the formation of a fluorescent band. Successful infection and spread was observed in all plants. Scale bar = 0.1 mm

The green fluorescent band indicates the presence of MP:GFP while the red colour at the centre of the ring is due to leaf chlorophyll autofluorescence.

[Figure 13](#) shows that in both mutants and the wild types the inoculation was successful, and that the virus encoded MP:GFP spreads outwards from the centre of infection.

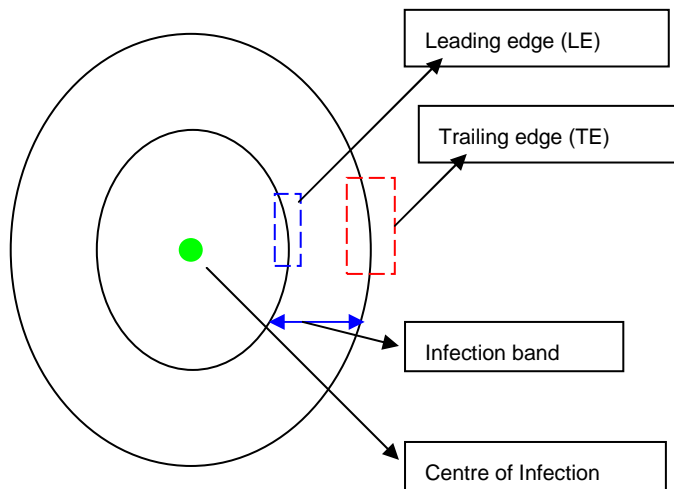


Figure 14: Schematic representation of TMVMP:GFP spread following successful inoculation.

The fluorescent infection band has an internal and external boundary (**Figure 14**). At the outer boundary (leading edge of infection) of the band, a stronger fluorescence is observed compared to the inner boundary (trailing edge of infection) (**Figure 15**).

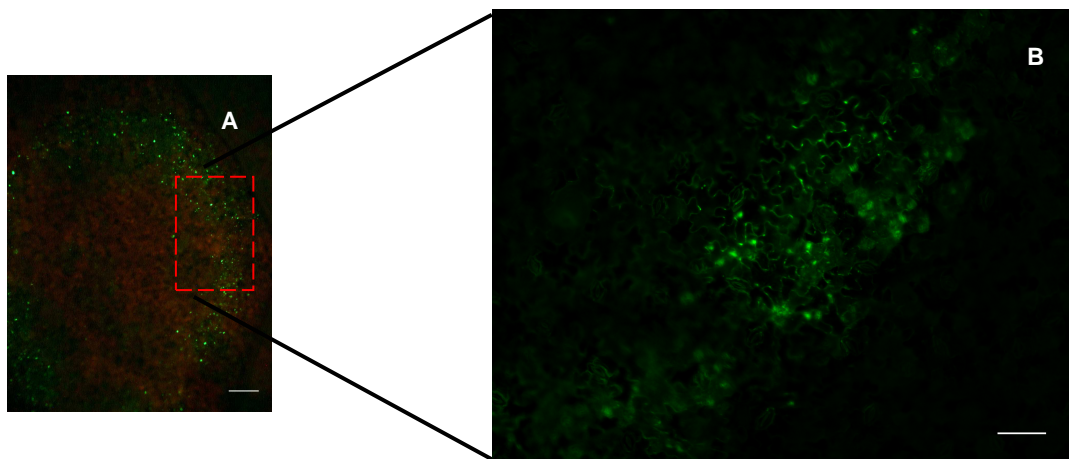


Figure 15: Infection band in tobacco plants showing direction of spread of the MP:GFP as indicated by increasing fluorescence towards the outer boundary. Plants were inoculated with an *in vitro* transcript of TMVMP:GFP. Scale bars A =0.1 μ m, B= 10 μ m

The fluorescence intensity indicates the direction in which the MP:GFP is moving. The movement of the virus was elucidated by following the movement of the virus encoded MP:GFP.

Results

To test, whether viral movement is influenced by microtubule dynamics, the width of the infection band in plants with differing microtubule dynamics was analyzed by calculating the difference between the diameter of the internal ring and that of the external ring. Measurements were taken at 5 and 7 days post inoculation (dpi).

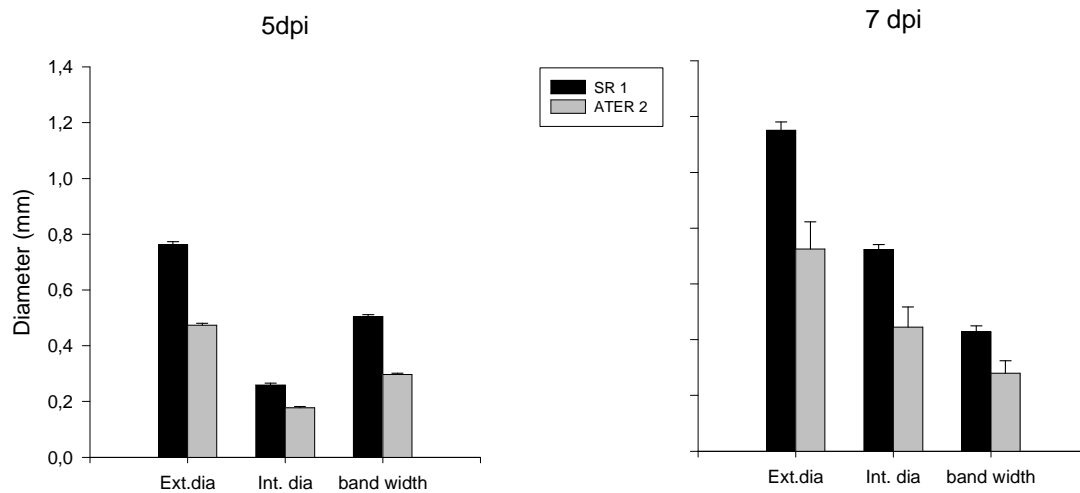


Figure 16: TMVMP:GFP movement in tobacco. Differences in TMV movement are dependent on microtubule dynamics. MP: GFP spreads at a constant rate (Ext dia. - External diameter, Int dia. - Internal diameter) n= 39 and 33 respectively for SR1 and ATER 2 at 5dpi. At 7 dpi n = 19 and 10 for SR1 and ATER 2 respectively).

It was observed that in the wild type the infection band was broader than in the mutants. In *ATER 2* the band was thinnest, and intermediate in *ATER 5* (data not shown) at both 5 and 7dpi ([Figure 16](#)).

An increase in both internal and external diameters of the fluorescent band in all the plants between 5 dpi and 7 dpi was observed, (0.2 mm/day in SR1 and 0.15 mm/day in *ATER 2*), the width of the fluorescent band however did not differ significantly.

The results demonstrate that the spread of TMV in *N. tabacum* is altered in the *ATER* mutants indicating a role of microtubule dynamics on viral movement.

5.7 Intracellular Localisation of TMV

5.7.1 Are Microtubules Involved in the Spread of TMV?

The actin network as well as microtubules and ER bodies have all been suggested to play a role in the spread of TMV. To study the movement of the virus and its interaction with cytoskeleton components, we made observations of the intercellular movement of TMV in tobacco plants with differing microtubule dynamics.

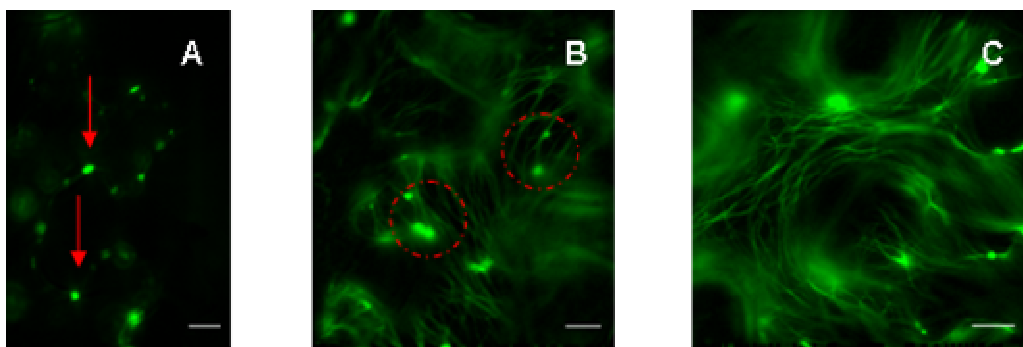


Figure 17: Intracellular localization of TMVMP:GFP in epidermal cells of tobacco (*Nicotiana benthamiana*) at 5 dpi. Localisation at the leading edge of infection (A) middle edge (B) and the trailing edge (C). Arrows show plasmodesmata labelling, circles show aggregation of ER inclusion bodies. Scale bars = 10 μm .

Figure 17, shows localization of TMV-MP:GFP in *Nicotiana benthamiana* with different cytoskeletal components. At the leading edge of infection the MP associates with the plasmodesmata (Pd). At the middle edge of infection single and aggregated ER inclusion bodies are seen; in addition the MP labels Pd and microtubules. At the trailing edge, there is reduced Pd labelling and enhanced association of MP with microtubules. Observations such as these have led to the view that microtubules are not involved in the spread of TMV (Padgett *et al.*, 1996), since TMV spread occurs at the leading edge and as shown in our study microtubule labelling in *N. benthamiana* does not occur at the leading edge. It has therefore been suggested that microtubules play a deciding role only at the trailing edge of infection where MP degradation occurs (Padgett *et al.*, 1996; Reichel and Beachy, 1998; Más and Beachy, 1999; for review, see Tzfira *et al.*, 2000).

Formatie
Gelöscht

Viral spread is host dependant; this implies that host specific factors play a significant role in TMV spread. Comparisons were made between the spread of TMV in *N. benthamiana* and that in *N. tabacum*.

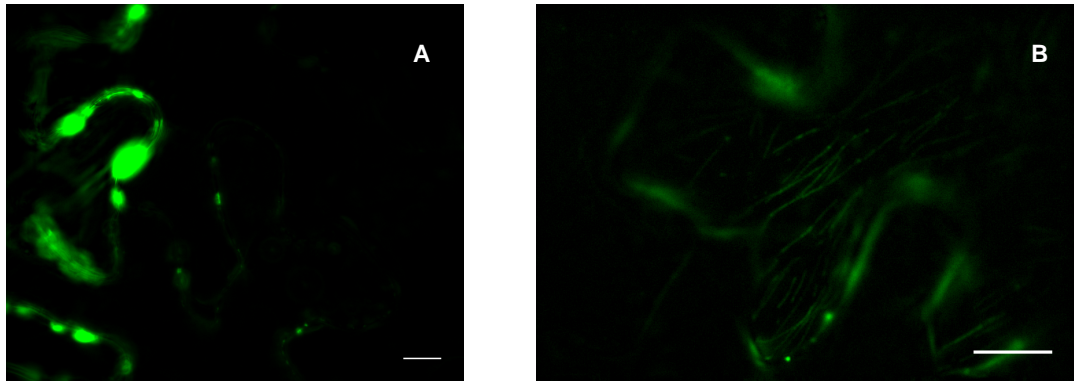


Figure 18: Differences in MP localization between *N. tabacum* and *N. benthamiana* at the leading edge 5 dpi. Plasmodesmata labelling in *N. benthamiana* (A). Plasmodesmata labelling and association of MP with microtubules in *N. tabacum* (B). TMV interaction with cytoskeleton components differs in *N. tabacum* and *N. benthamiana* Plants were inoculated with an *in-vitro* transcript of TMV-MP: GFP. Scale bars = 10 µm.

In *N. tabacum*, the association of MP:GFP with cytoskeleton components differs to that of *N. benthamiana* in one major aspect. At the leading edge of infection association of microtubules with MP is observed in *N. tabacum*, whereas in *N. benthamiana* at this stage only Pd labelling is visible (**Figure 18**).

It has been suggested that in *N. benthamiana* microtubules do not play a role in cell to cell spread of TMV, because of the lack of microtubule labelling at the leading edge of infection at either 3 dpi or 5 dpi. A series of experiments was conducted to investigate this phenomenon.

Formatie
Gelöscht

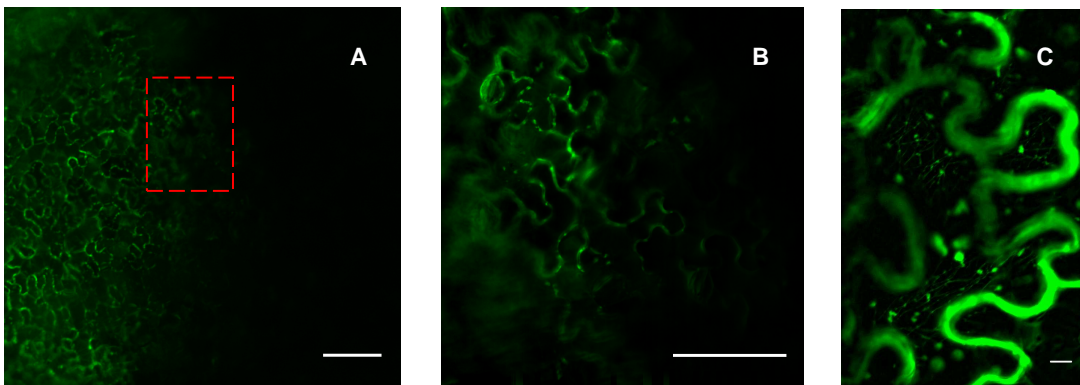


Figure 19: MP labelling at the leading edge of infection in *N. benthamiana* plants 10 dpi. The outlined area in (A) shows the leading edge, a close up view reveals plasmodesmatal labelling (B) and microtubule associations (C). Microtubule labelling in *N. benthamiana* at the leading edge of infection occurs late in infection. Plants were inoculated with in vitro transcripts of TMV-MP:GFP. Scale bars in A and B = 100µm and 10 µm in C.

Observations made at 10 dpi in *N. benthamiana* revealed microtubule labelling at the leading edge of infection, thereby suggesting a role for microtubule in the spread of TMV (**Figure 19**) could be further investigated.

In *N. tabacum*, microtubule labelling at the leading edge occurs earlier (5 dpi) than in *N. benthamiana* (10 dpi). This suggests that the interaction of the virus with the cytoskeletal host components differs between *N. tabacum* and *N. benthamiana*.

5.7.2 TMV:MP Association during TMV Spread in Tobacco.

With the leading edge as the focus of attention (since spread occurs in this region), *N. tabacum* plants with differing microtubule dynamics were studied with the aim of elucidating, whether the rate of microtubule treadmilling has an influence on TMV spread.

The plants were mechanically inoculated with TMV-MP:GFP, and at 7 dpi association of MP with cytoskeleton components was studied using fluorescence microscopy.

Formatie
Gelöscht

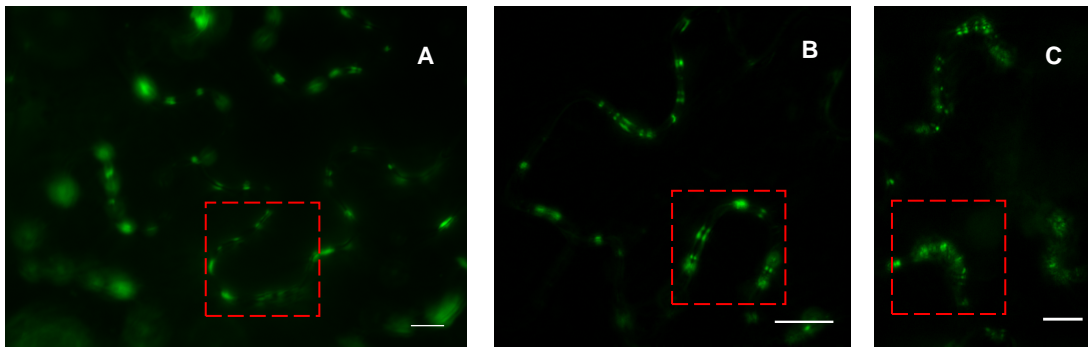


Figure 20: Pd labelling at the leading edge in *N. tabacum*. Higher amount of plasmodesmata labelling occurs in SR1 (A) in comparison to *ATER 2* (B) and *ATER 5* (C). Red squares show Plasmodesmata labelling. Plants were inoculated with an *in-vitro* transcript of TMVMP:GFP. Bars 0 10 μ m.

Association of MP with the Pd is indicated by the fluorescence spots at the edge of the cell wall. At the leading edge of infection, a stronger Pd labelling was exhibited by the wild type compared to the mutants (**Figure 20**). This raises the question, whether this response is influenced by microtubule dynamics.

ER inclusion bodies are recognized as the sites where virus replication occurs. It has been suggested that microtubules are involved in conveying this viral complex through the Pd. To study this aspect, MP association with ER inclusion bodies was analysed at the leading and middle edge of infection.

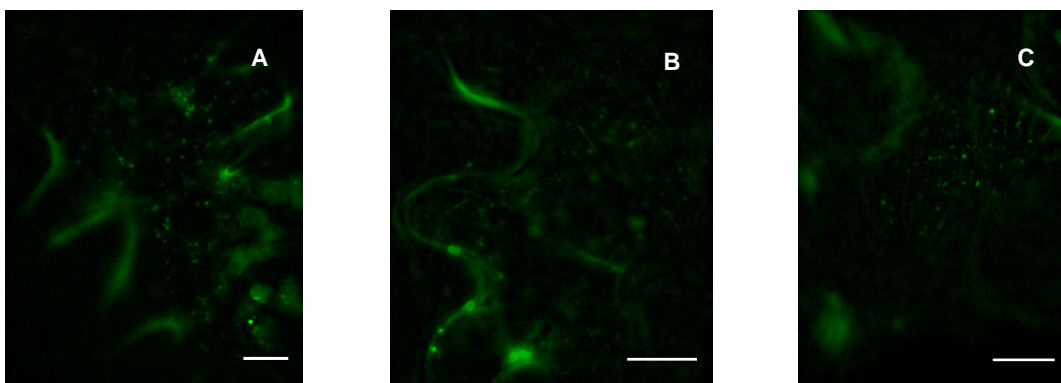


Figure 21: Association of MP with ER inclusion bodies at the middle edge of infection in *N. tabacum*. Most localisation observed in SR1 (A) and the least in *ATER 2*(B); *ATER 5* shows intermediate localisation (C). Plants were inoculated with an *in-vitro* transcript of TMV-MP:GFP. Scale bars = 10 μ m.

At the middle edge of infection, the ER bodies were observed to be most numerous in the wild type, the mutants showed reduced association of MP with

these bodies. The least amount of association of the MP with the ER bodies was observed in *ATER 2* mutant ([Figure 21](#)).

In both *ATER 2* and *ATER 5*, MP association with microtubules was observed as early as the leading edge of infection. However, in SR1 microtubule labelling was first observed at the middle edge of infection ([Figure 22](#)), which corresponds to the movement pattern observed in *N. benthamiana* ([Figure 17](#)).

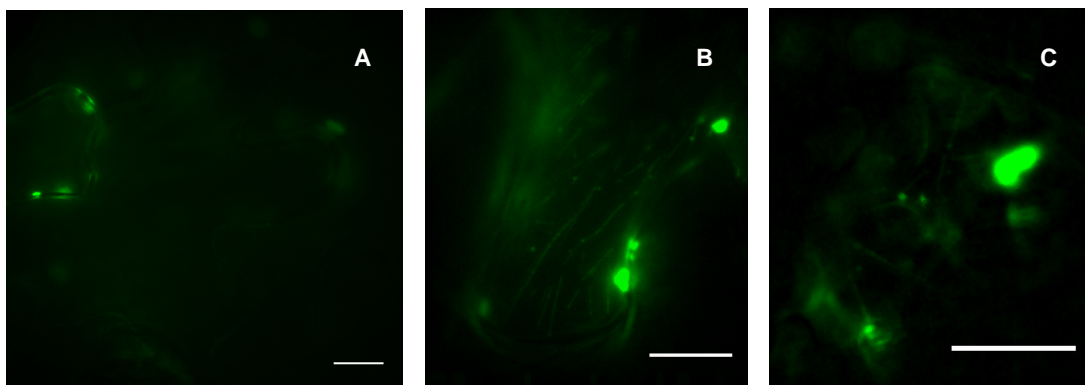


Figure 22: Association of MP with microtubules at the leading edge of infection in *N. tabacum*. In the *ATER 2* (B) and *ATER 5* (C) the MP associates with microtubules whereas in SR1 (A) this does not happen at this stage. Plants were inoculated with an *in vitro* transcript of TMVMP:GFP. Scale bars = 10µm

The most prominent association of MP with microtubules was observed in *ATER 2*; there was less MP-MT localisation in *ATER 5* and none at all in SR1 at the leading edge of infection.

Therefore, in tobacco mutants with reduced microtubule dynamics, the association of MP with microtubules network commences earlier as in the wild type.

5.8 TMV:MP Intracellular Association in the Absence of Viral Infection

To study the interaction of MP with cytoskeleton components in the absence of viral infection, a construct in which the 30 kDa MP of TMV was coupled to GFP, and driven by the 35S promoter of the CaMV was used. This was agro-infiltrated into the leaves of *N. tabacum* plants. 48h later the intracellular localization of the MP in the epidermis was traced.

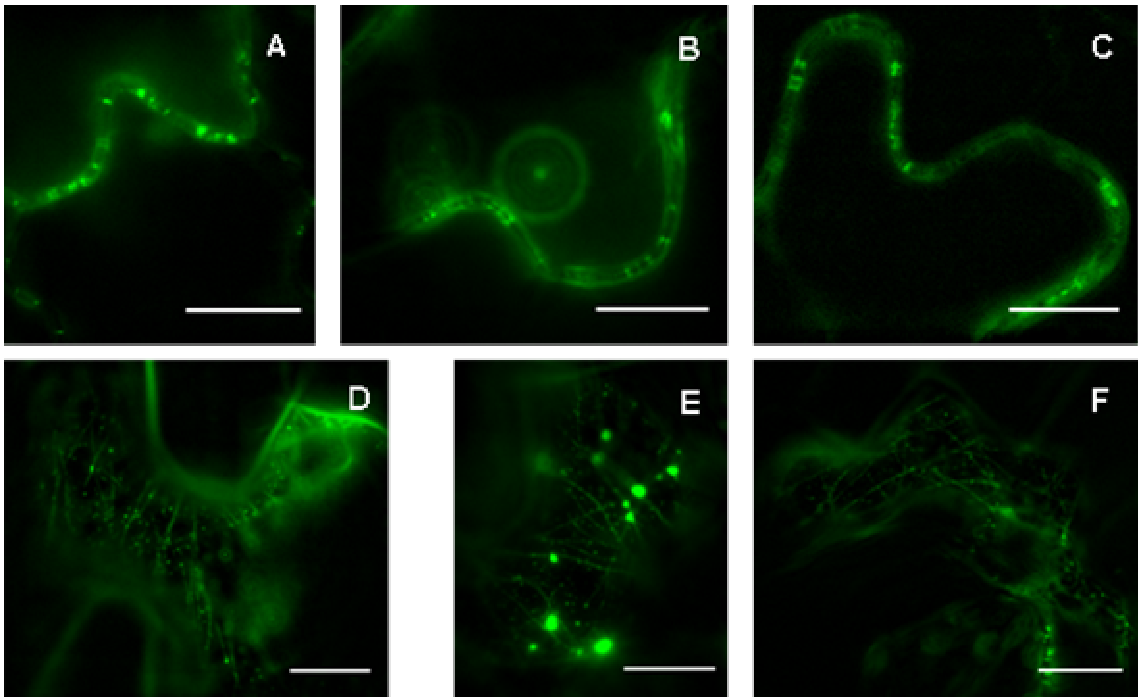


Figure 23: Intracellular localization of MP in *N. tabacum* in the absence of viral infection. MP associates with the plasmodesmata in SR1 (A), ATER 2 (B) and ATER 5, as well as with their microtubules D, E and F respectively. Plants were agro-infiltrated with MP:GFP and observed after 48 h. Scale bars = 10 μ m.

Even in the absence of viral infection, the MP still associates with plasmodesmata, microtubules and small punctae lying along or close to microtubules (**Figure 23**). These associations are similar to those observed when plants were inoculated with TMV-MP:GFP. Thus implying that the mobility of MP is independent of viral infection or viral associated factors.

To confirm whether the filamentous associations observed during the experiments were indeed microtubules, a tubulin marker, MAP4 fused to red fluorescent protein, was co agroinfiltrated with MP:GFP (green).

Formatie
Gelöscht

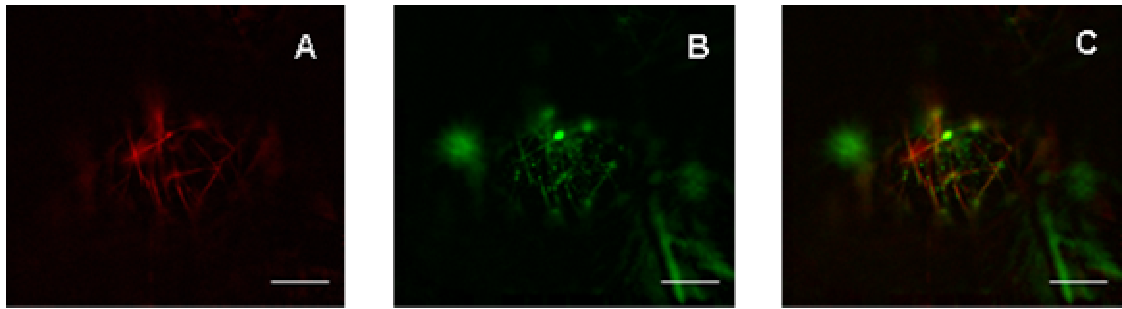


Figure 24: Visualization of filaments in leaf epidermis of *N. tabacum* plants following co-agrofiltration with a microtubule marker MAP4 (A) and the 30-kDa TMVMP coupled to GFP (B). An overlay of the A and B shows a 100% merge of the filamentous structures labelled by MP:GFP are indeed microtubules(C).

MAP4 is a well-known microtubule marker and was used in this case as a control. MP:GFP has been shown to associate with filamentous structures both in the presence and absence of viral infection. [Figure 24](#) shows that MAP4 and MP:GFP label microtubules. An overlay of the two images shows a 100% merge and reveals that the filamentous structures observed using MP:GFP are indeed microtubules.

5.9 ATER Mutants are Less Susceptible to TMV Infection.

Using a plasmid construct that carries the full length TMV cDNA, experiments were designed to establish the impact of microtubule dynamics on the long distance movement of TMV. At 4 weeks the mutant plants as well as the wild type were mechanically inoculated using the viral construct as described in.4.6.3

[Figure 26](#) shows necrosis levels of SR1, ATER 2 and ATER 5 at 6 weeks post inoculation.

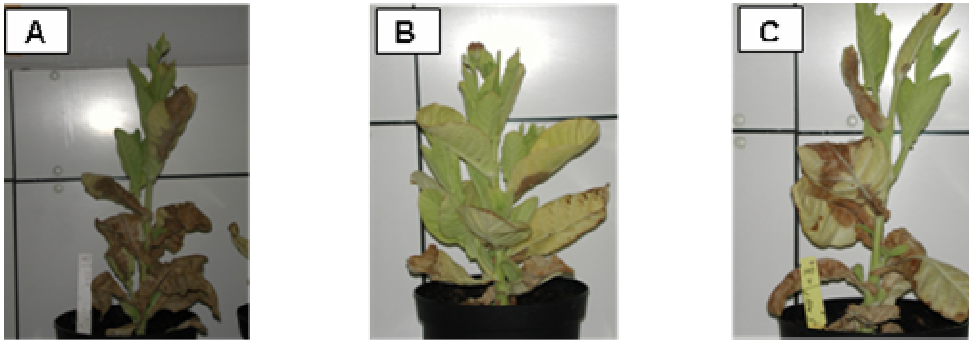


Figure 25: Tobacco plants infected with TMV at 6 weeks post inoculation. Severity of necrosis is most pronounced in SR1 (A), less in *ATER 5* (C) and the least in *ATER 2* (B). Thus, symptom expression in mutant plants with reduced microtubule dynamics is reduced than in the wild type. Plants were inoculated with TLW3 transcript which carries the full length ToMV cDNA.

Symptom expression as indicated by the level of necrosis was highest in the SR1 and lowest in *ATER 2*. *ATER* mutants appear to be less susceptible to TMV infection compared to the wild-type.

Necrosis levels in tobacco (*N. tabacum*) plants infected with TMV

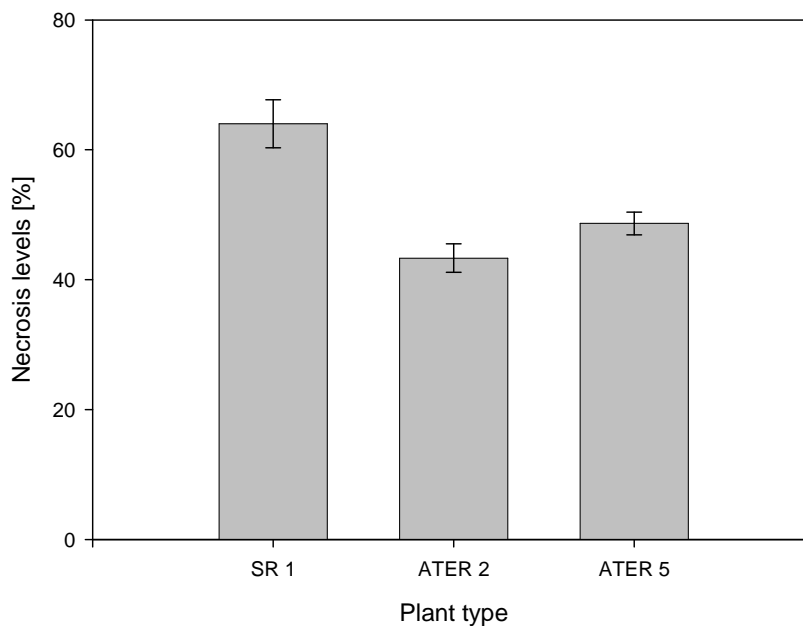


Figure 26: Symptom expression in *N. tabacum* at 6 weeks post inoculation. Mutants show slower disease progression (5 independent experimental series were conducted).

Figure 26 shows quantified data of the symptom expression (necrosis) as a percentage of the total plant i.e. number of leaves showing more than 50 % necrosis as a percentage of the total number of leaves that the plant had. *ATER*

Formatie
Gelöscht

5 showed intermediate symptom expression when compared to SR1 and *ATER* 2.

From these results we can see that the mutant plants with reduced microtubule dynamics are less susceptible (more resistant) to TMV infection, since disease progression as indicated by symptom levels is lower in these plants.

5.10 Summary of the Results

To gain an insight into the impact of microtubule dynamics on the sensitivity to a microtubule disassembly drug EPC, 7 tobacco mutants with reduced microtubule dynamics were grown under increasing concentrations of EPC and their growth monitored over a 14 day period. Mutant plants were less sensitive to high concentrations of EPC. The mutants *ATER* 1, *ATER* 2 and *ATER* 5 showed highest tolerance to EPC.

To test whether the tolerance to EPC was caused by a reduced affinity of α -tubulin for this inhibitor, the affinity of α -tubulins was measured directly using EPC affinity chromatography in the mutant lines *ATER* 2 and *ATER* 5, and in the wild type tobacco plants. In *ATER* 2, the tolerance to EPC could not be explained by a reduced affinity of α -tubulins. In fact, the α -tubulin is mostly present as de-tyrosinylated tubulin (indicative of reduced turnover of microtubules) with increased affinity for EPC. In *ATER* 5, the situation seems to be more complex. Here, the increased tolerance to EPC is accompanied by a 2.5-fold upregulation of α -tubulin expression whereby the ratio between de-tyrosinylated tubulin and tyrosinylated tubulin seems to be unchanged. Therefore, in *ATER* 2, the increased physiological tolerance to EPC can be clearly attributed to a reduced treadmilling of microtubules. A similar conclusion, however, not as straightforward, can be drawn for *ATER* 5.

It has been suggested that the stability of microtubules is dependent on their orientation (Nick *et al.*, 2002). In order to test this, microtubules in mutants with stable microtubules were visualized via immunolabelling experiments. It was

shown that the mutants have a higher percentage of longitudinally inclined microtubules.

Not much is known about the association of microtubules with actin filaments. To establish whether a correlation exists between the two components, actin filaments were visualized in *ATER 2* and *ATER 5*, where microtubule dynamics is reduced. Mutant plants had a higher percentage of longitudinally oriented actin filaments.

In order to study the impact of microtubule dynamics on TMV spread, mutant and wild type plants were mechanically inoculated with TMVMP:GFP, a viral construct that allows visualization of viral movement (through the coupling of MP to GFP). It was also possible to follow association of the MP with cytoskeletal components.

Mutant plants were susceptible to TMV infection inspite of their reduced microtubule dynamics.

The MP of TMV associates with microtubules in both *N. tabacum* and *N. benthamiana*, this association commences earlier in *N. tabacum* as compared to *N. benthamiana*.

MP also localizes to plasmodesmata, however, in the mutant plants tested this association is not as pronounced as in the wild type plants.

At the middle edge of infection, association of MP with ER bodies was stronger in the wild type as compared to the mutant plants.

Using a microtubule marker (MAP4:RFP) and MP:GFP, it was possible to confirm via co-agroinfiltration that the filaments observed associating with MP when plants were inoculated with the TMVMP:GFP transcript were indeed microtubules.

To establish whether the mutant plants with their reduced microtubule dynamics had a comparative advantage with regard to TMV infection and spread, a TMV viral construct capable of long distance transport was used to mechanically inoculate mutant and wild type tobacco plants. Mutant plants with reduced microtubule turnover show less susceptibility to TMV infection.

6 Discussion

Once a plant becomes infected with TMV, it will always harbour the virus. No measures exist to eliminate TMV. An effective means of control once TMV has set in can be accomplished through resistance.

It has been shown that microtubules are involved in the spread of TMV (Gillespie *et al.*, 2002; Heinlein *et al.*, 1995, 1998). The nature of their involvement is, however, not known. It is therefore plausible that disruption in the ability of microtubules to distribute the virus would confer a comparative advantage to plants infected with TMV.

In this section, I shall first discuss some physiological and biochemical properties of the *N. tabacum* plants with reduced microtubule dynamics. I then consider the impact of these changes in microtubule dynamics on α -tubulin levels and affinity to Ethyl-N-phenylcarbamate (EPC). In the final part the question of the role of microtubule dynamics in the spread of TMV is discussed. At the end of I present a model on a possible movement mechanism of TMV-MP complex via microtubule treadmilling.

6.1 Resistance to EPC is Dependant on Microtubule Dynamics

Microtubules play an important role in key cell processes such as cell division, organelle transport etc, and as such are a tempting target for herbicides. EPC is a common herbicide that is also used as a microtubule disrupting drug; it functions by binding to tubulin heterodimers and thus prevents their addition to the growing end of a microtubule (Mizuno and Suzaki, 1991). This has the effect of limiting polymerization. However since depolymerization proceeds, the microtubules become shorter and eventually disappear. Microtubule disrupting drugs are therefore in essence blockers of microtubule assembly.

It has been suggested that the response of plant shoots and roots to various stimuli such as auxin is dependent on the microtubule array in these tissues. In this study, tobacco seedlings with reduced microtubule dynamics were used in combination with EPC to study growth response of shoots and roots to anti-microtubular drugs, as well as look at the sensitivity of microtubule driven functions such as cell elongation and cell expansion to EPC. In rice, EPC was observed to affect normal seedling development. EPC interfered with cell elongation and this in turn limited coleoptile growth. It was also observed that EPC affected auxin dependent growth processes (Nick *et al.*, 1994).

EPC functions by interfering with microtubule assembly. Microtubules with low turnover are therefore expected to be less sensitive to microtubule blockers, because they can better tolerate the reduced microtubule assembly caused by the drugs (Wiesler *et al.*, 2002).

EPC interferes with plant germination and growth by blocking normal microtubule functioning. Germination is only hindered at high EPC concentrations, whereas at low concentrations only growth is affected.

In all the plants tested, shoots and roots show a dose-related response to EPC, implying that, mitotic arrays (responsible for cell expansion in roots) and cortical arrays (responsible for cell elongation in the hypocotyl) are affected similarly by EPC.

A concentration of 30 μM EPC hinders germination in the wild-type, whereas 3 mutant plants are able to germinate and grow at this concentration. Results obtained in this study show that plants with reduced microtubule dynamics can tolerate higher levels of EPC. This corresponds with results obtained by Kreis (1987) and Piperno *et al.*, (1987) where it was shown that stable interphase microtubules are more resistant to higher concentrations of microtubule disrupting drugs.

In *ATER 5*, growth is promoted by a 3 μM EPC concentration which corresponds to observations made by Ahad *et al.*, (2003) where growth of calli from tobacco mutants appeared to be stimulated by addition of EPC.

Before EPC enters into targeted tissue, it has to move through the epidermis and vascular tissues. This raises the question whether the resistance exhibited by the *ATER* mutants is due to a hindrance of the translocation ability of these plants. Such a hindrance would ensure that the plants have reduced levels of the drug and thus still thrive when the external EPC concentration is high.

A clear dose-response in the tested plants indicates that the resistance is due to factors other than reduced permeability to EPC. Emerging root tips of the seedlings were swollen and club like shaped which typifies drugs affecting mitosis.

By binding to tubulin heterodimers, EPC prevents their incorporation into microtubules. Plants in which the mutated tubulin has a low affinity to EPC would therefore be more resistant to this microtubule assembly blocker. The *ER31* rice mutant which is resistant to aryl carbamates (Nick *et al.*, 1994) harbours a tubulin isotype with reduced affinity for EPC due to truncation of the carboxyterminus as a consequence of a precocious codon stop. When the mutated tubulin, lacking the binding site for Arylcarbamate is truncated to calli, the calli acquired tolerance to otherwise inhibitory doses of phenyl urethane (reviewed in Nick *et al.*, 2003).

Resistance to EPC can also be as a result of changes in the binding sites for tubulin (Keates *et al.*, 1981; Cabral *et al.*, 1986) or to alteration in tubulin isotypes (Ranganathan *et al.* 1996; Kavallaris *et al.*, 2001; Cabral, 2003). Such changes would result in an alteration in the rates of assembly and disassembly such as exhibited by the *ATER* mutants. An alteration in the α -and/or β -subunit would confer enhanced stability, and therefore resistance to EPC. In mammalian cells it has been shown that alterations in the M-loop of β -tubulin resulted in resistance to microtubule disrupting drugs (Cabral *et al.*, 2003). The location of amino acids and changes in the tertiary structure of tubulin is consistent with a role in modulating the assembly of microtubules. Considering that the *ATER* mutants were developed via activation tagging (**see section 2.1.1**), if the tag would insert into a coding exon, it would result in a knockdown of the protein. The scenario of an altered binding site is thus improbable as this

would only occur via point mutation. If, however, the tag inserts into a tubulin promoter or intron, it would result in the upregulation of the respective gene product. Thereby initiating an increase in tubulin levels, resistance to EPC would thus be elevated as the system is better buffered against this drug. The elevated tubulin levels in *ATER 5* (Figure 7) point out to such a scenario. An increase in the expression of MAPs would result in increased microtubule stability. Such microtubules would have lower dynamics, this seem to be the case in *ATER 2* mutant.

To confirm, whether the resistance to EPC is indeed caused by alteration in tubulin, it is necessary to determine if there are changes in the mobility of α -tubulin in the mutants. It would also be necessary to determine if the mutants are cross resistant to other microtubule disrupting drugs that have distinct binding sites.

Plant types with reduced microtubule dynamics such as the *ATER* mutants confer a comparative advantage in the face of blockers of microtubule assembly.

6.2 Tubulin Separation using EPC Affinity Chromatography

Aryl carbamates such as Ethyl-N-phenylcarbamate usually display different affinities for tubulin from plant cells (Anthony and Hussey, 1999, Nick *et al.*, 2002). It is possible to separate tyrosinylated from detyrosinylated α -tubulins, based on this principle. These two α -tubulin modifications can then be detected using the antibodies ATT and DM1A respectively.

In the mutant plants the tyrosinylated tubulin weakly binds to EPC compared to the wild type. In *ATER 2*, the elution buffer with a 0.1 mM KCl concentration was sufficient to elute out the entire tyrosinylated α -tubulin whereas for SR1, double the concentration was required. Detyrosinylated α -tubulin in the mutants has a higher affinity to EPC compared to the wild type. Concentration of 0.5 to 3mM KCl were required to elute it in *ATER 2* and *ATER 5*, whereas in the wild type the elution buffer with a 0.25 mM KCl concentration was sufficient.

Gelöscht

The results show that via a simple method based on the affinity of tubulin to EPC it is possible to distinguish between tyrosinylated and detyrosinylated α -tubulin.

The binding site for EPC is located in the last 13 amino acids of α -tubulin. When this binding site is masked, which is the case when carboxy terminal tyrosine (CTT) is present, binding is weak. Detyrosinylation uncovers this binding site and favours strong binding of EPC to tubulin (Wiesler *et al.*, 2002). The *ATER* mutants were selected for resistance to EPC. It has since been shown that this resistance to EPC is due to the reduced rates of polymerisation and depolymerisation of the microtubules in these plants. Since the microtubules are less dynamic, they live longer and hence are exposed for a longer time to tubulin-tyrosine carboxypeptidase (TTC). This results in unmasking of the binding site and in consequence detyrosinylation of tubulin. In the *ATER* mutants the binding site is exposed and hence the affinity to EPC is increased.

6.3 Microtubule Stability and Detyrosinylation

Kreis (1987), showed that *glu*-microtubules are less dynamic (more stable) and have higher amounts of detyrosinylated tubulin. The author then posed the question whether this enhanced stability is due to detyrosinylation, or vice versa. It has since been suggested that detyrosinylation is due to stability (Skoufias and Wilson 1998). This is logical since dynamic microtubules are short lived and hence less prone to detyrosinylation.

When a microtubule is exposed for a longer time to tubulin-tyrosine carboxypeptidase (TTC), this results in tubulin detyrosinylation. This implies that stable microtubules such as those in the *ATER* mutants which have a longer life time are more prone to be detyrosinylated. Tyrosinylation levels can thus be used to define microtubule dynamism.

In this study the mutant plants with reduced microtubule dynamics had relatively higher amounts of detyrosinylated α -tubulin compared to the wild type. Measurements were made from total protein extract of the plant leaves.

Thereby confirming results obtained by Kreis, (1987) in which enhanced microtubule stability was linked to detyrosinylation. The higher amounts of detyrosinylated tubulin in the mutants is logical since the stable microtubules are exposed for a longer time to TTC compared to the wild type, and this results in detyrosinylation.

Both *ATER 2* and *ATER 5* can tolerate high levels of EPC. Ahad *et al.*, (2003) showed that the microtubules of these mutants remain stable even at high EPC concentrations. Our observations suggest that these plants use different strategies to cope with elevated EPC levels.

In *ATER 2*, the overall abundance of α -tubulin is not elevated; however, there is a shift into the detyrosinylated form. Thus a tolerance to EPC cannot be explained in terms of reduced affinity to EPC. Reduced microtubule turnover would ensure that these microtubules have a longer life time. In addition a reduced polymerisation/depolymerisation rate has the effect that these microtubules are less sensitive to the effects of microtubule antagonists such as EPC. This is the base for the resistance of *ATER 2* to EPC.

In *ATER 5* the situation is different. Both tyrosinylated and detyrosinylated forms of tubulin are elevated to the same extent. Therefore resistance cannot be explained in terms of reduced affinity to EPC as the reduced affinity of tyrosinylated tubulin is hardly detectable. The elevated tubulin levels point to a scenario whereby an increase in cytosolic tubulin results in competitive inhibition of EPC.

Changes in microtubule dynamics such as those exhibited by *ATER 2* or tubulin levels as seen in *ATER 5* would ultimately influence the cytoskeleton network. In the following section I discuss the impact of these changes to microtubule and actin organization.

6.4 Microtubule Stability Depends on their Orientation

The orientation of microtubules determines the preferential axis of growth in plant tissue. In living cells, transverse and longitudinal microtubules have been

shown to co-exist (Lloyd, 1994; Himmelspach *et al.*, 1999; Wiesler *et al.*, 2002). Studies conducted by Wiesler *et al.*, (2002) inferred that microtubule dynamics is dependent on microtubule orientation. Microtubules with reduced dynamics have higher amounts of deetyrosinated α -tubulin and are characteristically longitudinally oriented, whereas dynamic microtubules are transversely oriented to the direction of the growing axis.

In this study, the orientation of microtubules was visualized *in vitro* following immunolocalization. All plants examined had a cross section of transverse and longitudinally inclined cortical microtubules. The wild-type, SR1 had a higher percentage of transversely inclined cortical microtubules compared to the *ATER* mutants. The *ATER* mutants, on the other hand, had a majority of their microtubules longitudinally oriented.

Our results show a correlation between microtubule stability and deetyrosination levels. This is supported by results from EPC affinity chromatography as well as total protein extract, where it was shown that the mutants have higher levels of deetyrosinated tubulin compared to the wild type. These findings are in agreement with those of Wiesler *et al.* (2002). The extent of the correlation between microtubule stability and orientation has not been elucidated in the scope of this study. It is proposed that the longer longitudinally inclined microtubules live longer and therefore are more likely to be deetyrosinated. In order to understand the relationship between microtubule orientation and stability, it would be necessary to clarify the co-relation between microtubule stability and deetyrosination levels.

6.5 Microtubules Influences the Orientation of Actin Filaments

Historically, the two major cytoskeleton networks in plants, microtubules and actin microfilaments are viewed as independent entities. Research usually focuses on important functions associated with each network. Actin microfilaments have been found to be involved in cell polarity and contractile migratory processes whereas microtubules are involved in intracellular

trafficking and/or determination of cell axis. Further research revealed that agents that interfere with one network often affected processes mediated by the other network, thus indicating an interaction between the two components (reviewed in Collings *et al.*, 1998; Goode *et al.*, 2000; Waterman Storer *et al.*, 2000; Dehmelt and Halpain, 2003).

Actin filaments have been shown to align transversely in elongating cells parallel to transversely aligned microtubules (Traas *et al.*, 1987; Sonobe and Shibaoka, 1989; Blancaflor, 2000; Collings *et al.*, 2001; Collings and Wasteneys, 2005). Colocalization has also been observed in the phragmoplast (Gunning and Wick, 1985). This apparent colocalization of the two networks is however no conclusive proof of interaction.

Evidence of microtubule-actin microfilament interaction is provided by studies involving cytoskeleton antagonists. Stabilization of the microtubule network using taxol enhances the presence of microtubule associated microfilaments in maize roots (Chu *et al.*, 1993; Blancaflor, 2000). In tobacco BY-2 suspension cells, a similar treatment promoted their co-alignment (Collings *et al.*, 1998). Thus pointing out that cortical organization of actin microfilaments may rely on microtubules. Hussey *et al.*, (1998), suggest that orientation of newly formed microfilaments is controlled by microtubules.

Observations on the effect of microfilament disruption on microtubule organization are divided. Hush and Overall, (1992) and Collings *et al.*, (2006) have shown that microtubules remain unaffected. Whereas other reports indicate impaired or abnormal microtubule re-organization following microfilament disruption (Kobayashi *et al.*, 1988; Seagull, 1990; Blancaflor, 2000; Ueda and Matasuyama, 2000; Collings and Allen, 2000).

Further evidence of microtubule-microfilament interaction is provided by molecular studies using mutants (Schwab *et al.*, 2003; Saedler *et al.*, 2004; Zhang *et al.*, 2005; Timmers *et al.*, 2007) Of notable interest is the rice mutant *Yin-Yang* which has been selected for resistance to EPC. The auxin dependent cell elongation of these plants showed higher sensitivity to microfilament disruption using Cytochalasin D (Wang and Nick, 1998; Waller *et al.*, 2000).

In this study, the orientation of actin microfilaments from *N. tabacum* plants were observed *in vitro*. The majority of actin microfilaments in SR 1 were transversely inclined whereas those in the mutants were longitudinally oriented. These orientations of actin microfilaments correspond to that of microtubules. Just as in the microtubules, *ATER 2* had the largest percentage of longitudinally oriented microtubules as well as actin filaments. These results indicate an obvious interaction between microtubule and actin filament orientation. The nature of this association was however not elucidated. Three possible scenarios can be considered;

- a) Actin microfilaments direct microtubule orientation.
- b) Microtubules direct actin orientation.
- c) Both networks are independently directed by a third factor.

It is tempting to suggest that microtubules direct actin filament orientation. One can argue that the mutation resulted in *ATER* plants with reduced microtubule dynamics and a larger percentage of longitudinally inclined microtubules. The only linkage between the two networks is this mutation, which had an effect on microtubules. It is therefore not farfetched to suggest that microtubules do indeed direct the orientation of actin filaments.

The scope of this study did not identify whether the nature of this association is regulatory i.e. two systems indirectly controlling each other (Ingber, 2003) or structural i.e. when actin and microtubules are physically linked (Waterman Storer *et al.*, 2000).

Continuing investigations of the plant cytoskeleton will undoubtedly shed light to the nature of this cross-talk between microtubules and actin filaments. In animals cells, proteins (myosins and formins) have been identified that link both actin microfilaments and microtubules. The identification of similar cross linking proteins in plants would help establish why cross talk between the two networks occurs.

6.6 MP Phosphorylation is a Viral Strategy

To monitor infection of *N. tabacum* by Tobacco Mosaic Virus leaves *in vivo*, TMV derivatives, in which the MP is fused to a fluorescent protein derived from the jelly fish (*Aequorea victoria*) are commonly used to inoculate plant leaves (Epel *et al.*, 1996; Oparka *et al.*, 1997; Padgett *et al.*, 1996; Heinlein *et al.*, 1995; Heinlein *et al.*, 1998a; Heinlein *et al.*, 2000; Heinlein *et al.*, 2002). In these viral constructs the MP is expressed as a functional MP:GFP fusion protein and can thus be used to analyse infection sites in a near real time manner.

Successful inoculation using such transcripts of these viral constructs is indicated by fluorescent disc shaped infection spots (Heinlein *et al.*, 1995; Heinlein *et al.*, 1998). As infection proceeds, the fluorescent disc expands outwards, whereas the fluorescence at the centre of the disc diminishes and finally disappears, this eventually results in an infection spot in the form of a “halo”-shaped fluorescent ring.

Since the MP is coupled to the GFP, this is used as an indicator for the expression level of MP. At the outer boundary of the ring a stronger fluorescence signal indicates a higher MP expression level whereas the reduced fluorescence in the interior of the ring is indicative of diminished MP expression levels. It has been suggested that MP is downregulated/degraded via phosphorylation at the trailing edge of infection and this accounts for the lack of fluorescence at the centre of infection and the expanding interior diameter. Boyko *et al.*, (2000), propose that two forms of MP exist, an active form at the outer boundary and an inactive form at the interior boundary.

Excessive MP would most likely interfere with the size exclusion limit (SEL) of the plasmodesmata; it seems plausible to argue that the virus degrades the MP at the trailing edge to ensure that normal cellular activities of the cytoskeleton are not disrupted.

The wild type *N. tabacum* plants as well as the mutants with reduced microtubule dynamics were successfully infected using transcripts of the viral construct and showed expanding “halo”-shaped fluorescent infection spots.

Thus showing that reduced microtubule turnover does not hinder viral infection. This points out that an intact and functional microtubule cytoskeleton is not necessary for viral infection and spread. A similar view is supported by studies where TMV spread continues despite disruption of microtubule or actin filament networks. It has since been shown that these antagonists do not entirely destroy the networks (Seemanpillai *et al.*, 2006) and hence TMV spread proceeds even though a large part of the microtubule or actin network is destroyed.

Microtubules have been implicated to play a role in degradation of MP (Padgett *et al.*, 1996; Reichel and Beachy, 2000; Gillespie, 2002). In this study the internal diameter of the fluorescent ring is larger in the wild type compared to that of the *ATER* mutants. This suggests that microtubule turnover plays a significant role in phosphorylation of MP and that the dynamic microtubules in the wild type are more efficient in facilitating MP phosphorylation

Already infected spots are not re-infected, this is demonstrated when two expanding infection spots come into contact with each other. Infection does not proceed beyond this point. This would lay credence to the phosphorylated or inactive MP theory at the centre of the infection spot. It has been shown that the plasmodesmata at this point are no longer gated. Since gating is however indispensable for viral movement, viral spread cannot proceed beyond this point. With the plasmodesmata restored to normal size, macromolecular trafficking in this region proceeds normally. It also ensures that other viruses do not take advantage of the gated plasmodesmata to further harm the host. It ensures that the infected host does not switch on a counter defence strategy and TMV can exclusively “milk” the host. This may explain why TMV appears to avoid the effects of viral induced gene silencing (Baulcombe *et al.*, 1998). Phosphorylation of MP appears to be virus triggered as a strategy to ensure that virus spread proceeds undisturbed.

An alternative scenario is to consider TMV infection leaves a “message” on already infected spots. Subsequent infections read the “I have been here” message and avoid this area, as there is nothing to be gained by re-infection.

This ensures that the virus invades new areas and spreads more efficiently in the host plant.

6.7 Reduced Microtubule Dynamics Lower TMV Cell-To-Cell Movement Efficiency

The efficiency by which local spread of TMV in infected plants occurs can be determined by measuring the area of the infection spot at different time points and establishing a rate of size increase over a specific time period. Such studies have been conducted to determine the extent to which disruption of the microtubule or actin filament cytoskeleton using disrupting drugs interferes with viral spread (Kawakami *et al.*, 2004; Ashby *et al.*, 2006).

In this study, the efficiency of cell to cell movement was analysed by determining the external and internal diameters as well as the band width of the fluorescent infection spots at 5 and 7 dpi in *N. tabacum* plants inoculated with a TMVMP:GFP. In both the control plants and the mutants with reduced microtubule dynamics, an increase in both external and internal diameters was observed over a 48 h period indicating active local transport of the virus. The width of the band at 5 dpi did not differ significantly with that at 7 dpi, implying that the rate of spread is constant. This would suggest that the rate at which the MP spreads at the leading edge of infection is equal to the rate at which the MP is degraded at the trailing edge of infection.

In *ATER 2*, local transport was at least 1.5 times slower than in *SR1*. The fluorescent band in the wild type was broader than that of the *ATER 2*, indicating less MP accumulation in plants having reduced microtubule dynamics.

The involvement of microtubules in viral movement was first inferred by Heinlein *et al.*, (1995). Doubts were cast as to the involvement of microtubules in viral spread when Gillespie *et al.*, (2002) pointed out that viral spread occurs at the leading edge whereas association of the microtubules with MP was only observed late stages of infection. Further credence to this observation was laid

by reports showing that viral movement occurs despite disruption of the microtubule network using microtubule disrupting drugs (Kawakami *et al.*, 2004). Recently Seemanpillai *et al.*, (2006) have shown that microtubule disrupting drugs do not entirely destroy the microtubule cytoskeleton, thus lending credence to the involvement of microtubules in TMV spread. Even though the actual role of microtubules has not been shown, Boyko *et al.*, (2000, 2002), implicated microtubules in this process and thus fuelled the debate even further.

The differences in the efficiency of local transport of TMV in plants of differing microtubule dynamics, point to an end to this debate by explicitly showing that diminished TMV spread corresponds to reduced microtubule dynamics. An increase in the external diameter of the infection spot is accompanied by a corresponding increase in the internal diameter. This points out that, microtubules play a role both in MP spread (at the leading age) and MP degradation (at the trailing edge).

Immunoblotting assays to measure the accumulation of MP in infected tissues would help lay further credence to the role of microtubules in TMV spread.

6.8 Intracellular Association of MP:GFP during Viral Infection.

Following inoculation with TMV-MP:GFP, it has been shown that the MP associates intracellularly with various components of the cytoskeleton. The association of MP with cytoskeleton components is dependent on the stage of infection (Heinlein *et al.*, 1998). In this study, an association of the MP with plasmodesmata, ER inclusion bodies and microtubules was shown. This indicates that the MP associations observed are comparable to that used in other studies.

When the association of the MP with ER inclusion bodies was analysed; it was found that these bodies contain viral replicase proteins and are as such referred

to as viral replication complexes (VRCs) (Más and Beachy, 2000; Heinlein, 1998).

Similar studies analysing the association of MP with cytoskeleton components have mainly used the highly susceptible *N. benthamiana* tobacco species (Ding *et al.*, 1992; Padgett *et al.*, 1996, Oparka, 1999; Más and Beachy, 2000; Heinlein, 2002). In these studies the patterns of association observation at 3 - 5 dpi was as follows. Plasmodesmata labelling at the leading edge of infection, followed by ER inclusion bodies immediately behind the leading front, and the middle stages of infection, the ER inclusion bodies disappear and microtubules immerge, larger VRCs are also observed at late stage plasmodesmata labelling and microtubules localization. It has been suggested that microtubules transport the ER inclusion bodies to the plasmodesmata (Heinlein *et al.*, 2002b). Other reports suggest that the small ER bodies observed are in fact nucleation sites for microtubules (Sambade, personal communication).

In the *N. tabacum* plants used in this study, MP labelled microtubules already at the leading edge of infection. This is consistent with observations by Padgett *et al.*, (1996) confirming that the MP:GFP distribution observed here represents a functional MP that is capable of mediating viral movement.

In *N. benthamiana* at 5 dpi, microtubules labelling is not observed at the early stage which contrasts with our observations in *N. tabacum*, where association of MP with microtubules is observed at this stage. At 10 dpi microtubules labelling is observed at the leading edge in *N. benthamiana*. The argument by Oparka *et al.* (1999), that microtubules are not involved in viral spread because they are not observed at the leading edge is thus not justified.

These differences in intracellular distribution of MP between the two tobacco species points out to a host-dependent strategy of the TMV virus. Several reports outlining the significance of host-viral interaction have been shown (Schaad *et al.*, 1997; Huang and Zhang, 1999; Kawakami *et al.*, 1999; Más *et al.*, 2000; Bressan *et al.*, 2003). It has been further suggested that viruses are bits of nucleic acids, which “escaped” from cellular organisms; this would explain their host specificity.

In cell-to-cell transport of TMV following viral infection, the VRCs spread from the sites of replication, to and through the plasmodesmata and into neighbouring cells where they initiate infection.

Even though a functional relationship between the association of microtubules and the intracellular redistribution of VRCs has been established (Boyko *et al.*, 2000a, 2000b), it is not exactly clear, how this occurs.

It has been suggested that TMV uses the motility function of microtubules for transport of VRCs throughout the cytoplasm. Although no direct evidence has been presented for this hypothesis, the appearance of microtubules corresponds with disappearance of MP containing inclusion bodies and their relocation at the cell periphery. In our study association of MP with the plasmodesmata was most pronounced in the wild type. Taking into consideration that the treadmilling in the mutants is reduced, one can speculate that the reduced treadmilling is responsible for the reduced efficiency in transport of the VRCs to the plasmodesmata. This would implicate a scenario where the VRCs cargo dock onto one end of the microtubules, and, via polymerisation and depolymerisation of the microtubules, emerges at the other end. Plant microtubules with a lower treadmilling rate would therefore require a longer time to deliver their cargo. Alternative models proposed by McLean *et al.*, (1995) or (Carrington *et al.*, 1996) where the microtubule network is proposed to function as a track where the viral complex is guided along appear flawed. In such a model a stable microtubule network would favour faster viral movement. Our results however show that viral movement is reduced in the mutants which have a stable microtubule network.

ER inclusion bodies observed at the leading edge of infection are later replaced by larger complexes that have been shown to contain MP and replicase proteins. These ER bodies are aligned close to or along microtubules. Evidence suggested that the ER network is involved in MP trafficking is conclusive (Reichel and Beachy, 1998; Boevink and Oparka, (2005). It is proposed that the MP moves via a dynamic ER membrane flow.

In this study evidence is presented those plants with reduced microtubule dynamics have fewer ER inclusion bodies compared to the wild type. These punctae are closely associated with microtubules at the leading edge of infection. It is not clear what their role is, even though it is obvious that their presence is significant to viral movement.

6.9 Association of MP with the Cytoskeleton in the Absence of Infection.

By agroinfiltration of a construct encoding MP:GFP under the influence of a 35S promoter, MP:GFP was transiently expressed in leaves of *N. tabacum* plants. The 30-kDa MP used in this construct is that which is present in the TMVMP:GFP plasmid construct that was used for transcription inoculation.

Results in this thesis show that the MP localized to plasmodesmata, microtubules and small punctae that resembled ER inclusion bodies. This is in agreement with similar associations observed by Ashby *et al.*, (2006) and proves that neither viral replication nor virus-host interactions are necessary for association of TMV-MP with various cytoskeleton components. It is therefore likely that MP binds directly to microtubules. This is supported by findings of Boyko *et al.*, (2000a), showing that a domain in the MP has structural similarity with the M-loop domain in tubulin that mediates tubulin:tubulin associations. MP may thus use mimicry to bind directly to microtubules.

The small punctae observed lie along or close to microtubule filaments and raise the question of their involvement in microtubule formation.

Co-agroinfiltration of MP:GFP with a microtubule marker MAP4, showed a perfect match and served to prove that the filaments observed associating with MP are indeed microtubules.

6.10 *ATER* Mutants are More Resistant to TMV

Symplastic continuity between cell to cell movement and long distance viral transport is provided by plasmodesmata in the phloem. Long distance transport is a passive process that occurs with the flow of photo assimilates. Successful infection of plants with TMV begins with local transport followed by systemic transport of the viral complexes. This eventually results in visible expression of the disease (symptom expression).

Symptom expression depends on the plant species and may be a combination of one of the following: mosaic pattern on leaves, necrosis, stunting, leaf mottling, and leaf distortion.

In this study the level of symptom expression was determined as a measure of necrosis per individual plant on a total leaf basis at 6 weeks after inoculation. It was observed that the wild type plants had a higher symptom expression level compared to the mutants. This suggests that the mutants have an altered competence for TMV viral infection. This hypothesis is, however, unlikely as the mutation only affected EPC tolerance of the plants. A more likely scenario is presented when results from the intracellular distribution of MP are examined. The fluorescence infection band is broader in the wild type compared to the mutants, indicating that the wild type accumulates more of the viral infection complexes and when this is translated to symptom expression it explains why the mutants are less affected. An alternative explanation is that since the rate of viral movement is faster in the wild type, the viral complex arrives to the vascular system faster in the wild type compared to the mutants. A combination of the two factors i.e. higher amount of viral material, being delivered quickly to the vascular system would account for our observations.

It appears therefore that activities affecting cell to cell movement have an effect on long distance transport and, in consequence, symptom expression.

It is therefore plausible to suggest that reduced microtubule dynamics confer a form of resistance to *N. tabacum* plants in the face of TMV infection.

A measure of viral accumulation in plant tissue would help cement these findings.

In-situ hybridization experiments have demonstrated that vRNA colocalizes with movement proteins and microtubules (Beachy *et al.*, 1999), other studies linking microtubules to vRNA movement involved temperature sensitive virus mutants. At high temperatures (where MP:microtubules association did not occur) there is no viral movement. Movement of the virus is however restored when temperatures are permissive (Boyko *et al.*, 2000; Boyko *et al.*, 2007).

Findings in this dissertation show that the 30-kDa MP of TMV interacts with microtubules and that these microtubules play a significant role in viral trafficking. These observations complement several other findings implicating microtubules in viral transport (Heinlein *et al.*, 1995; Padgett *et al.*, 1996; Boyko *et al.*, 2000; Seemanpillai *et al.*, 2006).

Doubts have been raised on the importance of microtubules by observations showing that MP can target to plasmodesmata independently of microtubule association (Boyko *et al.*, 2000; Khan, 1998; Wright *et al.*, 2007). In some of these studies, conclusions were drawn based on MP localization at the plasmodesmata despite the use of microtubule inhibitors. It has since been shown that microtubule antagonists are incapable of completely destroying the microtubule network (Seemanpillai *et al.*, 2006).

Results from this study show that reduced microtubule turnover lowers the efficiency of plasmodesmatal targeting by MP, thus bring microtubules again into focus. These observations suggest that microtubule treadmilling is used in the transport of the viral complex, and challenges the commonly held view of microtubules being used as tracks for motor driven viral transport. The treadmilling hypothesis was first proposed by Boyko *et al.*, (2000), and was based on the interesting sequence homology motif between TMV-MP and tubulin. It was suggested that the MP+vRNA complex is incorporated into the microtubule polymer.

It is therefore clear that microtubules play a significant role at both the leading and trailing edge of infection. The model that I have generated is based on comparisons of viral spread as well as the radially expanding trailing edge in mutants with reduced dynamics, speculates that MP together with the vRNA binds directly onto the microtubule polymer and the viral complex moves along the length of the microtubule via treadmilling. Microtubules with lower turnover such as in the ATER 2 mutant require a longer time to deposit their load at the other end.

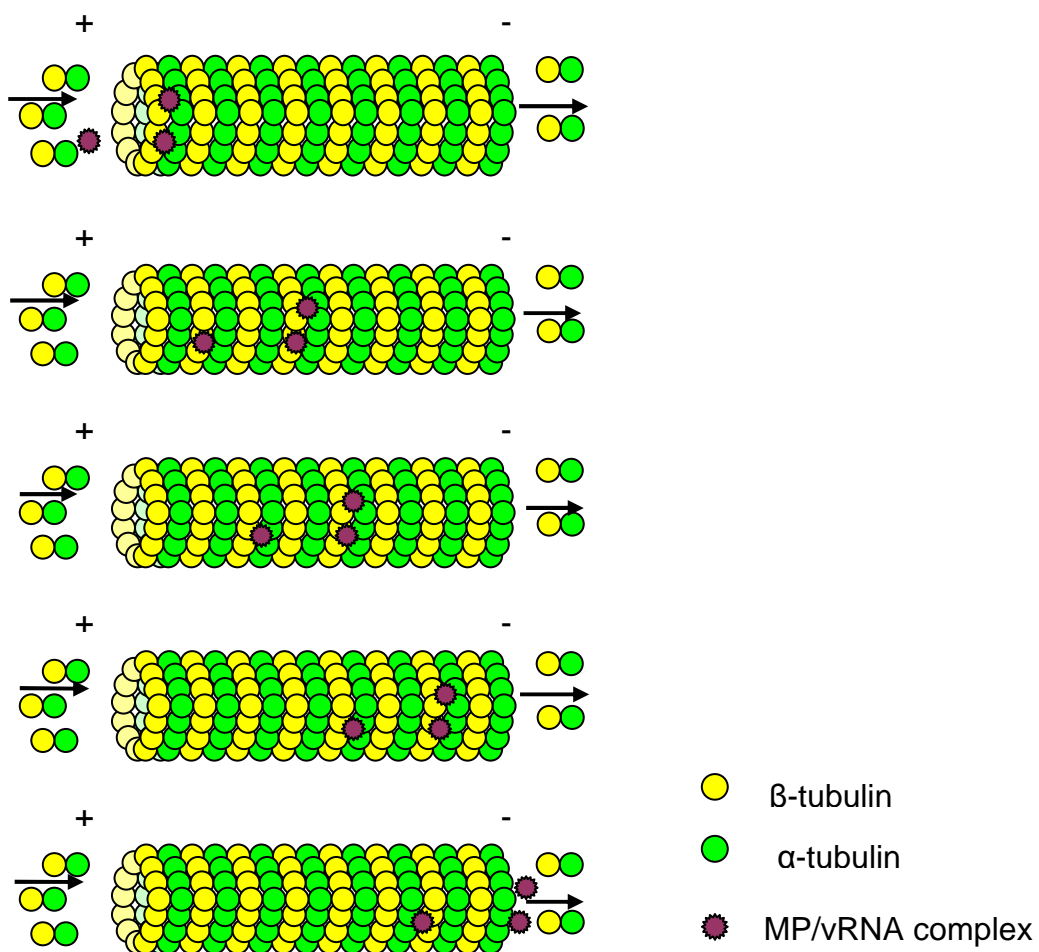


Figure 27: working model depicting TMV movement via microtubule treadmilling. MP+vRNA complexes bind onto tubulin dimers at one end and emerge at the other end.

An ideal situation would be to develop plants, where microtubule turnover is reduced to such an extent that viral trafficking is too slow to cause plant damage.

7 Conclusions and Future Outlook

Dose-response studies of the *ATER* plants to increasing EPC concentrations highlighted their resistance to microtubule disassembly. In *ATER 2* this resistance was due to reduced microtubule turnover, whereas in *ATER 5* this was caused by elevated tubulin levels. It is, however, not enough to show that the plants tolerate high levels of EPC, of paramount importance is the identification of the gene(s) that were activated following insertion of the T-DNA tag that resulted in the EPC tolerance phenotype. Identification of this gene would pave way for concrete studies on TMV spread in *N. tabacum*. Reproducibility of this phenotype in the wild type would serve as sufficient proof of identification of the gene. Plasmid rescue as described by Walden *et al.* (1995), is the method of choice.

A post translational modification of tubulin; detyrosinylation, can be used to define microtubule dynamism. Dynamic microtubules have high levels of tyrosinylated α -tubulin whereas stable microtubules (reduced dynamics) have higher levels detyrosinylated α -tubulin. Using biochemical means it was possible to show (in the tested plants) differences in levels of these tubulin modifications as well as differences in their affinity to EPC. However, immunolocalization experiments using the antibodies DM1A and ATT did not reveal different populations of microtubules (**Figure 30**), a result that contrasts with that of Wiesler *et al.* (2002). By transiently or stably expressing microtubule markers such as the microtubule end binding protein 1 (EB1), in the *ATER* mutants. It would be possible to follow microtubule dynamics *in vivo*.

In this study the analysis of cytoskeletal organization was limited to the simple characterization of microtubules and actin microfilaments. *In-vitro* observations showed that microfilament alignment corresponded to the orientation of the microtubules. Such a view, however, does not give conclusive evidence of cross talk between the two cytoskeleton components. A better understanding of the interaction between actin microfilaments and microtubules would be

achieved by conducting *in-vivo* studies, coupled with pharmacological experiments. Shutting down of one component with inhibitors and analysing the effect on activities associated with the other. Effort concentrated on the identification of crosslinker proteins in plants would go a long way in elucidating this problem.

In addition, actin filaments in the *ATER* mutants were bundled compared to those in the wild-type (see appendix), thus implicating cross-talk between the two systems, a result that relates to the findings associated with the *Yin-Yang* rice mutant and raises the question, what happens when the actin bundling phenotype is rescued by use of Latrunculin B or auxin. This opens interesting prospects in the event that the EPC resistance is affected by this rescue process.

Viruses are known to adapt existing intracellular communication host channels for their own benefit. Viral infection is thus very host specific, in this study, differences were observed in the interaction of *N. tabacum* and *N. benthamiana* with the same virus (TMV). Specifically in *N. tabacum* microtubule association at the leading edge of infection is observed much earlier than in *N. benthamiana*.

In *N. benthamiana* association of MP with microtubules at 3 - 5 dpi does not occur at the infection front, thus leading to the suggestion that microtubules are involved in auxiliary activities other than viral trafficking (Padgett *et al.*, 1996; Gillespie *et al.*, 2002; Curin *et al.*, 2007). However in *N. tabacum* plants inoculated with transcripts of TMVMP:GFP, MP associated microtubules are observed already at the leading front, thus highlighting the host specificity of TMV.

Conclusive statements on the role of microtubules in the spread of TMV must be host related. Further insights are necessary to understand the molecular virus-host interactions and to determine the specific roles of these interactions in each host system. Experiments designed to compare subcellular localization of the virus, viral movement, viral accumulation in the two host systems would help answer this question.

Using fluorescence spectroscopy it is possible to determine symptom expression before visible signs occur. This could be used to compare rates of spread between the mutants on a leaf-to-leaf basis as well as on a global scale and would help establish a linkage between events occurring during local transport and their influence on long distance transport.

Conclusive evidence presented here shows that reduced microtubule turnover confers resistance to *N. tabacum* plants infected with TMV. In this study symptom expression as well as the rate of viral spread were used to establish a link between microtubules and viral trafficking. Further proof of the differences in viral spread could be established via real-time PCR studies by measuring the levels of RNA accumulated following infection, quantification of plasmodesmata labelling and ER inclusion bodies. Research focusing on identifying how plasmodesmata labelling occurs would be necessary to help establish clarity. The movement protein is known to stabilize microtubules (Ashby *et al.*, 2006). This raises the question of the role MP in already stabilized microtubules such as in *ATER 2*.

It is unlikely that the microtubule network alone is responsible for conveying the VRC to the plasmodesmata. It has been shown that the ER is contiguous between adjacent cells (Ding *et al.*, 1992b; Epel 1994; Overall and Blackman, 1996). Furthermore, associations of MP with ER (Heinlein *et al.*, 1998a; Más and Beachy, 1999) and actin filaments (McClean *et al.*, 1995) suggest that other cytoskeletal components also play a role. The extent to which each component mediates viral movement still needs to be elucidated. New findings on cross-talk between these components as well as comparisons with animal systems would help shed light to this debate.

Acknowledgements

“Research is teamwork“, an on this note would like to mention some members of this team who played significant roles in my studies.

Prof Dr. Peter Nick for giving me an opportunity to pursue my scientific dreams, and introducing me to the fascinating world of microtubules. And for his ability to fish out information from this network of filamentous structures. And to Dr. Claus Buschmann for kindly agreeing to co-referee my dissertation

I am also grateful to the staff of the Institut Biologie Moléculaire des Plantes (IBMP)-Strasbourg-France especially Prof Manfred Heinlein of the for providing me with working tools (TMVMP:GFP) and lab space, Dr Adrian Sambade for microscopy, Mark Seemanpillai, Christian Hoffman and Katrin Brandner for help with the *in vitro* transcriptions.

A plasmid construct carry the full length TMV cDNA was kindly provided by Prof Tetsuo Meshi of the Plant Physiology Department, National Institute of Agrobiological Sciences, Kannondai-Japan.

I would also like to thank the gardeners at the IBPM as well as those at the Botany garden-Karlsruhe university, for growing my plants and ensuring that they remained green.

“I was a stranger and you took me in“, with these words I would like to show appreciation to all my work mates at the Botanik institute 1, for providing a suitable working environment and for tips and tricks into the not so familiar world of cell and molecular biology. Special thanks to Aleksandra Jovanović (*soon to be doctor*) and Dr. Michael Riemann for tirelessly correcting draft after draft of my manuscript.

And to my wife Sabrina and my son Romeo, thank you for showing understanding, even without understanding what the TMV fuss is all about.

Financial support for this study was provided in part by the PROCOPE grant funded by the German Academic Exchange Service (DAAD) as well as a fellowship from the Landesgraduierten-Programm of the State of Baden-Württemberg

8 References

- Aaziz, R., Dinant, S. Epel, B.L.** (2001). The cytoskeleton and plasmodesmata: For better or for worse. *Trends Plant Sci.*, **6**: 326–330.
- Ahad, A., Wolf, J Nick, P.** (2003). Activation-tagged tobacco mutants that are tolerant to antimicrotubular herbicides are cross-resistant to chilling stress. *Transgenic Research.*, **1222**: 1–15.
- Abdrakhamanova, A., Wang, Q. Y., Khokhlova, L., Nick, P.** (2003). Is microtubule disassembly a trigger for cold acclimation? *Plant Cell Physiol.*, **44**: 676-686.
- Anthony, R.G and Hussey, P.J.** (1998). Suppression of endogenous α - and β -tubulin synthesis in transgenic maize calli overexpressing α - and β -tubulins. *Plant J.*, **16**: 297-304.
- Anthony, R.G., Reichelt, S Hussey, P.J.** (1999). Dinitroaniline herbicide-resistant transgenic tobacco plants generated by cooverexpression of a mutant α -tubulin and a β -tubulin. *Nat. Biotechnol.*, **17**: 712-716.
- Ashby, J., Boutant, E., Seemanpillai, M., Groner, A., Sambade, A., Ritzenthaler, C., Heinlein, M.** (2006). Tobacco mosaic virus movement protein functions as a structural microtubule-associated protein. *J Virol.*, **80**: 8329-8344.
- Atkins, D., Hull, R., Wells, B., Roberts, K., Moore, P., Beachy, R.N.** (1991). The tobacco mosaic virus 30K movement protein in transgenic tobacco plants is localized to plasmodesmata. *J. Gen.Virol.*, **72**: 209-211.
- Bassel, G. and Singer, R.H.** (1997). mRNA and cytoskeletal filaments. *Curr. Opin. Cell Biol.*, **9**:109–115.
- Baulcombe, D.C., Chapman, S.N., Santa Cruz, S.** (1995). Jellyfish green fluorescent protein as a reporter for virus infections. *Plant J.*, **7**: 1045-1053.
- Beachy, R.N.** (1998). Changing patterns of localization of the tobacco mosaic virus movement protein and replicase to the endoplasmic reticulum and microtubules during infection. *Plant Cell.*, **10**: 1107-1120.
- Boyko, V., Ashby, J.A., Suslova, E., Ferralli, J., Sterthaus, O., Deom, C.M., Heinlein, M.** (2002). Intramolecular complementing mutations in Tobacco mosaic virus movement protein confirm a role for microtubule association in viral RNA transport. *J. Virol.*, **76**: 3974-3980.

References

- Boyko, V., Ferralli, J., Ashby, J., Schellenbaum, P., Heinlein, M.** (2000a). Function of microtubules in intercellular transport of plant virus RNA. *Nat. Cell Biol.*, **2**: 826-832.
- Boyko, V., Ferralli, J., Heinlein, M.** (2000b). Cell-to-cell movement of TMV RNA is temperature-dependent and corresponds to the association of movement protein with microtubules. *Plant J.*, **22**: 315-325.
- Boyko, V., Hu, Q., Seemanpillai, M., Ashby, J., Heinlein, M.** (2007). Validation of microtubule-associated TMV RNA movement and involvement of microtubule-aligned particle trafficking. *Plant J.* in press
- Boyko, V., van der Laak, J., Ferralli, J., Suslova, E., Kwon, M-O., Heinlein, M.** (2000c). Cellular targets of functional and dysfunctional mutants of tobacco mosaic virus movement protein fused to GFP. *J. Virol.*, **74**: 11339-11346.
- Goode, B. L., Drubin, D. G. and Barnes, G.** (2000). Functional cooperation between the microtubule and actin cytoskeletons. *Curr. Opin. Cell Biol.*, **12**: 63-71.
- Cabral, F.** (2000). Factors determining cellular mechanisms of resistance to antimetabolic drugs. *Drug Resist Updat.*, **3**: 1–6.
- Cabral, F., and Barlow, S. B.** (1989). Mechanisms by which mammalian cells acquire resistance to drugs that affect microtubule assembly. *FASEB J.*, **3**: 1593–1599.
- Carr T, Whitham SA.** (2007). An emerging model system: Arabidopsis as a viral host plant. In: Waigmann E, Heinlein M (eds) *Viral Transport in Plants*. Springer, Heidelberg, pp 159-183.
- Carrington, J.C., Kasschau, K.D., Mahajan, S.K., Schaad, M.C.** (1996). Cell-to-cell and long distance transport of viruses in plants. *Plant Cell.*, **8**: 1669-1681.
- Chen, M.-H., Sheng, J., Hind, G., Handa, A. K., Citovsky, V.** (2000). Interaction between the tobacco mosaic virus movement protein and host cell pectin methylesterases is required for viral cell-to-cell movement. *EMBO J.*, **19**: 913-920.
- Citovsky, V., Knorr, D., Schuster, G., Zambryski, P.** (1990). The P30 movement protein of tobacco mosaic virus is a single-stranded nucleic acid binding protein. *Cell.*, **60**: 637-647.
- Citovsky, V., McLean, B.G., Zupan J.R., Zambryski, P.** (1993). Phosphorylation of tobacco mosaic virus cell-to-cell movement protein by a developmentally regulated plant cell wall-associated protein kinase. *Genes Dev.*, **7**: 904-910.

References

- Citovsky, V.** (1993). Probing plasmodesmal transport with plant viruses. *Plant Physiol.*, **102**: 1071-1076.
- Citovsky, V and Zambryski, P.** (1991). How do plant virus nucleic acids move through intercellular connections? *Bioessays.*, **13**: 373–379.
- Citovsky, V.** (1999). Tobacco mosaic virus: a pioneer of cell-to-cell movement. *Philos Trans R Soc Lond B Biol Sci.*, **354**: 637–647.
- Citovsky, V. and Zambryski, P.** (1993). Transport of nucleic acids through membrane channels: snaking through small holes. *Annu. Rev. Microbiol.*, **47**: 167-197.
- Citovsky, V., Knorr, D. & Zambryski, P.** (1991). Gene I, a potential cell-to-cell movement locus of cauliflower mosaic virus, encodes an RNA binding protein. *Proc Natl Acad Sci U S A.*, **88**: 2476–2480.
- Citovsky, V., Knorr, D., Schuster, G., Zambryski, P.** (1990). The P30 movement protein of tobacco mosaic virus is a single-strand nucleic acid binding protein. *Cell.*, **60**: 637-647.
- Citovsky, V., McLean, B.G., Zupan, J. and Zambryski, P.** (1993). Phosphorylation of tobacco mosaic virus cell-to-cell movement protein by a developmentally-regulated plant cell wall-associated protein kinase. *Genes Dev.*, **7**: 904–910.
- Citovsky, V., Wong, M.L., Shaw, A.L., Prasad, B.V.V., and Zambryski, P.** (1992) Visualization and characterization of tobacco mosaic virus movement protein binding to single-stranded nucleic acids. *Plant Cell.*, **4**: 397-411.
- Waterman-Storer, C., Duey, D. Y., Weber, K. L., Keech, J., Cheney, R. E., Salmon, E. D. and Bement, W. M.** (2000). Microtubules remodel actomyosin networks in *Xenopus* egg extracts via two mechanisms of F-actin transport. *J. Cell Biol.*, **150**: 361-376.
- Collings, D.A., Allen, N.S.** (2000). Cortical actin interacts with the plasma membrane and microtubules. In: Staiger CJ, Baluška F, Volkmann D, Barlow PW (eds) *Actin: A Dynamic Framework for Multiple Plant Cell Functions*. Kluwer Academic, Dordrecht, pp 145-163.
- Collings, D.A, Asada, T., Allen, N.S., Shibaoka, H.** (1998). Plasma membrane-associated actin in Bright Yellow 2 tobacco cells: Evidence for interaction with microtubules. *Plant Physiol.*, **118**: 917-928.

References

- Collings D.A., Harper, J.D.I., Vaughn, K.C.** (2003). The association of peroxisomes with the developing cell plate in dividing onion root cells depends on actin microfilaments and myosin. *Planta.*, **218**: 204-216.
- Collings D.A., Lill A.W., Himmelspach, R., Wasteneys, G.O.** (2006). Drug sensitisation studies show actin microfilaments and microtubules interact during root elongation in *Arabidopsis thaliana*. *New Phytol.*, **170**: 275-290.
- Collings, D.A., Wasteneys, G.O.** (2005). Actin microfilament and microtubule distribution patterns in the expanding root of *Arabidopsis thaliana*. *Can J Bot.*, **83**: 579-590.
- Collings, D.A., Wasteneys, G.O., Williamson, R.E.** (1996) Actin-microtubule interactions in the alga *Nitella*: analysis of the mechanism by which microtubule depolymerization potentiates cytochalasin's effects on streaming. *Protoplasma.*, **191**: 178-190.
- Collings, D.A., Zsuppan, G., Allen, N.S., Blancaflor, E.B.** (2001) Demonstration of prominent actin filaments in the root columella. *Planta.*, **212**: 392-403.
- Collings, D.A., Asada, T., Allen, N.S., Shibaoka, H.** (1998). Plasma membrane-associated actin in Bright Yellow 2 tobacco cells: Evidence for interaction with microtubules. *Plant Physiol.*, **118**: 917-928.
- Dawson, W.O., Bubrick, P., Grantham, G.L.** (1988). Modifications of the tobacco mosaic virus coat protein gene affecting replication, movement, and symptomatology. *Phytopathology.*, **78**: 783-789.
- Dehmelt L, Halpain S.** (2004). Actin and microtubules in neurite initiation: are MAPs the missing link? *J Neurobiol.*, **58(1)**:18-33.
- Deom, C.M. and He, X.Z.** (1997). Second-site reversion of a dysfunctional mutation in a conserved region of the tobacco mosaic virus movement protein. *Virology.*, **232**: 13-18.
- Deom, C.M., Oliver, M.J., Beachy, R.N.** (1987). The 30-kilodalton gene product of tobacco mosaic virus potentiates virus movement. *Science.*, **237**: 384-389.
- Deom C.M, Schubert, K.R., Wolf, S., Holt, C.A., Lucas, W.J., Beachy, R.N.** (1990). Molecular characterization and biological function of the movement protein of tobacco mosaic virus in transgenic plants. *Proc. Natl. Acad. Sci. USA.*, **87**: 3284-3288.

References

- Deom, C.M., Lapidot, M. Beachy, R.N.** (1992). Plant virus. movement proteins. *Cell.*, **69**: 221-224.
- Diaz-Griffero, F., Cancino, C. E., Arevalo, C. M., & Arce-Johnson, P.** (2006). Expression of the crucifer-infecting TMV-Cg movement protein in tobacco plants complements in trans a TMV-U1 trafficking-deficient mutant. *Biological Research.*, **39(2)**: 269-279.
- Ding, B., Haudenshield, J.S., Hull R.J., Wolf S., Beachy; R.N., Lucas, W.J.** (1992a). Secondary plasmodesmata are specific sites of localization of the tobacco mosaic virus movement protein in transgenic tobacco plants. *Plant Cell.*, **4**: 915-928.
- Ding, B., Turgeon, R., Parthasarathy, M.V.** (1992b) Substructure of freeze-substituted plasmodesmata. *Protoplasma.*, **169**: 28-41.
- Ding, B., Kwon, M.-O. and Warnberg, L.** (1996). Evidence that actin filaments are involved in controlling the permeability of plasmodesmata in tobacco mesophyll. *Plant J.*, **10**:157-164.
- Ding, S.W.** (2000) RNA silencing. *Curr. Opin. Biotech.*, **11**: 152–156.
- Dingwall, C. and Laskey, R. A.** (1992). The nuclear membrane. *Science.*, **258**: 942-947.
- Dorokhov, Y.L., Alexandrov, N.M., Miroshnichenko, N.A., Atabekov, J.G.** (1983) Isolation and analysis of virus-specific ribonucleoprotein of tobacco mosaic virus-infected tobacco. *Virology.*, **127**: 237-252.
- Dorokhov, Y.L., Alexandrova, N.M., Miroshnichenko, N.A., Atabekov, J.G.** (1984) The informosome-like virus-specific ribonucleoprotein (vRNP) may be involved in the transport of tobacco mosaic virus infection. *Virology.*, **137**: 127-134.
- Dumontet, C. and Sikic, B. I.** (1999) Mechanisms of action of and resistance to antitubulin agents: microtubule dynamics, drug transport, and cell death. *J. Clin. Oncol.*, **17**: 1061-1070.
- Epel B.** (1994) Plasmodesmata: composition, structure and trafficking. *Plant Mol. Biol.*, **26**: 1343-1356.
- Epel, B.L., Padgett, H.S., Heinlein M., Beachy, R.N.** (1996). Plant virus movement protein dynamics probed with a GFP-protein fusion. *Gene.*, **173**: 75-79.

References

Escuin, D., Kline, E.R., Giannakakou, P. (2005). Both microtubule-stabilizing and microtubule-destabilizing drugs inhibit hypoxia-inducible factor-1alpha accumulation and activity by disrupting microtubule function. *Cancer Res.*; **65(19)**:9021-9028.

Ferralli, J., Ashby, J., Fasler, M., Boyko, V., Heinlein, M. (2006). Disruption of microtubule organization and centrosome function by expression of Tobacco mosaic virus movement protein. *J. Virol.*, **80**: 5807-5821.

Gibbs, (1976) in *Intercellular communication in plants: studies on plasmodesmata*, p.149, ed. B. E. S. Gunning & A. W. Robards, Springer-Verlag, 1976.

Giddings, T.H. Jr, Staehelin, L.A. (1991). Microtubule-mediated control of microfibril deposition: a re-examination of the hypothesis. In CW Lloyd, eds, *The Cytoskeletal Basis of Plant Growth and Form*. Academic Press, San Diego, CA, pp 85-100.

Gillespie, T., Boevink, P., Haupt, S., Roberts, A.G., Toth, R., Vantine, T., Chapman, S., Oparka K.J. (2002). Functional analysis of a DNA shuffled movement protein reveals that microtubules are dispensable for the cell-to-cell movement of tobacco mosaic virus. *Plant Cell.*, **14**: 1207-1222.

Goode, B.L., Drubin, D.G., Barnes, G. (2000) Functional cooperation between the microtubule and actin cytoskeletons. *Curr Op Cell Biol.*, **12**: 63-71.

Goode, B.L., Drubin, D.G., Lappalainen, P. (1998). Regulation of the cortical actin cytoskeleton in budding yeast by twinfilin, a ubiquitous actin monomer-sequestering protein. *J. Cell Biol.*, **142**:723-733.

Gunning, B.E.S. and Wick, S.M. (1985). Preprophase bands, phragmoplasts and spatial control of cytokinesis. *J Cell Sci Suppl.*, **2**: 157-179.

Hasezawa, S. and Nagata, T. (1993). Microtubule organizing centers in plant cells: localization of a 49 kDa protein that is immunologically cross-reactive to a 51 kDa protein from sea urchin centrosomes in synchronised tobacco BY-2 cells. *Protoplasma.*, **176**: 64-74.

Hasezawa. S., Sano, T., Nagata, T. (1998). The role of microfilaments in the organization and orientation of microtubules during the cell cycle transition from M phase to G1 phase in tobacco BY-2 cells. *Protoplasma.*, **202**: 105-114.

Hazelrigg, T. (1998). The destinies and destinations of RNAs. *Cell.*, **95**: 451-460.

References

- Heinlein, M.** (2002). The spread of Tobacco mosaic virus infection: insights into the cellular mechanism of RNA transport. *Cell. Mol. Life Sci.*, **59**: 58-82.
- Heinlein, M (2005)** Systemic RNA silencing. In: Oparka K (eds) *Plasmodesmata*. Blackwell, Oxford, pp 212-240.
- Heinlein M (2006)** TMV movement protein targets cell-cell channels in plants and prokaryotes: possible roles of tubulin- and FtsZ-based cytoskeletons. In: Baluska F, Volkmann D, Barlow PW (eds) *Cell-cell channels*. Landes Bioscience, pp 176-182.
- Heinlein M, Epel BL (2004)** Macromolecular transport and signaling through plasmodesmata. *Int. Rev. Cytol.*, **235**: 93-164.
- Heinlein, M., Epel, B.L., Padgett, H.S., Beachy, R.N.** (1995). Interaction of tobamovirus movement proteins with the plant cytoskeleton. *Science.*, **270**: 1983-1985.
- Heinlein, M., Padgett, H.S., Gens, J.S., Pickard, B.G., Casper, S.J., Epel, B.L., Beachy, R.N.** (1998a). Changing patterns of localization of the tobacco mosaic virus movement protein and replicase to the endoplasmic reticulum and microtubules during infection. *Plant Cell.*, **10**: 1107-1120.
- Heinlein, M., Wood, M.R., Thiel, T., Beachy, R.N.** (1998b). Targeting and modification of prokaryotic cell-cell junctions by tobacco mosaic virus cell-to-cell movement protein. *Plant J.*, **14**: 345-351.
- Heinlein, M., Epel, B.L., Padgett, H.S. and Beachy, R.N. (1995).** Interaction of tobamovirus movement proteins with the plant cytoskeleton. *Science.*, **270**: 1983-1985.
- Heinlein, M.** (2002). The spread of tobacco mosaic virus infection: insights into the cellular mechanism of RNA transport. *Cell Mol Life Sci.*, **59**: 58–82.
- Heinlein, M., Padgett, H.S., Gens, J.S., Pickard, B.G., Casper, S.J., Epel, B.L.**
- Hesketh, J.** (1994). Translation and the cytoskeleton: a mechanism for targeted protein synthesis. *Mol Biol Rep.*, **19**: 233-243.
- Himmelspach, R, Nick, P.** (2001). "Gravitropic microtubule reorientation can be uncoupled from growth" *Planta.*, **212**: 184-189.
- Huang, M. and Zhang, L.** (1999). Association of the movement protein of alfalfa mosaic virus with the endoplasmic reticulum and its trafficking in epidermal cells of onion bulb scales. *Mol Plant Microbe Interact.*, **12**: 680–690.

References

- Huang, S., An, Y-Q., McDowell, J.M., McKinney, E.C., Meagher, R.B.** (1997). The Arabidopsis ACT11 actin gene is strongly expressed in tissues of the emerging inflorescence, pollen, and developing ovules. *Plant Mol Biol.*, **33**: 125-139.
- Huang Z., Han, Y., Howell, S.H.** (2000). Formation of surface tubules and fluorescent foci in Arabidopsis thaliana protoplasts expressing a fusion between the green fluorescent protein and the cauliflower mosaic virus movement protein. *Virology.*, **271**: 58-64.
- Huang, Z., Yeakley, J.M., Garcia, E.W., Holdridge, J.D., Fan, J.B., Whitham, S.A.** (2005). Salicylic acid-dependent expression of host genes in compatible Arabidopsis-virus interactions. *Plant Physiol.*, **137**: 1147-1159.
- Hussey, P.J., Hawkins, T.J., Igarashi, H., Kaloriti, D., Smertenko, A.** (2002). The plant cytoskeleton: recent advances in the study of the plant microtubule-associated proteins MAP-65, MAP-190 and the Xenopus MAP215-like protein, MOR1. *Plant Mol Biol.*, **50**: 915-924.
- Hussey, P.J., Yuan, M., Calder, G., Khan, S., Lloyd, C.W.** (1998). Microinjection of pollen-specific actin-depolymerizing factor, ZmADF1, reorientates F-actin strands in Tradescantia stamen hair cells. *Plant J.*, **14**: 353-357.
- Ishikawa, M., Meshi, T., Motoyoshi, F., Takamatsu, N., Okada, Y.** (1986). In vitro mutagenesis of the putative replicase genes of tobacco mosaic virus. *Nucleic Acids Res.*, **14**: 8291-8305.
- Jansen, R.P.** (1999). RNA-cytoskeletal association. *FASEB J.*, **13**: 455–466.
- Jordan, M.A. and Wilson L.** (1998). Microtubules and actin filaments: dynamic targets for cancer chemotherapy. *Curr. Opin. Cell Biol.*, **10**: 123-130.
- Kahn, T.W., Lapidot, M., Heinlein, M., Reichel, C., Cooper, B., Gafny, R., Beachy, R.N.** (1998). Domains of the TMV movement protein involved in subcellular localization. *Plant J.*, **15**: 15-25.
- Karger, E.M., Frolova, O.Y., Fedorova, N.V., Baratova, L.A., Ovchinnikova, T.V., Susi, P., Makinen, K., Ronnstrand, L., Dorokhov, Y.L., Atabekov, J.G.** (2003b). Dysfunctionality of tobacco mosaic virus movement protein mutant mimicking threonine 104 phosphorylation. *J. Gen. Virol.*, **84**: 727-732.

References

- Karpova, O.V., Rodionova, N.P., Ivanov, K.I., Kozlovsky, S.V., Dorokhov, Y.L., Atabekov, J.G.** (1999). Phosphorylation of tobacco mosaic virus movement protein abolishes its translation repressing ability. *Virology.*, **261**: 20-24.
- Kavallaris, M., Tait, A.S., Walsh, B.J., He, L., Horwitz, S.B., Norris, M.D., Haber, M.** (2001a). Multiple microtubule alterations are associated with Vinca alkaloid resistance in human leukemia cells. *Cancer Res.*, **61**: 5803–5809.
- Kavallaris, M., Verrills, N.M., Hill, B.T.** (2001b). Anticancer therapy with novel tubulin-interacting drugs. *Drug Resist. Updates.*, **4**: 392–401.
- Kawakami, S., Watanabe, Y., Beachy, R.N.** (2004). Tobacco mosaic virus infection spreads cell to cell as intact replication complexes. *Proc Natl Acad Sci USA.*, **101**: 6291–6296.
- Keates, R. A. B., Sarangi, F., and Ling, V.** (1981). Structural and functional alterations in microtubule protein from Chinese hamster ovary mutants. *Proc. Natl. Acad. Sci. USA.*, **78**: 5638–5642.
- Kobayashi, T., Beuchat, M.H., Lindsay, M., Frias, S., Palmiter, R.D., Sakuraba, H., Koonin, E.V. and Dolja, V.V.** (1993). Evolution and Taxonomy of Positive-Strand RNA Viruses. Implications of Comparative Analysis of Amino Acid Sequences. *Crit Rev Biochem. Molec. Biol.*, **28**: 546-547.
- Kreis, T.E.** (1987) Microtubules containing detyrosinylated tubulin are less dynamic. *EMBO J.*, **6**: 2597–2606.
- Laemmli, U. K.** (1970). Cleavage of structural proteins during the assembly of the head of bacteriophage T4. *Nature.*, **227**: 680-685
- Lazarowitz, S.G. and Beachy, R.N.** (1999). Viral movement proteins as probes for intracellular and intercellular trafficking in plants. *Plant Cell.*, **11**: 535–548.
- Leisner, S.M. and S.H. Howell.** (1993). Long-distance movement of plant viruses. *Trends Microbiol.*, **1**: 314-317.
- Lloyd, C.W.** (1994). Why should stationary plant cells have such dynamic microtubules? *Mol. Biol. Cell.*, **5**: 1277–1280.
- Lloyd, C.W., Slabas, A.R., Powell, A.J., Peace, W.** (1982). Novel Features Of The Plant Cytoskeleton *Cell Biology International Reports.*, **6**: 171-175.
- Lucas W.J., Yoo, B-C., Kragler, F.** (2001). RNA as a long-distance information macromolecule in plants. *Nat. Rev. Mol. Cell Biol.*, **2**: 849-857.

References

- Lucas, W. J.** (2006). Plant viral movement proteins: agents for cell-to-cell trafficking of viral genomes. *Virology.*, **344**: 169-184.
- Lucas, W. J., and Lee, J. Y.** (2004). Plasmodesmata as a supracellular control network in plants. *Nat. Rev. Mol. Cell Biol.*, **5**:712-726.
- Maliga, P., Sz-Breznovits, A., Marton, L.** (1973). Streptomycin resistant plants from callus culture of haploid tobacco. *Nat New Biol.*, **244**: 29–30.
- Más, P. and Beachy, R.N.** (1999) Replication of tobacco mosaic virus on endoplasmic reticulum and role of the cytoskeleton and virus movement in intracellular distribution of viral RNA. *J. Cell Biol.*, **147**: 945-958.
- Más, P. and Beachy, R.N.** (2000). Role of microtubules in the intracellular distribution of tobacco mosaic virus movement protein. *Proc. Natl. Acad. Sci. USA.*, **97**: 12345-12349.
- McLean, B.G., Zupan, J., Zambryski, P.C.** (1995). Tobacco mosaic virus movement protein associates with the cytoskeleton in tobacco plants. *Plant Cell.*, **7**: 2101-2114
- Meshi, T., Hosokawa, D., Kawagishi, M., Watanabe, Y., Okada, Y.** (1992). Reinvestigation of intra-cellular localization of the 30k protein in tobacco protoplasts infected with tobacco mosaic virus RNA. *Virology.*, **187**: 809-813.
- Meshi, T., Watanabe, Y., Saito, T., Sugimoto, A., Maeda, T., Okada, Y.** (1987). Function of the 30 kd protein of tobacco mosaic virus: involvement in cell-to-cell movement and dispensability for replication. *EMBO J.*, **6**: 2557-2563.
- Mizuno, K. and Suzaki, T.** (1991). Effects of anti-microtubule drugs on in vitro polymerization of tubulin from mung bean. *Bot Mag Tokyo.*, **103**: 435–448.
- Moore, P., Fenczik, C.A., Deom, C.M., Beachy, R.N.** (1992). Developmental changes in plasmodesmata in transgenic tobacco expressing the movement protein of tobacco mosaic virus. *Protoplasma.*, **170**: 115-127
- Nick P, ed.** **2000**. Plant microtubules: potential for biotechnology. 209 pp. Berlin, Heidelberg, New York: Springer.
- Nick, P., Yatou, O., Furuya, M., Lambert, A.M.** (1994). Auxin-independent microtubule response and seedling development are affected in a rice mutant resistant to EPC. *Plant J.*, **6**: 651–663.

References

- Nick, P., Christou, P., Breviario, D.** (2003). Generating transgenic plants by minimal addition of exogenous DNA - a novel selection marker based on plant tubulins. *AGBiotechNet AGB.*, **5**:105
- Nick, P.** (1998). Signalling to the microtubular cytoskeleton in plants. *International Rev. Cytol.*, **184**: 33-80.
- Nick, P., Schäfer, E., Hertel, R., Furuya, M.** (1991). On the putative role of microtubules in gravitropism of maize coleoptiles. *Plant Cell Physiol.*, **32**:873–880.
- Olga C. Rodriguez, Andrew W. Schaefer, Craig A. Mandato, Paul Forscher, William M. Bement and Clare M. Waterman-Storer.** (2003). Conserved microtubule-actin interactions in cell movement and morphogenesis. *Nature Cell Biology.*, **5**: 599–609
- Oparka K, ed.** (2005) *Plasmodesmata*. Blackwell Publishing, Oxford .
- Oparka, K.J., Prior, D.A.M., Santa Cruz, S., Padgett, H.S., Beachy, R.N.** (1997). Gating of epidermal plasmodesmata is restricted to the leading edge of expanding infection sites of tobacco mosaic virus. *Plant J.*, **12**: 781-789.
- Oparka, K.J., Roberts, A.G., Boevink, P., Santa Cruz, S., Roberts, I.M., Pradel, K.S., Imlau, A., Kotlizky, G., Sauer, N., and Epel, B.E.** (1999). Simple, but not branched, plasmodesmata allow the non-specific trafficking of proteins in developing tobacco leaves. *Cell.*, **97**: 743–754.
- Osman, T.A., Buck, K.W.** (1996). Complete replication in vitro of tobacco mosaic virus RNA by a template-dependent, membrane-bound RNA polymerase. *J. Virol.*, **70**: 6227-6234.
- Padgett, H.S., Epel, B.L., Kahn, T.W., Heinlein, M., Watanabe, Y., Beachy, R.N.** (1996). Distribution of tobamovirus movement protein in infected cells and implications for cell-to-cell spread of infection. *Plant J.*, **10**: 1079–1088.
- Parton, R.G. and Gruenberg, J.** (1999). Late endosomal membranes rich in lysobisphosphatidic acid regulate cholesterol transport. *Nature Cell Biol.*, **1**: 113–118.
- Pasick, J. M. Kalicharran, M., K. Dales, S.** (1994). Distribution of trafficking of JHM coronavirus structural proteins of virions in primary neurons and the OBL-21 neuronal cell line. *J. Virol.*, **68**: 2915-2928.

References

- Boevink, P. and Oparka, K. J.** (2005). Virus-Host Interactions during Movement Processes. *Plant Physiol.*, **138**: 1815-1821
- Piperno, G., LeDizet, M., Chang, X.** (1987). Microtubules containing acetylated alpha-tubulin in mammalian cells in culture. *J. Cell Biol.*, **104**: 298-302.
- Ploubidou, A. and Way, M.** (2001). Viral transport and the cytoskeleton. *Curr. Opin. Cell Biol.*, **13**: 97-105.
- Ramachandran, S., Christensen, H.E., Ishimaru, Y., Dong, C.H., Chao-Ming, W., Cleary, A.L., Chua, N.H.** (2000) Profilin plays a role in cell elongation, cell shape maintenance, and flowering in Arabidopsis. *Plant Physiol.*, **124**: 1637–1647.
- Reichel, C. and Beachy, R.N.** (1998). Tobacco mosaic virus infection induces severe morphological changes of the endoplasmatic reticulum. *Proc. Natl. Acad. Sci. USA.*, **95**: 11169-11174.
- Reichel, C. and Beachy, R.N.** (2000). Degradation of the tobacco mosaic virus movement protein by the 26S proteasome. *J. Virol.*, **74**: 3330-3337.
- Heil-Chapdelaine, R. A., Adames, N. R. and Cooper, J. A.** (1999). Formin' the connection between microtubules and the cell cortex. *J. Cell Biol.*, **144**: 809-811.
- Sacristan, S., Malpica, J.M., Fraile, A., Garcia-Arenal, F.** (2003). Estimation of population bottlenecks during systemic movement of tobacco mosaic virus in tobacco plants. *J Virol.*, **77**: 9906-9911.
- Saedler, R., Mathur, N., Srinivas, B.P., Kernebeck, B., Hülkamp, M., Mathur, J.** (2004). Actin control over microtubules suggested by DISTORTED2 encoding the Arabidopsis ARPC2 subunit homolog. *Plant Cell Physiol.*, **45**: 813-822.
- Saito, T., Yamanaka, K., Okada, Y.** (1990). Long-distance movement and viral assembly of tobacco mosaic virus mutants. *Virology.*, **176**: 329-336.
- Schaad, M.C., Jensen, P.E., and Carrington, J.C.** (1997). Formation of plant RNA virus replication complexes on membranes: role of an endoplasmic reticulum-targeted viral protein. *EMBO (Eur. Mol. Biol. Organ) J.*, **16**: 4049-4059.
- Schnorrer, F., Bohmann, K. and Nüsslein-Volhard, C.** (2000). The molecular motor dynein is involved in targeting Swallow and *bicoid* RNA to the anterior pole of *Drosophila* oocytes. *Nat. Cell Biol.*, **2**: 185- 190.
- Schwab, B., Mathur, J., Saedler, R., Schwarz, H., Frey, B., Scheidegger, C., Hülkamp, M.** (2003) Regulation of cell expansion by the DISTORTED genes in

References

Arabidopsis thaliana: actin controls the spatial organization of microtubules. *Mol Gen Genomics.*, **269**: 350-360.

Seemanpillai, M., Elamawi, R., Ritzenthaler, C., Heinlein, M. (2006). Challenging the role of microtubules in Tobacco mosaic virus movement by drug treatments is disputable. *J. Virol.*, **80**: 6712-6715.

Shaw, S. L., Kamyar, R. and Ehrhardt, D. W. (2003). Sustained Microtubule Treadmilling in Arabidopsis Cortical Arrays. *Science.*, **300**: 1715 - 1718.

Bisgrove, S.R., Hable, W.E., Kropf, D.L. (2004). +TIPs and microtubule regulation. The beginning of the plus end in plants. *Plant Physiol.*, **136**: 3855–3863.

Shibaoka, H. (1994). Plant hormone-induced changes in the orientation of cortical microtubules: alterations in the cross-linking between microtubules and the plasma membrane. *Annu Rev Plant Physiol Plant Mol Biol.*, **45**: 527-544.

Shibaoka, H. and Nagai, R. (1994). The plant cytoskeleton. *Curr. Opin. Cell Biol.*, **6**: 10–15.

Skoufias, D. A. and Wilson, L. (1998). Assembly and colchicine binding characteristics of tubulin with maximally tyrosinated and detyrosinated alpha-tubulins. *Arch. Biochem. Biophys.*, **351**: 115-122.

Sodeik, B. (2000). Mechanisms of viral transport in the cytoplasm. *Trends Microbiol.*, **8**: 465–472.

Sonobe S. (1996). Studies on the plant cytoskeleton using miniprotoplasts of tobacco BY-2 cells. *J Plant Res.*, **109**: 437-448.

Sonobe, S. and Shibaoka, H. (1989) Cortical fine actin filaments in higher plant cells visualized by rhodamine-phalloidin after pretreatment with m-maleimidobenzoyl N-hydroxysuccinimide ester. *Protoplasma.*, **148**: 80-86.

Stahelin, L.A. (1997) The plant ER: a dynamic organelle composed of a large number of discrete functional domains. *Plant J.*, **11**: 1151-1165.

Staiger, C. (2000) Signaling to the actin cytoskeleton in plants. *Annu Rev Plant Physiol Plant Mol Biol.*, **51**: 257.

Staiger, C.J. and Lloyd, C.W. (1991). The plant cytoskeleton. *Curr Opin Cell Biol.*, **3**: 33-42.

References

- Szécsi, J., Ding, X.S., Lim, C.O., Bendahmane, M., Cho, M.J., Nelson, R.S., Beachy, R.N.** (1999). Development of tobacco mosaic virus infection sites in *Nicotiana benthamiana*. *Mol. Plant Microbe Interact.*, **2**: 143-152.
- Traas, J.A., Doonan, J.H., Rawlins, D.J., Shaw, P.J., Watts, J., Lloyd, C.W.** (1987). An actin network is present in the cytoplasm throughout the cell cycle of carrot cells and associates with the dividing nucleus. *J Cell Biol.*, **105**:387–395.
- Vale, R. D.** (1987). Intracellular transport using microtubule-based motors *Annu. Rev. Cell Biol.*, **3**: 347-378.
- van Lent J, Storms M, van der Meer F, Wellink J, Goldbach R.** (1991). Tubular structures involved in movement of cowpea mosaic virus are also formed in infected cowpea protoplasts. *J. Gen. Virol.*, **72**: 2615-2623.
- van Lent J.W.M. and Schmitt-Keichinger C.** (2006). Viral movement proteins induce tubule formation in plant and insect cells. In: Baluska F, Volkmann D, Barlow PW (eds) *Cell-cell channels*. Landes Bioscience,
- Vaughn, K.C.** (2000). Anticytoskeletal herbicides. In: Nick P (ed.), *Plant Microtubules: Potential for Biotechnology*. (pp. 193–205) Springer, Berlin, Heidelberg.
- Waigmann, E., Chen, M.H., Bachmaier, R., Ghoshroy, S., Citovsky, V.** (2000). Regulation of plasmodesmal transport by phosphorylation of tobacco mosaic virus cell-to-cell movement protein. *EMBO J.*, **19**: 4875–4884.
- Waigmann, E., Curin, M., Heinlein, M.** (2007). Tobacco mosaic virus - a model for macromolecular cell-to-cell spread. In: Waigmann E, Heinlein M (eds) *Viral Transport in Plants*. Springer, Heidelberg, pp 29-62.
- Waigmann, E., Lucas, W., Citovsky, V., Zambryski P.** (1994). Direct functional assay for tobacco mosaic virus cell-to-cell movement protein and identification of a domain involved in increasing plasmodesmal permeability. *Proc. Natl. Acad. Sci. USA.*, **91**: 1433-1437.
- Waller, F., Wang, Q-Y., Nick, P.** (2000). Actin and signal-controlled cell elongation in coleoptiles. In: Staiger CJ, Baluška F, Barlow PW, Volkmann D (eds) *Actin: A Dynamic Framework for Multiple Plant Functions*. Kluwer, Dordrecht, pp 477-496.
- Wang, Q-Y, Nick, P.** (1998). The auxin response of actin is altered in the rice mutant *Yin-Yang*. *Protoplasma.*, **204**: 22-33.

References

- Wang, Y-S., Motes, C.M., Mohamalawari, D.R., Blancaflor., E.B.** (2004). Green fluorescent protein fusions to Arabidopsis fimbrin 1 for spatio-temporal imaging of F-actin dynamics in roots. *Cell Motil Cytoskel.*, **59**: 79-93.
- Wasteneys, G.O., Williamson, R.E.** (1991) Endoplasmic microtubules and nucleus-associated actin rings in *Nitella* internodal cells. *Protoplasma.*, **162**: 86-98
- Wasteneys, G.O., Willingale-Theune, J., Menzel, D.** (1997) Freeze shattering: a simple and effective method for permeabilizing higher plant cell walls. *J Microscopy.*, **188**: 51-61
- Wasteneys, G.O.** (2002) Microtubule organization in the green kingdom: chaos or self-order? *J. Cell Sci.*, **115**: 1345–1354.
- Wernicke, W and Jung, G.** (1992) Role of cytoskeleton in cell shaping of developing mesophyll of wheat (*Triticum aestivum* L.). *Eur J Cell Biol.*, **57**: 88-94
- Wiesler, B., Wang, Q.Y., Nick, P.** (2002) The stability of cortical microtubules depends on their orientation. *Plant J.*, **32**: 1023-1032.
- Wolf, S., Deom, C.M., Beachy, R.N. Lucas, W.J.** (1989). Movement protein of tobacco mosaic virus modifies plasmodesmatal size exclusion limit. *Science.*, **246**: 377-379.
- Wright, K.M., Wood, N.T., Roberts, A.G., Chapman, S., Boevink, P., Mackenzie, K.M., Oparka, K.J.** (2007) Targeting of TMV Movement Protein to Plasmodesmata Requires the Actin/ER Network; Evidence From FRAP. *Traffic.*, **8**: 21-31.
- Zambryski, P.** (1995). Plasmodesmata: Plant channels for molecules on the move. *Science.*, **270**: 1943-1944.
- Zhang, D., Wadsworth, P., Hepler, P.K.** (1993) Dynamics of microfilaments are similar, but distinct from microtubules during cytokinesis in living, dividing plant cells. *Cell Motil Cytoskel.*, **24**: 151-155.

9 Appendix

High Tubulin Levels Hamper MP Dephosphoregulation

ATER 2 and *ATER 5* adopt different strategies with in dealing with high levels of EPC. *ATER 2* has reduced microtubule dynamics, whereas *ATER 5* has high tubulin levels. We therefore concentrated on the effect of reduced microtubule turnover in viral spread. The effect of increased tubulin on viral movement is epitomised by *ATER 5* as shown in Figure 28.

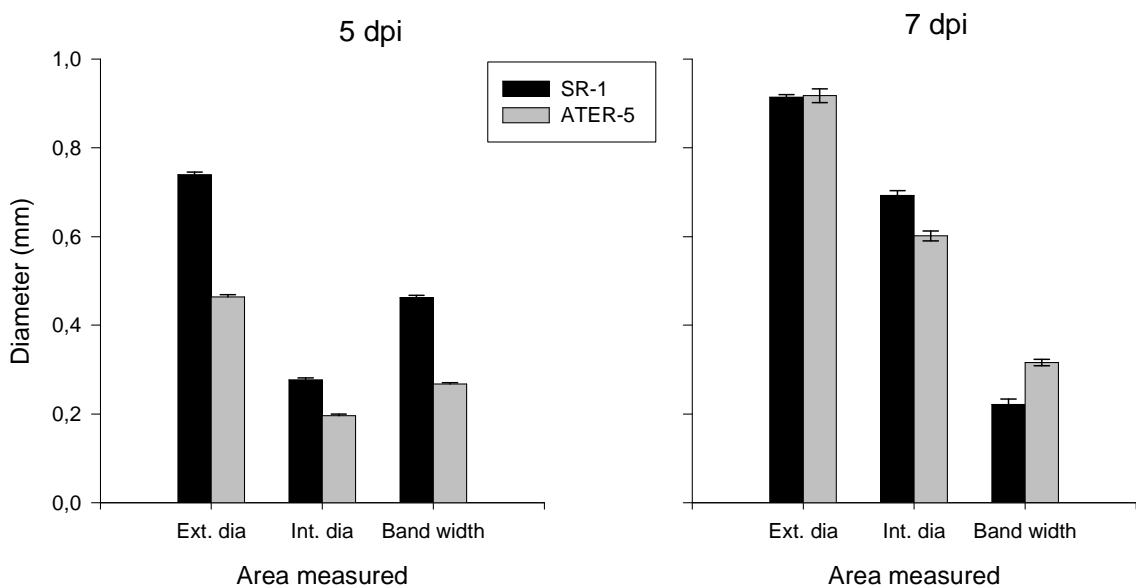


Figure 28: Effect of high tubulin levels on viral spread in *N. tabacum* following inoculation with TMV-MP:GFP. TMV spread at early infection stages is slower in *ATER 5*. However at 7 dpi it is faster than in the wild type tobacco plants.

The high tubulin levels probably interfere with the functioning of the MP, at 7dpi, the rate of MP degradation in the *ATER 5* is slower than in the wild type and hence a broader infection band in the mutant.

MP moves Actively through the Plasmodesmata

The MP localization is observed on both sides of the plasmodesmata indicating that the MP+vRNA complex moves across the cell wall through the plasmodesmata.

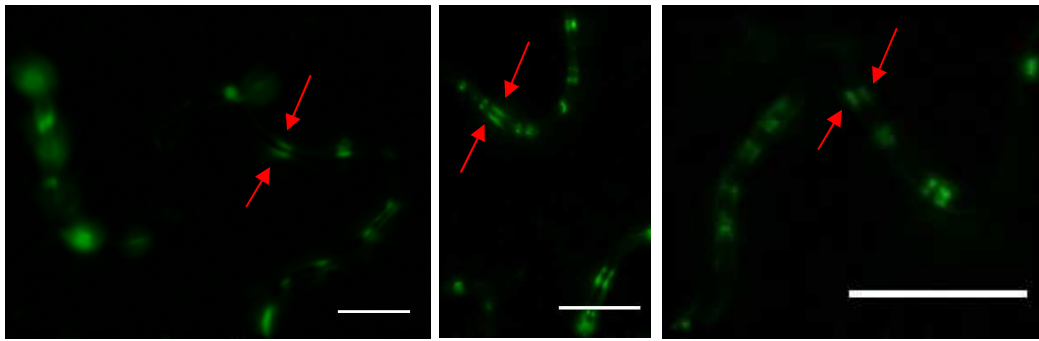


Figure 29: MP moves across the plasmodesmata. MP labels both sides of the plasmodesmata in SR1 (A), ATER 2 (B) and ATER (5). Indicating that the MP+vRNA cargo move across the plasmodesmata. Scale bars = 10 μ m.

The MP does more than just gating the plasmodesmata. It is also capable of movement as shown in **Figure 29**. Thus confirming observations by Waigmann *et al.*, 1994 and Kotlizky *et al.*, 2001.

Immunolocalization can not be used to separate Detyr- from Tyr- α -tubulin

Detyrosinated tubulin can be separated biochemically from the tyrosinated form by a simple method of affinity chromatography. Experiments conducted by Weisler *et al.*, (2002) suggested that dynamic and stable microtubules are distinguished using the antibodies ATT (dynamic microtubules) and DM1A (stable microtubules).

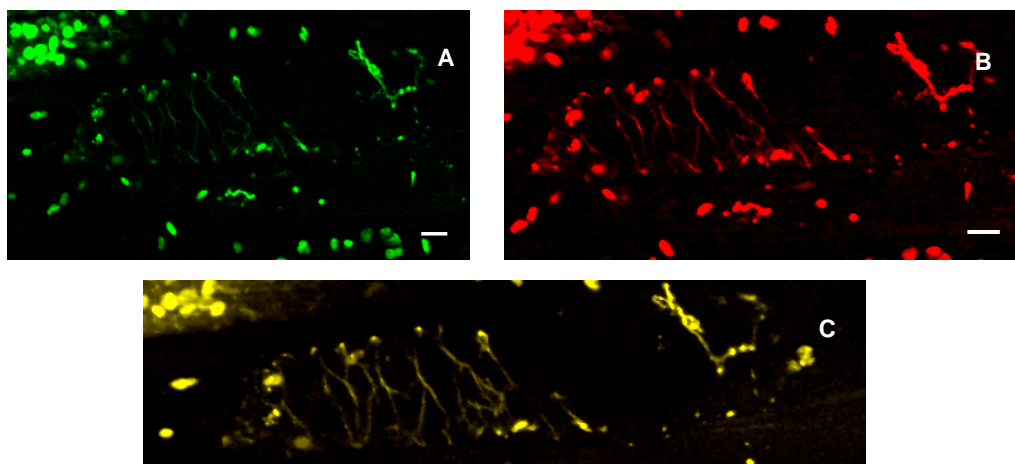


Figure 30: Double Immunolabelling of cortical microtubules in *N. tabacum* epidermal cells.

DM1A-FITC labelled microtubules (A). ATT labelled microtubules (B). An overlay of A and B shows a 100% merge (C). Scale bar = 10 μ m

Using the two antibodies we conducted double immunolabelling of microtubules in epidermal cells of tobacco plants under *in vitro* conditions (**Figure 30**). Our

results show that ATT and DM1A label the same microtubule arrays. Thus implying that it is not possible to distinguish between populations of dynamic and stable microtubules *in situ*.

Actin Bundling in *ATER* Mutants

Further evidence of cross talk is presented by images showing that EPC resistance in the *ATER* mutants which has been shown to be controlled by either microtubule turnover (*ATER 2*) or tubulin levels (*ATER 5*) results in bundling of actin filaments in these mutants.

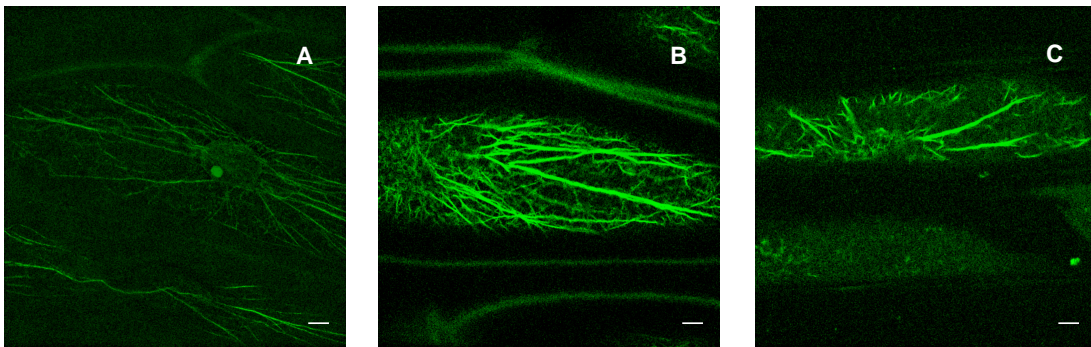


Figure 31: Actin bundling in *ATER* mutants. In *ATER 2* (B) and *ATER 5* (C), actin filaments appear bundled compared to the wild type (A). Scale bars = 10 μ m